Ice-shelf vibrations modeled by a full 3-D elastic finite-volume model: field equations (version 6)

Yuri V. Konovalov

ORCID: 0000-0002-8469-9706

Financial University under the Government of the Russian Federation, Leningradsky Prospekt 49, Moscow, Russian Federation, 125993

Correspondence to: Y.V. Konovalov (yu-v-k@yandex.ru)

Abstract

The propagation of elastic-flexural waves through the ice shelf was modeled with a full 3-D elastic model. This model is based on momentum equations discretized using the *finite volume* method (like in the previous version 5). An evolution of the previous version (version 5) is the application of a *finite volume* approach to the approximation of the boundary conditions at ice shelf boundaries. The flow of sea water under the ice shelf is described by the wave equation. Numerical experiments were undertaken for a crevasse-ridden ice shelf with different spatial periodicities of crevasses. In addition to the finite-difference model (described in versions 2 and 3) the finite volume model developed in this version 6 reveals a torsional component of deformation in modeled ice shelf vibration modes.

1. Model description and field equations

1.1 Basic equations (this item is completely the same as in the previous version 5)

The equations of momentum, written as balance equations of momentum in the volume V (bounded by the surface S) of an elastically deformable continuous medium have the following form (e.g. [1], [2], [3], [4])

$$\frac{\partial^2}{\partial t^2}\int_V \rho\, U_i\, dV = \int_V \left(\frac{\partial \sigma_{ik}}{\partial x_k} + \rho g_i\right) dV \tag{1.1}$$

or

$$\frac{\partial^2}{\partial t^2}\int_V \rho\, U_i\, dV = \int_S \sigma_{ik} dS_k + \int_V \rho g_i dV \tag{1.2}$$

where $\boldsymbol{\sigma}$ is the stress tensor; and ρ is the ice density; $i,k = 1,2,3$ or in terms of rectangular coordinate (XYZ) i,k means x,y,z; U_i are displacements of an elastic continuous medium (displacements of ice) which are also denoted in rectangular coordinates as U,V,W: U,V and W are two horizontal and one vertical ice displacements, respectively.

As in previous versions/models (XYZ) is a rectangular coordinate system with the X-axis along the center line, and Z-axis pointing vertically up. The ice shelf has a length L along the center line. The geometry of the ice shelf is assumed to be given by lateral boundary functions $y_{1,2}(x)$ at sides labeled 1 and 2 and functions for the surface and base elevation, $h_{s,b}(x,y)$, denoted by subscripts s and b, respectively. Thus, the domain, which includes the volume of integration in Eqs. (1), is $\Omega = \{0 < x < L,\ y_1(x) < y < y_2(x),\ h_b(x,y) < z < h_s(x,y)\}$.

Sub-ice water is assumed to be an incompressible inviscid fluid of uniform density. Other assumptions are

(i) the water flow in the cavity ander the ice shelf is a two-dimensional horizontal fluid flow, in which the vertical component of the flow velocity has a negligible zero value, that corresponds to the propagations of waves in a shallow water layer (e.g. the gravity waves) when the water depth is much less than the wavelength (e.g. [1],[2]). Moreover, the ice is considered as a continuous solid elastic medium (solid elastic plate).

(ii) the horizontal velocity of the water flow is small so that the non-linear term in the Euler equations can be neglected (e.g. [1], [2]), that corresponds the propagation of a wave, in which the amplitude of water vertical displacements is much less than the wavelength (e.g. [1], [2]).

Under these three assumptions, sub-ice water flow is independent of z in the vertical column. Manipulations with the governing equations of the shallow sub-ice water layer yield the wave equation [5]:

$$\frac{\partial^2 W_b}{\partial t^2} = \frac{1}{\rho_w}\frac{\partial}{\partial x}\left(d_0\frac{\partial P\prime}{\partial x}\right) + \frac{1}{\rho_w}\frac{\partial}{\partial y}\left(d_0\frac{\partial P\prime}{\partial y}\right), \qquad (2)$$

where ρ_w is sea water density; $d_0(x,y)$ is the depth of the sub-ice water layer; $W_b(x,y,t)$ is the vertical deflection of the ice-shelf base, and $W_b(x,y,t) = W(x,y,h_b(x,y),t)$; and $P'(x,y,t)$ is the deviation of the sub-ice water pressure from the hydrostatic value.

1.2 Boundary conditions

The boundary conditions are: (i) a stress-free ice surface; (ii) the normal stress exerted by seawater on the ice-shelf free edges and on the ice-shelf base; and (iii) rigidly fixed edges at the grounding line of the ice-shelf.

The model considered here also use a linear combination of boundary conditions [6]. This linear combination is expressed as [6]

$$\alpha_1 F_i(U,V,W) + \alpha_2 \Phi_i(U,V,W) = 0,\ i = 1,2,3, \quad (3)$$

where:

(i) $F_i(U,V,W) = 0$ is the typical form of the boundary conditions, i.e. $\sigma_{ik} n_k = f_i$ where, f_i is given forcing on the boundary ($\vec{n}$ is the unit vector normal to the surface);

(ii) $\Phi_i(U,V,W) = 0$ is the approximation based on the application of a *finite volume approach* to the approximation of the boundary conditions, taking in to account for the typical form of boundary conditions on the boundaries of an *elementary volume*;

(iii) the coefficients α_1 and α_2 satisfy the condition $\alpha_1 + \alpha_2 = 1$.

The boundary conditions for the seawater layer correspond to the frontal incident wave. They are

(i) at $x = 0$: $\frac{\partial P\prime}{\partial x} = 0$;

(ii) at $y = y_1, y = y_2$: $\frac{\partial P\prime}{\partial y} = 0$;

(iii) at $x = L$: $P' = A_0 \rho_w g\, e^{i\omega t}$, where A_0 is the amplitude of the incident wave.

1.3 Equations for ice-shelf displacements (this item is completely the same as in the previous version 5)

Constitutive relationships between stress tensor components and displacements correspond to Hooke's law, e.g., [3], [4]:

$$\sigma_{ij} = \frac{E}{1+\nu}\left(u_{ij} + \frac{\nu}{1-2\nu}\, u_{ll}\delta_{ij}\right) \quad , \tag{4}$$

where u_{ij} are the strain components, E - Young's modulus, ν - Poisson's ratio.

1.4 Discretization of the model

Numerical solutions were obtained by a finite volume method, which is based on the standard coordinate transformation $x, y, z \rightarrow x, \eta = \frac{y-y_1}{y_2-y_1}, \xi = (h_s - z)/H$, where H is the ice thickness ($H = h_s - h_b$). The coordinate transformation maps the ice domain Ω into the rectangular parallelepiped $\Pi = \{0 \le x \le L; 0 \le \eta \le 1; 0 \le \xi \le 1\}$, which simplifies the numerical discretization.

Considering an elementary volume, which is an elementary rectangular parallelepiped in coordinates x, η, ξ: $\Pi_{i,j,k} = \left\{x_{i-\frac{1}{2}} \le x \le x_{i+\frac{1}{2}}; \eta_{j-\frac{1}{2}} \le \eta \le \eta_{j-\frac{1}{2}}; \xi_{k-\frac{1}{2}} \le \xi \le \xi_{k+\frac{1}{2}}\right\}$, and applying Eq (1.2) to this volume, we obtain six momentum fluxes entering this volume, which are expressed by the stress tensor for an elastic continuum (which for an elastic continuum are defined as forces applied to the surfaces of the volume) (Figure 1):

$$I_p^{(1)} \approx \left\{-\sigma_{px}\xi'_x H - \sigma_{py}\xi'_y H + \sigma_{pz}\right\}_{k-\frac{1}{2}}^{i,j} B^{i,j}\Delta x\Delta\eta,\ p = 1,2,3\ (or\ x, y, z); \tag{5.1}$$

$$I_p^{(2)} \approx \left\{\sigma_{px}\xi'_x H + \sigma_{py}\xi'_y H - \sigma_{pz}\right\}_{k+\frac{1}{2}}^{i,j} B^{i,j}\Delta x\Delta\eta,\ p = 1,2,3\ (or\ x, y, z); \tag{5.2}$$

$$I_p^{(3)} \approx -\left\{\sigma_{px}\eta'_x B + \sigma_{py}\right\}_{k}^{i,j-\frac{1}{2}} H^{i,j-\frac{1}{2}}\Delta x\Delta\xi,\ p = 1,2,3\ (or\ x, y, z); \tag{5.3}$$

$$I_p^{(4)} \approx \left\{\sigma_{px}\eta'_x B + \sigma_{py}\right\}_k^{i,j+\frac{1}{2}} H^{i,j+\frac{1}{2}}\,\Delta x\Delta\xi,\ p = 1,2,3\ (or\ x,y,z); \quad (5.4)$$

$$I_p^{(5)} \approx -\left\{\sigma_{px}\right\}_k^{i-\frac{1}{2},j} B^{i-\frac{1}{2},j} H^{i-\frac{1}{2},j}\,\Delta\eta\Delta\xi,\ p = 1,2,3\ (or\ x,y,z); \quad (5.5)$$

$$I_p^{(6)} \approx \left\{\sigma_{px}\right\}_k^{i+\frac{1}{2},j} B^{i+\frac{1}{2},j} H^{i+\frac{1}{2},j}\,\Delta\eta\Delta\xi,\ p = 1,2,3\ (or\ x,y,z); \quad (5.6)$$

where $B = y_2 - y_1$ is ice shelf width in transverse direction.

Six momentum fluxes (5.1) - (5.6), entering the elementary volume, rewritten in terms of ice displacements, are presented in **Appendix A in the previous version 5** (https://doi.org/10.5281/zenodo.7697142).

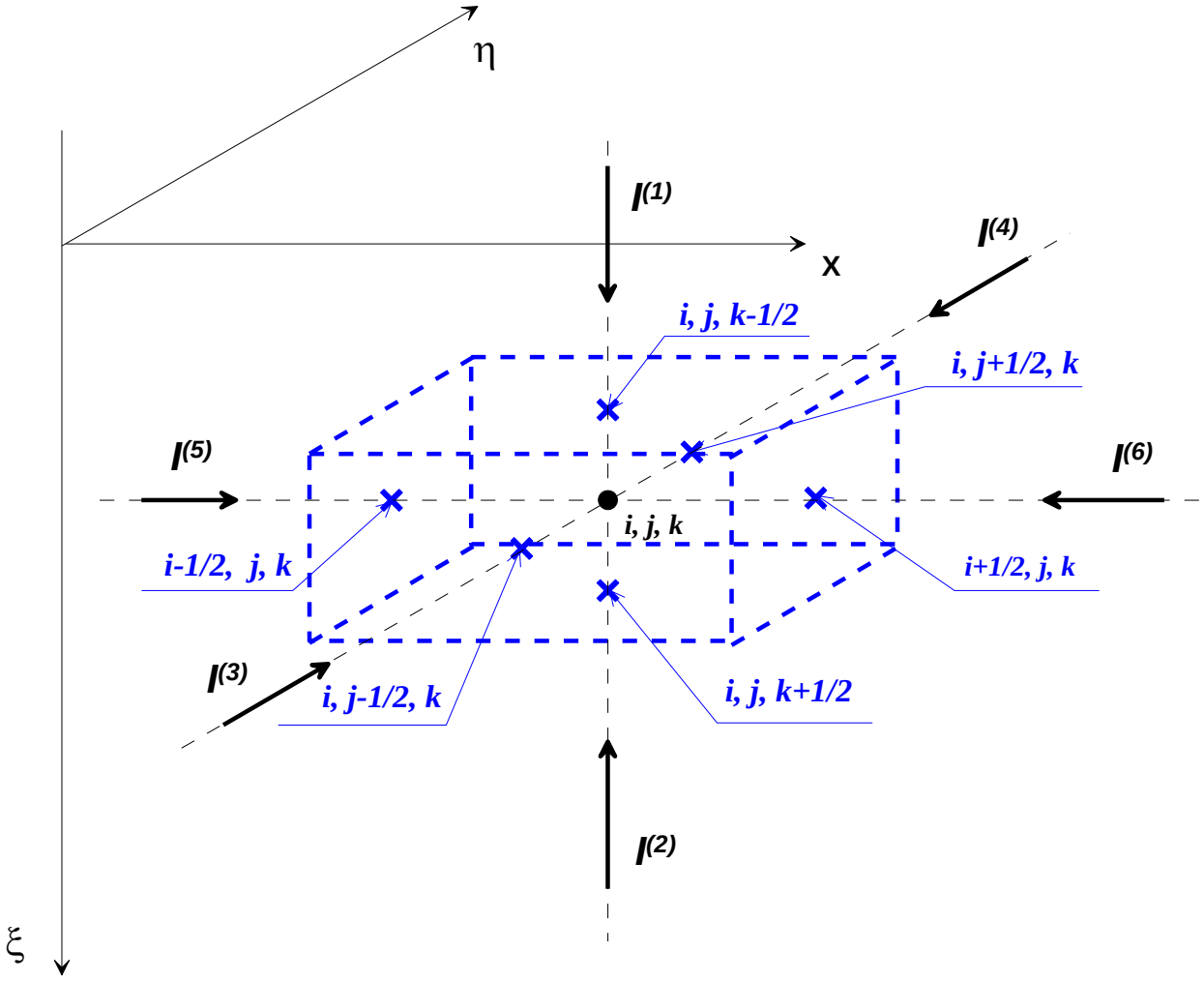

Figure 1. An elementary volume (an elementary rectangular parallelepiped) in which the momentum balance is considered in the model.

Accordingly, considering an elementary volume, which is located, for example, on the surface of ice, as shown in Figure 2, we obtain that $I_p^{(1)} = 0$ and remaining five momentum fluxes are determinated by equations (5.2) - (5.6), where $k = 1$. Thus, having made appropriate changes in the approximations of derivatives in equations (A1.1) – (A6.3) from **Appendix A** in the previous version 5 (https://doi.org/10.5281/zenodo.7697142), we obtain second type approximation $\Phi_i(U, V, W)$ from Eq (3):

1) **the corresponding lines 14839..23341 in the program code** contain an approximation of the second type of **boundary conditions on the ice surface at $z = h_s(x, y)$**
2) **the corresponding lines 750..3816 in the program code** contain an approximation of the second type of **boundary conditions on the ice shelf front/terminus**
3) **the corresponding lines 4000..9059 in the program code** contain an approximation of the second type of **boundary conditions on the ice shelf lateral edge at $y = y_1(x)$**
4) **the corresponding lines 9422..14471 in the program code** contain an approximation of the second type of **boundary conditions on the ice shelf lateral edge at $y = y_2(x)$**
5) **the corresponding lines 24147..32840 in the program code** contain an approximation of the second type of **boundary conditions on the ice shelf base at $z = h_b(x, y)$**

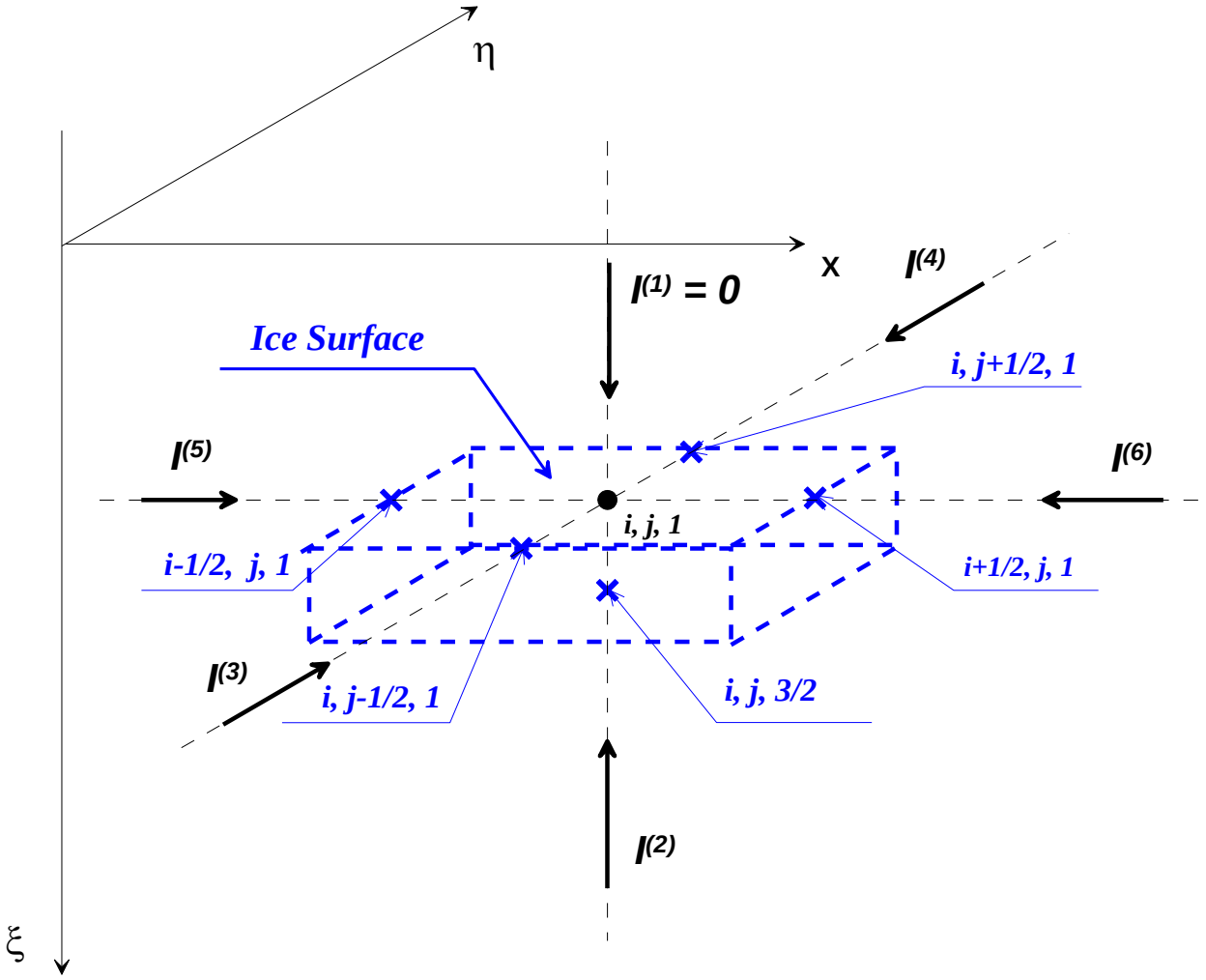

Figure 2. An elementary volume located on the ice surface.

1.5 Free energy of elastically deformed ice shelf

The free energy of elastic deformation of the bends of ice shelves per unit volume is defined by the expression, e.g., [3], [4],

$$F = \frac{E}{2(1+\nu)}\left(u_{ij}^2 + \frac{\nu}{1-2\nu}\, u_{ll}^2\right). \qquad (6)$$

Respectively, the free energy of the ice shelf bending is determined by integrating of energy density (6) over the volume of the ice shelf:

$$F_{overall} = \frac{E}{2(1+\nu)} \int_V \left(u_{ij}^2 + \frac{\nu}{1-2\nu} u_{ll}^2 \right) dV. \quad (7)$$

1.6 Ice-shelf harmonic vibrations. The eigenvalue problem.

(The content of this item is the same as in the description of previous models/versions [6])

It is assumed that for harmonic vibrations all variables are periodic in time, with the periodicity of the incident wave (of the forcing) given by the frequency ω, i.e.,

$$\tilde{\varsigma}(x, y, z, t) = \varsigma(x, y, z)\, e^{i\omega t}, \quad (8)$$

where $\tilde{\varsigma} = \{U, V, W, \ \sigma_{ij}\}$,

where we are interested in the real part of the variables expressed in complex form.

This assumption also implies that the full solution of the linear Eqs. (1) is a sum of the solution for the steady-state flexure of the ice shelf and solution (8) for the time-dependent problem. In other words, solution (8) implies that the deformation due to the gravitational forcing can be separated from the vibration problem, i.e. the term, which includes ρg, is absent from the final equations formulated for the vibration problem, because a time-independent solution accounting for them applies and is not of interest in this study.

The separation of variables in Eq. (8) and its substitution into Eqs. (1) yields the same equations, but with the operator $\frac{\partial^2}{\partial t^2}$ replaced with the constant $-\omega^2$, i.e. we obtain equation for $\varsigma(x, y, z)$:

$$\mathcal{L}\,\varsigma = -\omega^2 \varsigma, \quad (9)$$

where $\mathcal{L}$ is a linear integro-differential operator.

The numerical solution of Eq. (9) at different values of ω yields the dependence of ς on the frequency of the forcing ω. When the frequency of the forcing converges to the eigenfrequency of the system, we observe the typical rapid increase of deformation/stresses in the spectra in the form of the resonant peaks.

Note that here, the term "eigenvalue" refers to the eigenfrequency (ω_n) of the ice/water system or corresponding periodicity ($T_n = \frac{2\pi}{\omega_n}$). As mentioned previously, the term "eigenvalue" is employed in the same meaning like in a Sturm-Liouville Eigenvalue Problem, e.g. [7]. Eigenvalues (where resonant peaks would be observed) are denoted by the letters ω_n or T_n with the subscript n (or other), which is integer, because the array of the eigenvalues is a countable set.

Letters ω or T without the subscript denote the non-resonant values of frequency or periodicity of the ice/water system. They are defined by the frequency of the incident wave (of the forcing).

The eigenvalues can be derived from the equation $D(\omega) = 0$, where D is the determinant of the matrix, which results from the discretization of Eqs. (1), (2) and of the corresponding boundary conditions. However, the probability of the appearance of the forcing at any specific frequency is practically zero. This can be seen when we consider only events within the frequency range $(\omega_i - \Delta\omega,\ \omega_i + \Delta\omega)$. The probability of a forcing that is within the frequency range, is non-zero:

$$p\{\omega \in (\omega_i - \Delta\omega,\ \omega_i + \Delta\omega)\} = \frac{2\Delta\omega}{\Omega}, \qquad (10)$$

where Ω is the width of the range in omega space, which includes all possible frequencies of the forcing. Eq. (10) also assumes that the events have equal probabilities in different parts of Ω.

Thus, the probability of the resonant-like motion is higher when the value $\Delta\omega$, which is defined by the width of the resonant peak, is higher too. Therefore, the width of the resonant peaks is an important parameter, from a practical standpoint, because it defines the probability of the suitable resonant-like motion.

Thus, the computation of the spectra provides important information about the width of resonant peaks within the likely range of forcing frequencies found in nature. By assessing the widths of such peaks, a better understanding of the probability that any one specific forcing event, at a specific ω can be assessed.

2. Code input parameters and code output results

The geometric parameters of the ice shelf, considered here as a rectangular parallelepiped, are specified in **lines 20-26** in the program code. Corresponding changes in **lines 118-122**, where the lateral boundaries $(y_1(x), y_2(x))$ and the width of the ice shelf are defined, and in **lines 130-134**, where thickness of the ice shelf is defined, should be made in the case of a more general ice shelf geometry.

In this version a crevasse-ridden ice shelf [8] is considered. The parameters of crevasses are listed in the **lines 29-33** of the program code. They are

a) spatial periodicity of the crevasses T_{cr}

b) crevasse depth D_{cr};

c) crevasse width W_{cr}.

The shape of the crevasse was assumed as rectangular (**lines 147-167** in the code) or as triangular (**lines 170-197** in the code).

The elevation of the ice surface (**lines 204-208** in the code) and the elevation of the ice bed (**lines 224-228** in the code) correspond to the condition of floating ice.

Some of the modes generated by the finite-volume model are listed below (**Figures 4-16; 18-34; 36-50**).

The output of the code is the free energy spectrum, that is, the total free energy defined by equation (7) versus periodicity/frequency of the forcing (**lines 38667-38722** in the code).

Figure 51 shows the example of the output of the code, i.e. free energy spectrum.

The model reveals the torsion strain component in the deformations of the ice shelf (see e.g., Figures 10,b; 18,b; 18,c; 21,b; 22,c; 25,b; 36,c; 43,c; 45,b and others, highlighted in red), which is visibly observed in some cases of periodicity of the forcing, when $\alpha_1 < \alpha_2$ (see Eq. (3)). A torsion strain component is also observed in ice shelf modes obtained, in particular, using the thin plate elastic model [5] and by the model based on integro-differential momentum equations (see version 4) [9].

2.1 Vertical deflections of the ice shelf were obtained with spatial periodicity of the crevasses $T_{cr} = 2.0\ km$ and with crevasse depth $D_{cr} = 20m$.

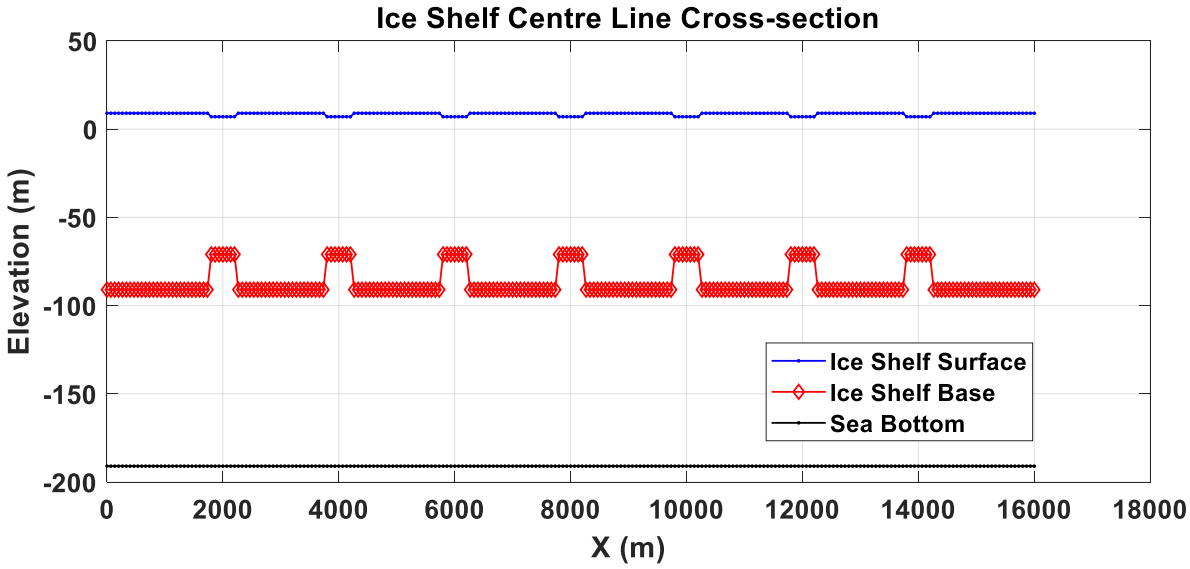

Figure 3. Ice shelf geometry. $T_{cr} = 2.0km$; $D_{cr} = 20m$.

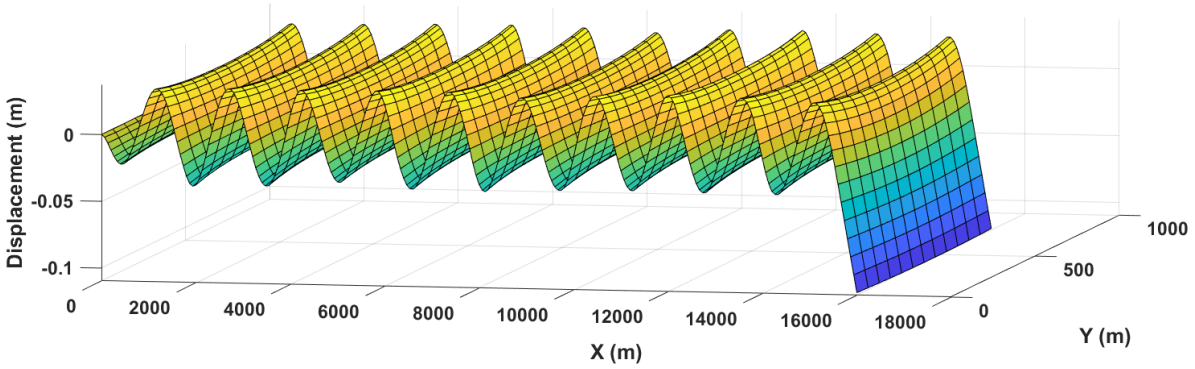

Fig. 4,a

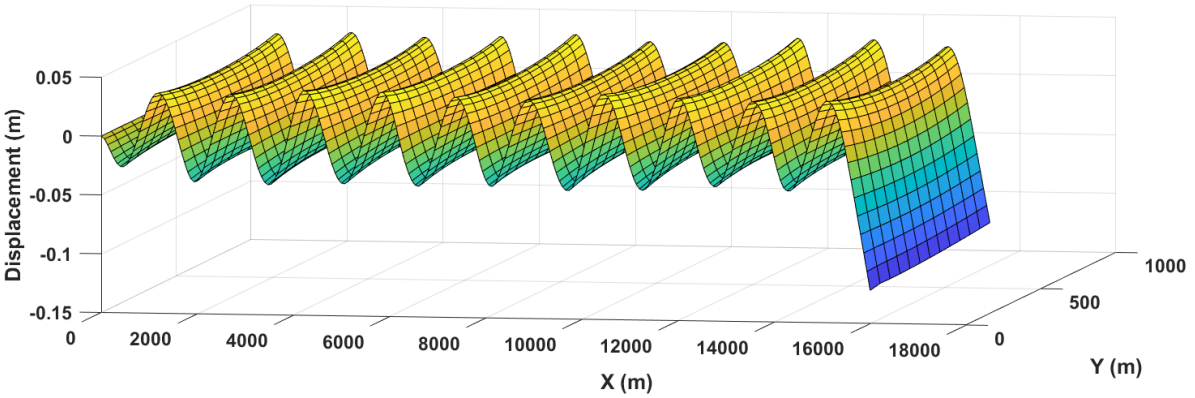

Fig. 4,b

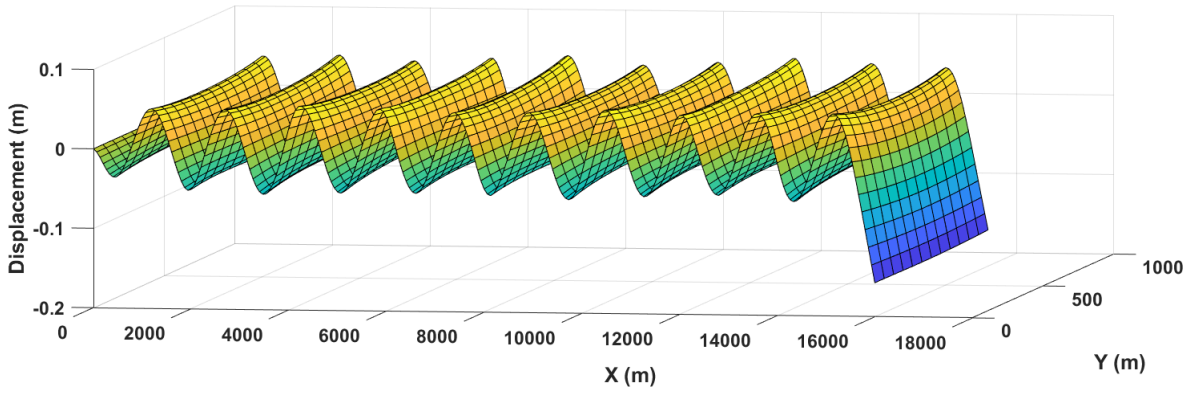

Fig. 4,c

Figure 4. Ice shelf vertical deflections result from the impact of the frontal incident wave. The periodicity of the forcing $\boldsymbol{T = 10s}$. The parameters of the model are **a)** $\boldsymbol{\alpha_1 = 0.6, \alpha_2 = 0.4}$; **b)** $\boldsymbol{\alpha_1 = 0.4, \alpha_2 = 0.6}$; **c)** $\boldsymbol{\alpha_1 = 0.0, \alpha_2 = 1.0}$.

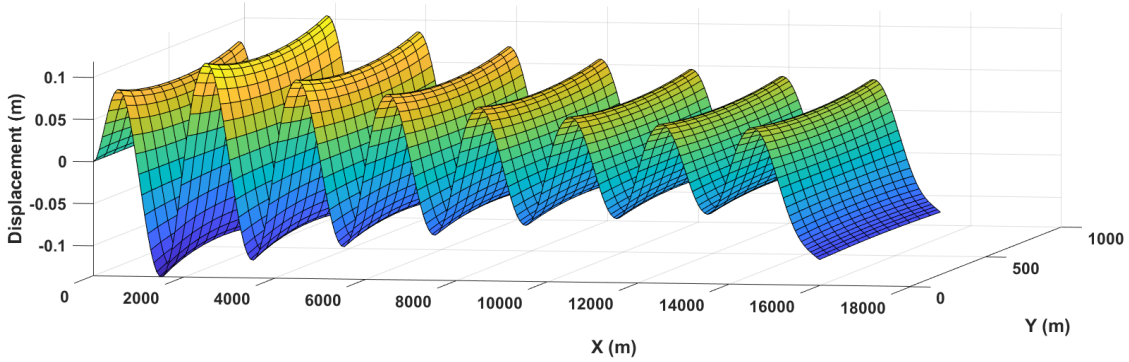

Fig. 5,a

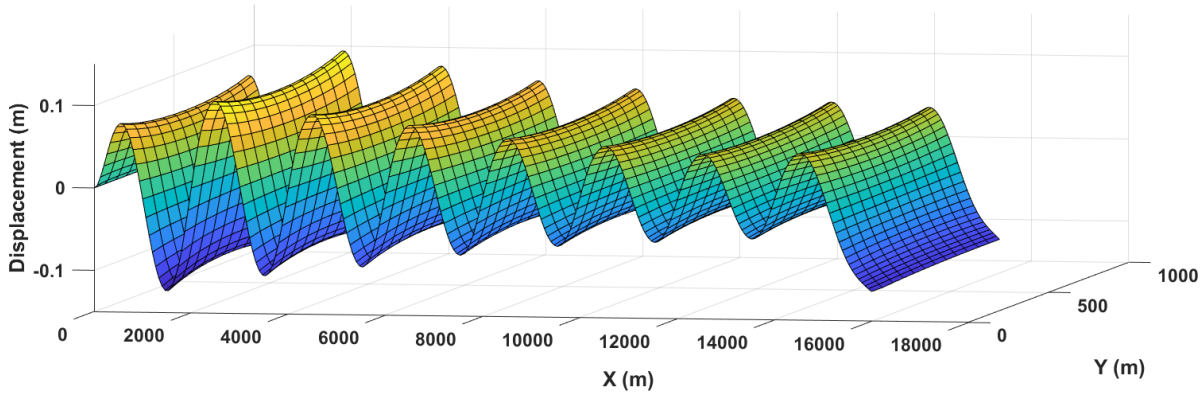

Fig. 5,b

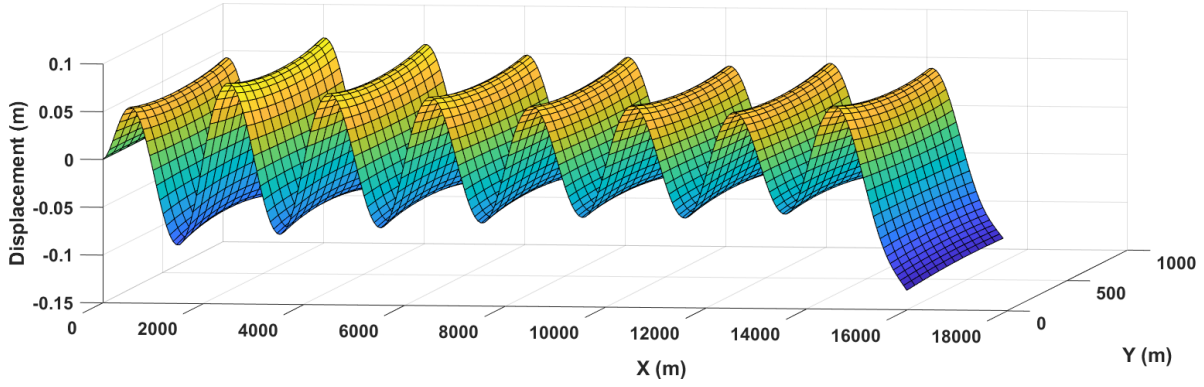

Fig. 5,c

Figure 5. Ice shelf vertical deflections result from the impact of the frontal incident wave. The periodicity of the forcing $\boldsymbol{T = 20s}$. The parameters of the model are **a)** $\boldsymbol{\alpha_1 = 0.6, \alpha_2 = 0.4}$; **b)** $\boldsymbol{\alpha_1 = 0.4, \alpha_2 = 0.6}$; **c)** $\boldsymbol{\alpha_1 = 0.0, \alpha_2 = 1.0}$.

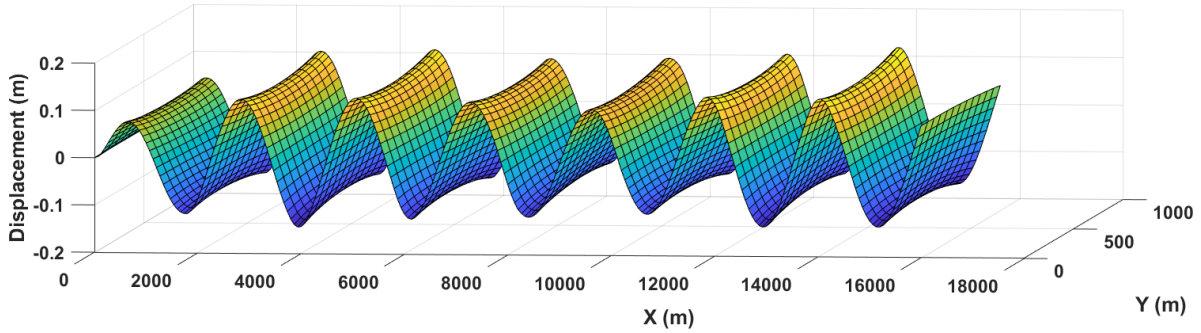

Fig. 6,a

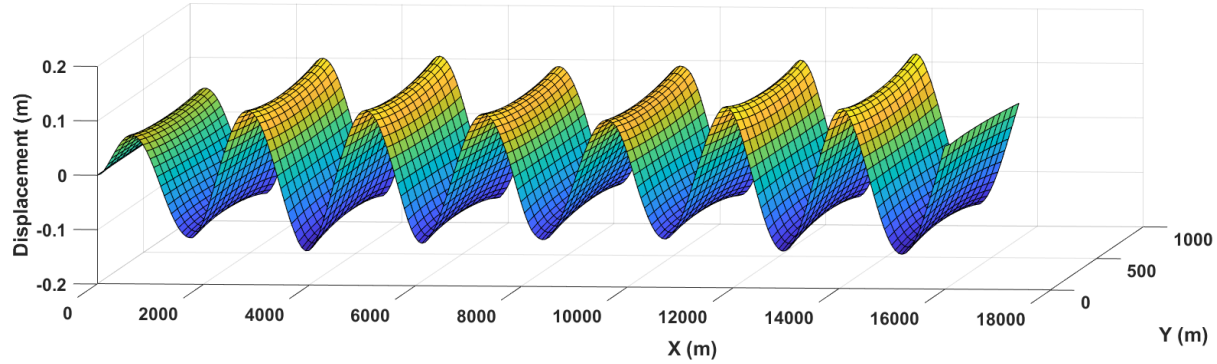

Fig. 6,b

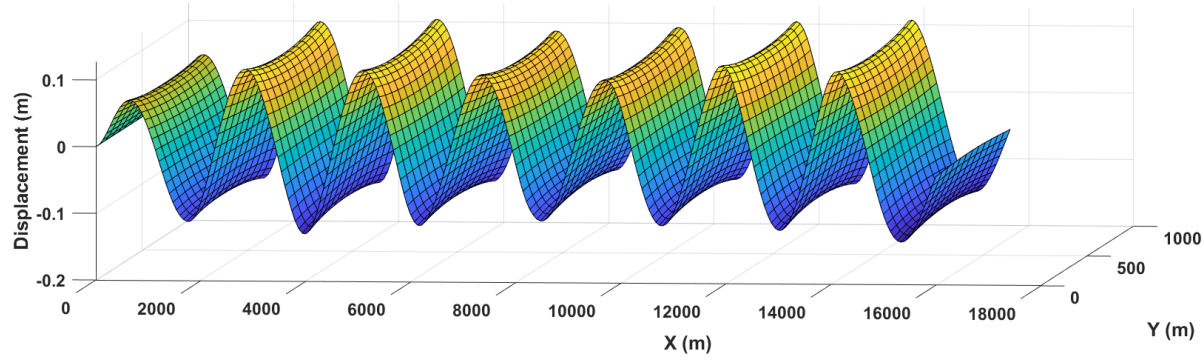

Fig. 6,c

Figure 6. Ice shelf vertical deflections result from the impact of the frontal incident wave. The periodicity of the forcing $\boldsymbol{T = 30s}$. The parameters of the model are **a)** $\boldsymbol{\alpha_1 = 0.6, \alpha_2 = 0.4}$; **b)** $\boldsymbol{\alpha_1 = 0.4, \alpha_2 = 0.6}$; **c)** $\boldsymbol{\alpha_1 = 0.0, \alpha_2 = 1.0}$.

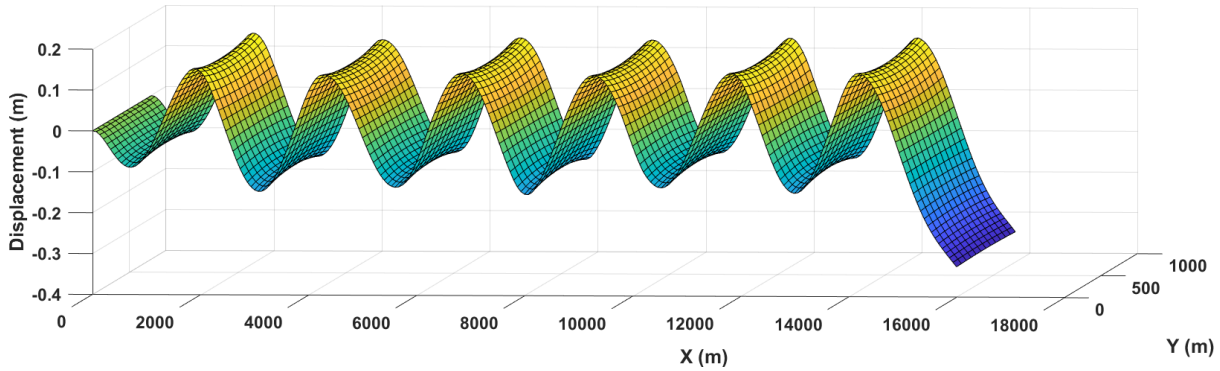

Fig. 7,a

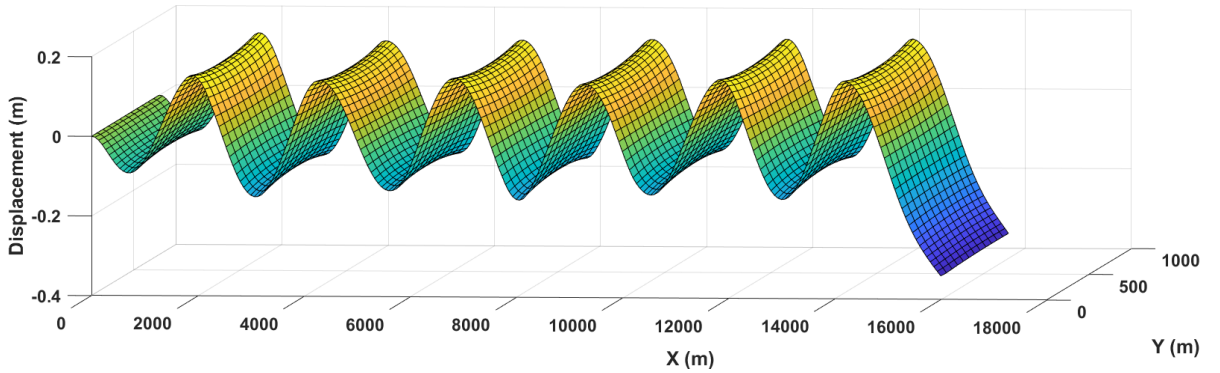

Fig. 7,b

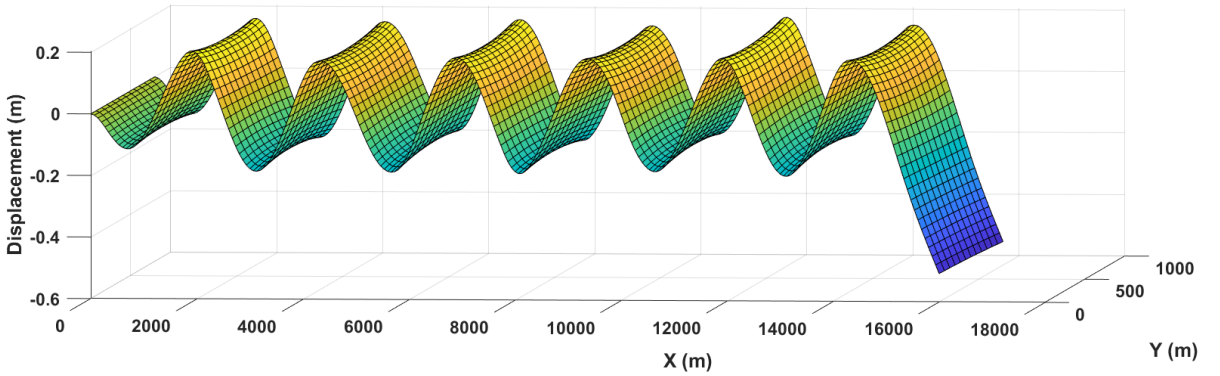

Fig. 7,c

Figure 7. Ice shelf vertical deflections result from the impact of the frontal incident wave. The periodicity of the forcing $\boldsymbol{T = 40s}$. The parameters of the model are **a)** $\boldsymbol{\alpha_1 = 0.6, \alpha_2 = 0.4}$; **b)** $\boldsymbol{\alpha_1 = 0.4, \alpha_2 = 0.6}$; **c)** $\boldsymbol{\alpha_1 = 0.0, \alpha_2 = 1.0}$.

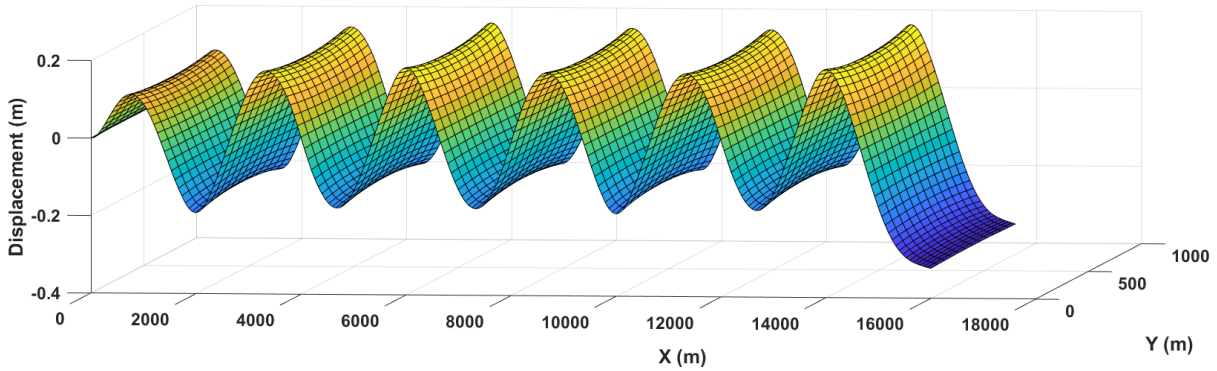

Fig. 8,a

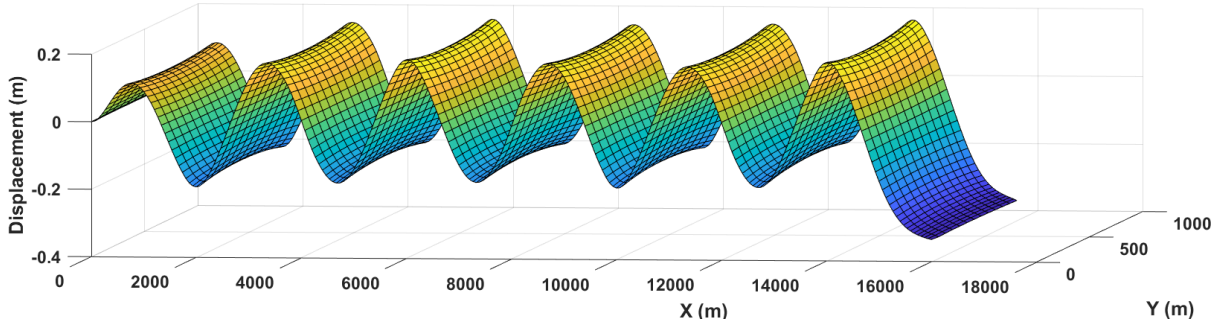

Fig. 8,b

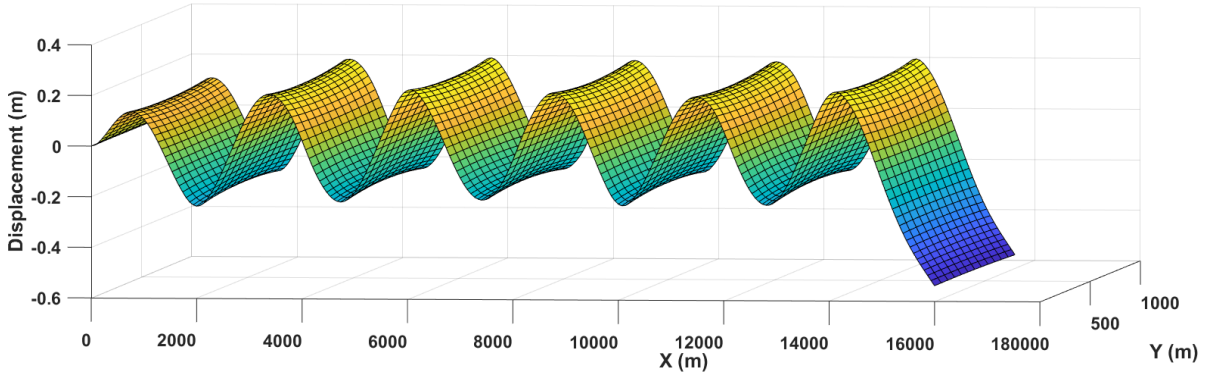

Fig. 8,c

Figure 8. Ice shelf vertical deflections result from the impact of the frontal incident wave. The periodicity of the forcing $\boldsymbol{T = 50s}$. The parameters of the model are **a)** $\boldsymbol{\alpha_1 = 0.6, \alpha_2 = 0.4}$; **b)** $\boldsymbol{\alpha_1 = 0.4, \alpha_2 = 0.6}$; **c)** $\boldsymbol{\alpha_1 = 0.0, \alpha_2 = 1.0}$.

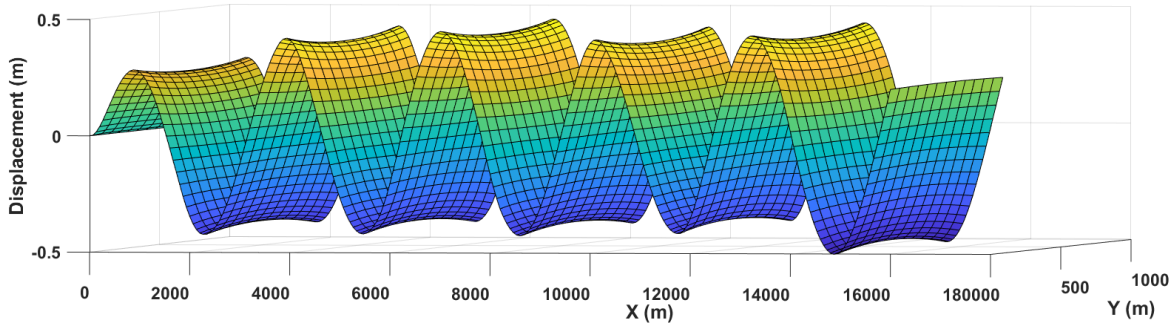

Fig. 9,a

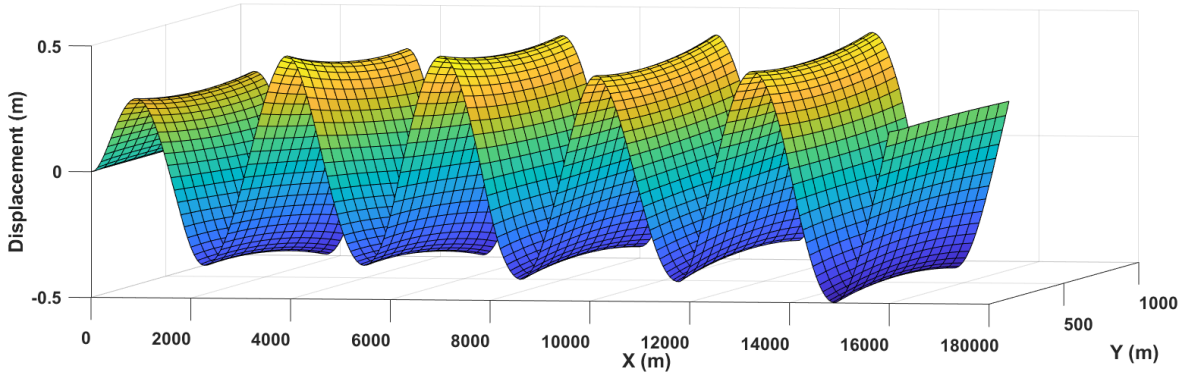

Fig. 9,b

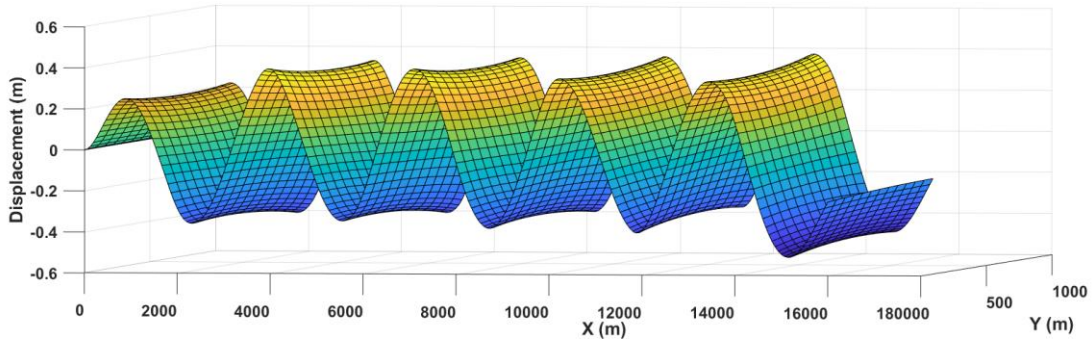

Fig. 9,c

Figure 9. Ice shelf vertical deflections result from the impact of the frontal incident wave. The periodicity of the forcing $\boldsymbol{T = 80s}$. The parameters of the model are **a)** $\boldsymbol{\alpha_1 = 0.6, \alpha_2 = 0.4}$; **b)** $\boldsymbol{\alpha_1 = 0.4, \alpha_2 = 0.6}$; **c)** $\boldsymbol{\alpha_1 = 0.0, \alpha_2 = 1.0}$.

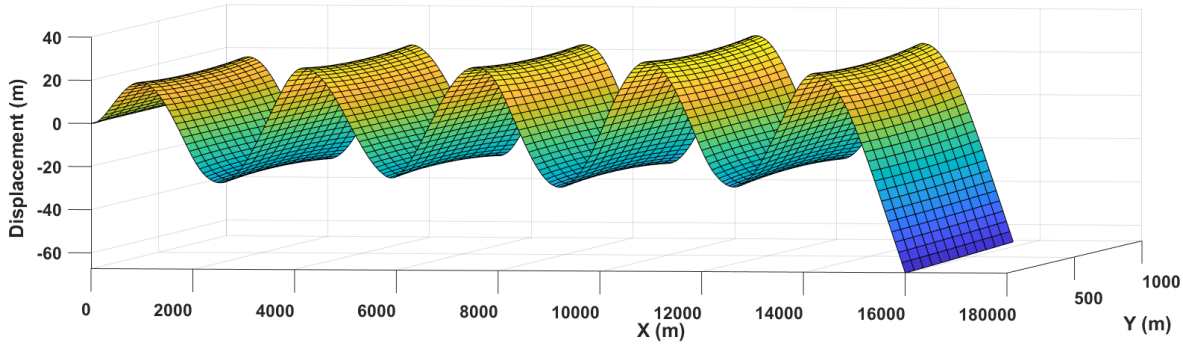

Fig. 10,a

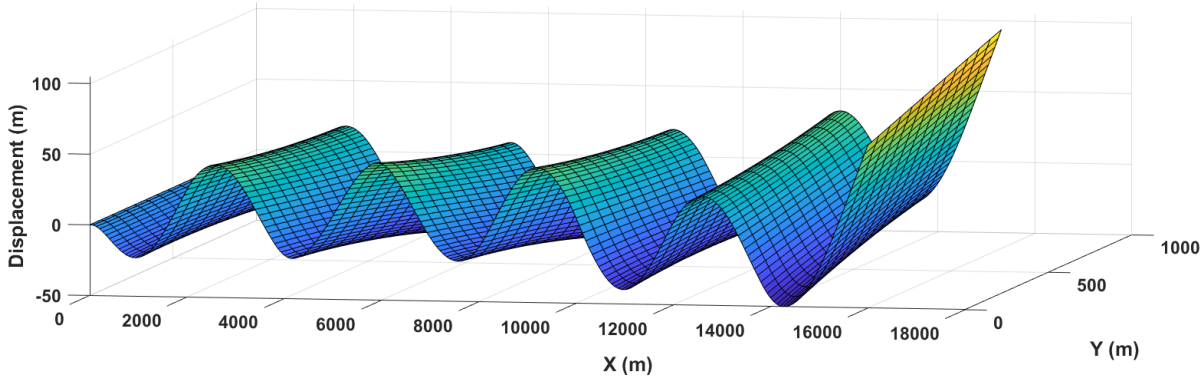

Fig. 10,b

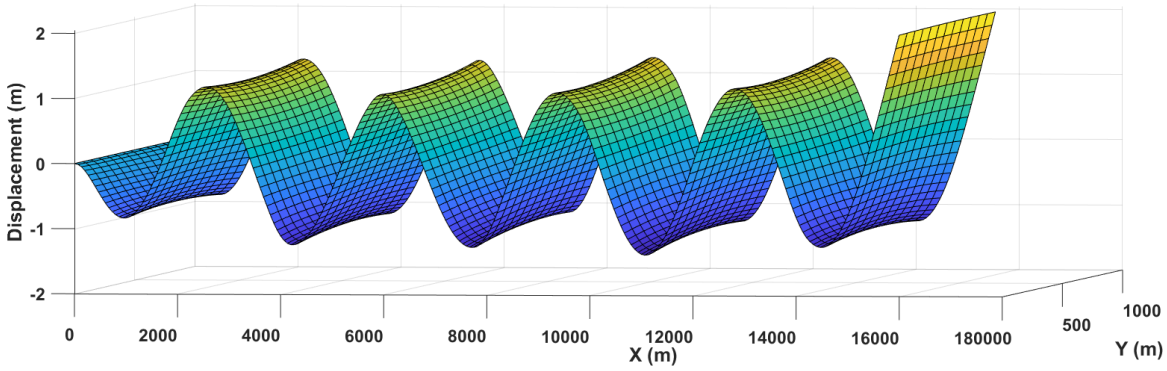

Fig. 10,c

Figure 10. Ice shelf vertical deflections result from the impact of the frontal incident wave. The periodicity of the forcing $\boldsymbol{T = 100s}$. The parameters of the model are **a)** $\boldsymbol{\alpha_1 = 0.6, \alpha_2 = 0.4}$; **b)** $\boldsymbol{\alpha_1 = 0.4, \alpha_2 = 0.6}$; **c)** $\boldsymbol{\alpha_1 = 0.0, \alpha_2 = 1.0}$.

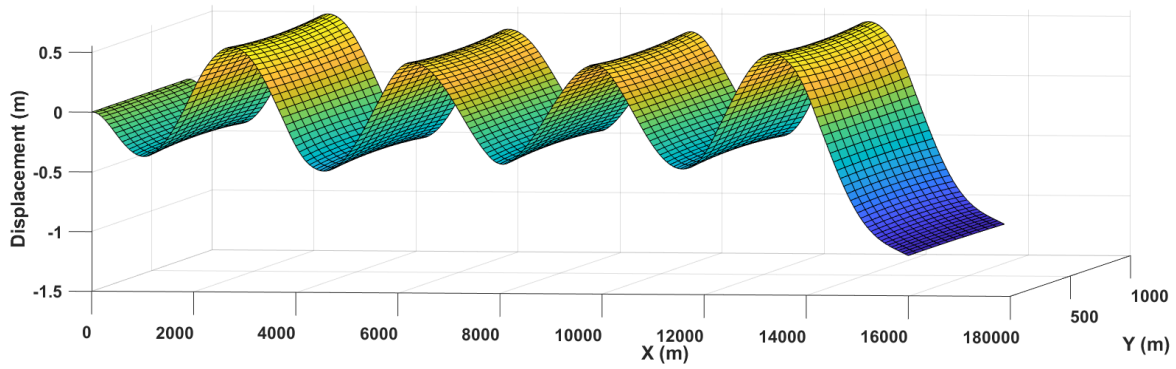

Fig. 11,a

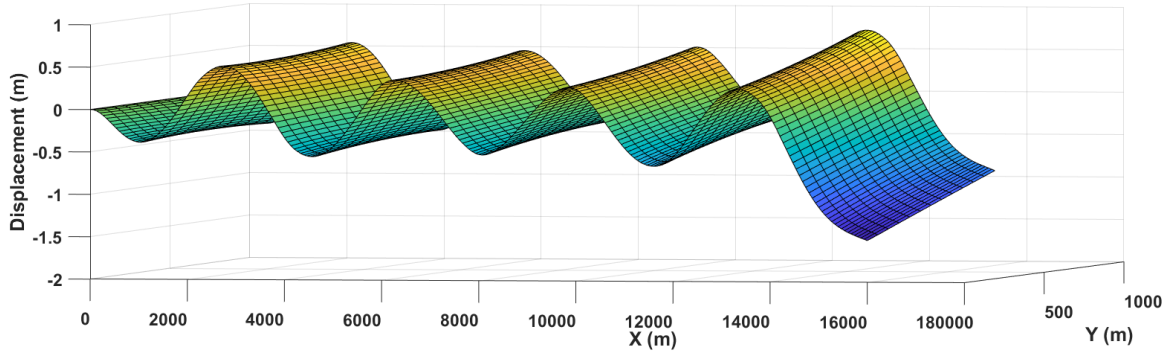

Fig. 11,b

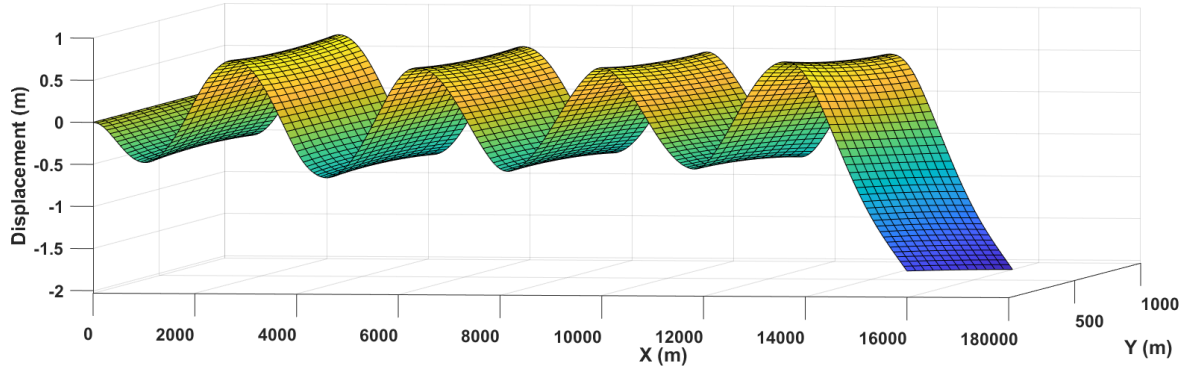

Fig. 11,c

Figure 11. Ice shelf vertical deflections result from the impact of the frontal incident wave. The periodicity of the forcing $\boldsymbol{T = 120s}$. The parameters of the model are **a)** $\boldsymbol{\alpha_1 = 0.6, \alpha_2 = 0.4}$; **b)** $\boldsymbol{\alpha_1 = 0.4, \alpha_2 = 0.6}$; **c)** $\boldsymbol{\alpha_1 = 0.0, \alpha_2 = 1.0}$.

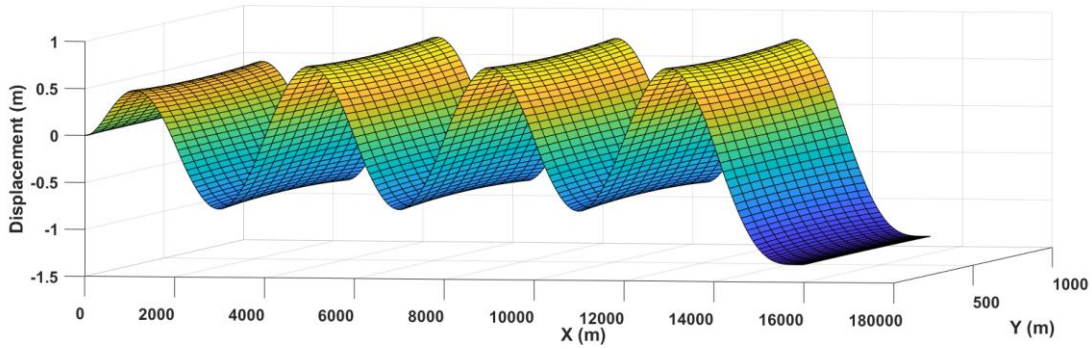

Fig. 12,a

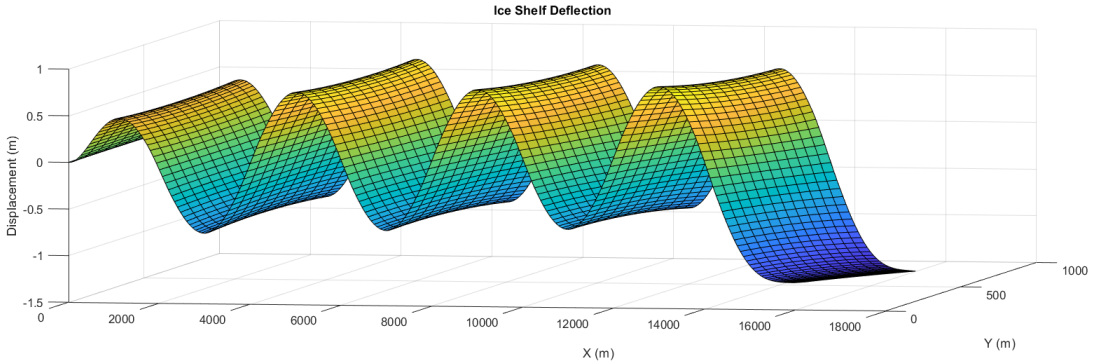

Fig. 12,b

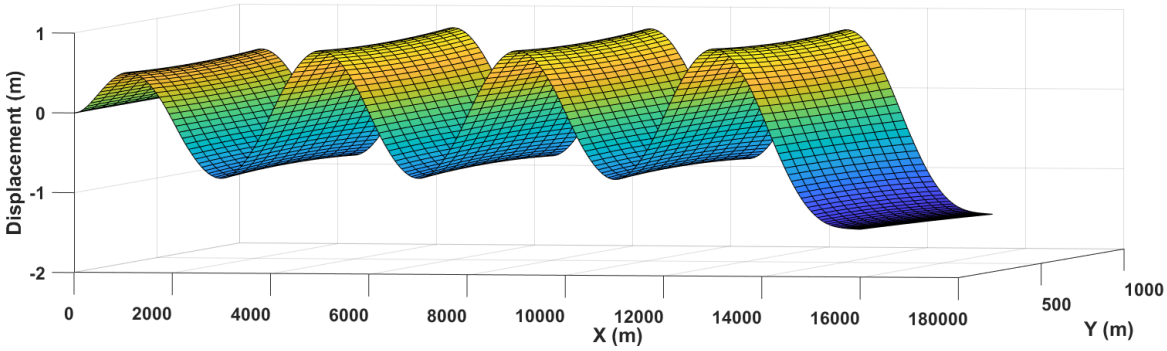

Fig. 12,c

Figure 12. Ice shelf vertical deflections result from the impact of the frontal incident wave. The periodicity of the forcing $\boldsymbol{T = 150s}$. The parameters of the model are **a)** $\boldsymbol{\alpha_1 = 0.6, \alpha_2 = 0.4}$; **b)** $\boldsymbol{\alpha_1 = 0.4, \alpha_2 = 0.6}$; **c)** $\boldsymbol{\alpha_1 = 0.0, \alpha_2 = 1.0}$.

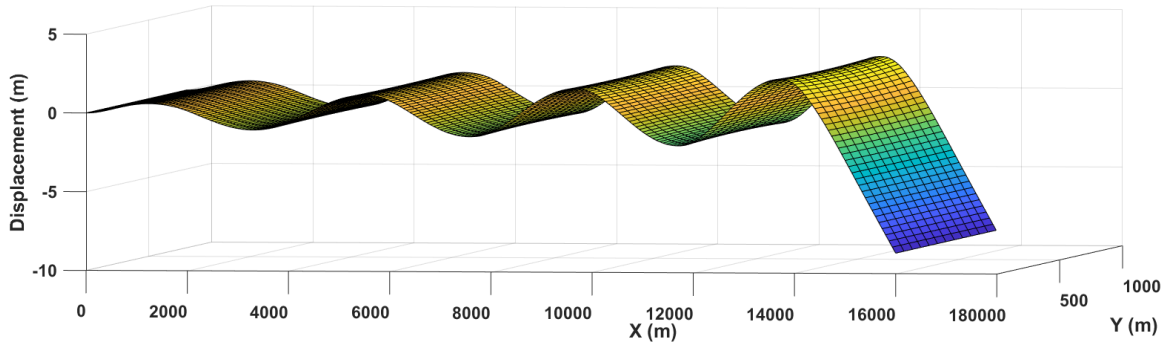

Fig. 13,a

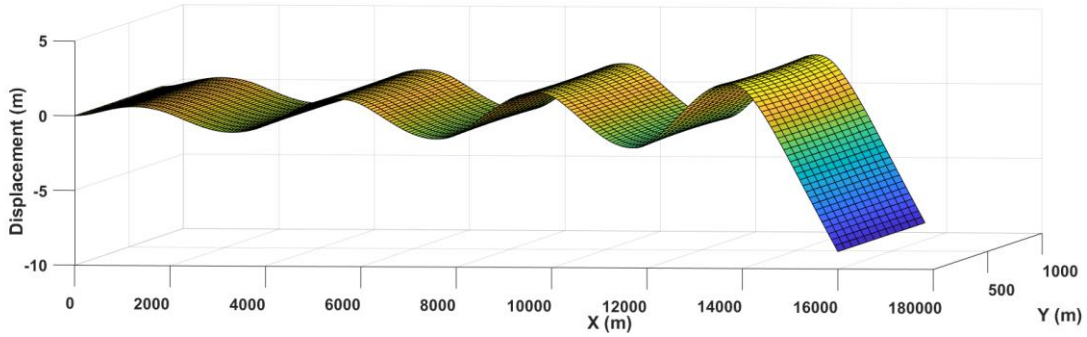

Fig. 13,b

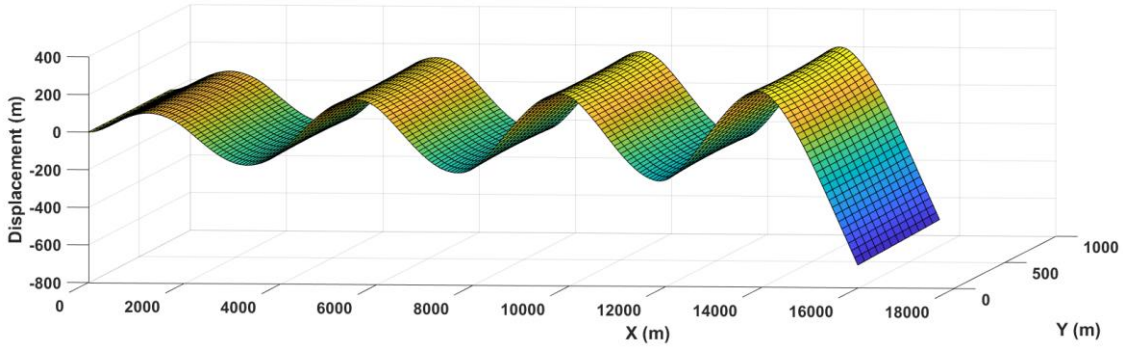

Fig. 13,c

Figure 13. Ice shelf vertical deflections result from the impact of the frontal incident wave. The periodicity of the forcing $\boldsymbol{T = 200s}$. The parameters of the model are **a)** $\boldsymbol{\alpha_1 = 0.6, \alpha_2 = 0.4}$; **b)** $\boldsymbol{\alpha_1 = 0.4, \alpha_2 = 0.6}$; **c)** $\boldsymbol{\alpha_1 = 0.0, \alpha_2 = 1.0}$.

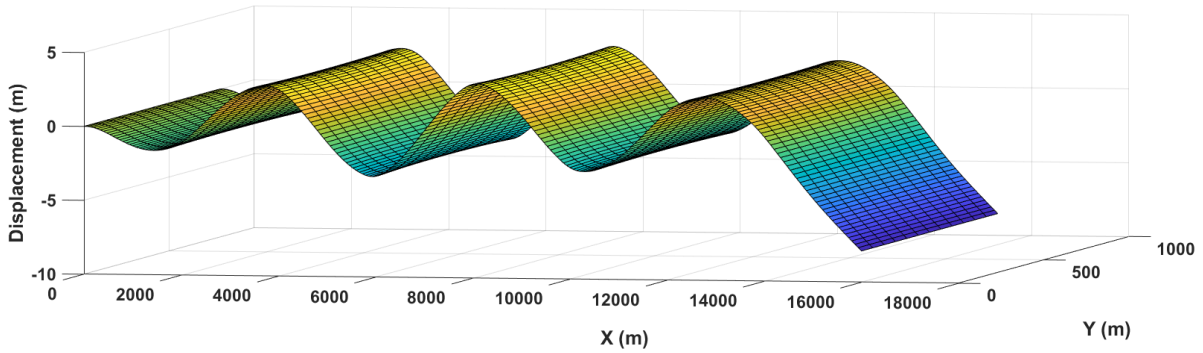

Fig. 14,a

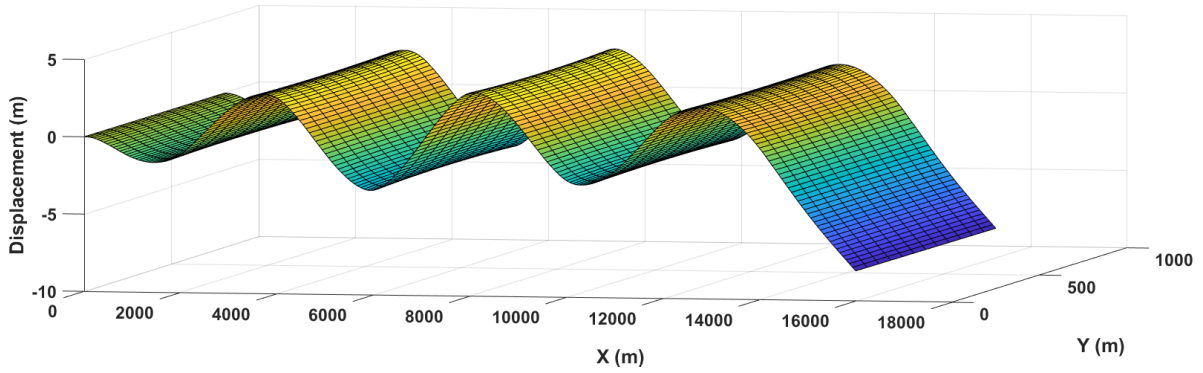

Fig. 14,b

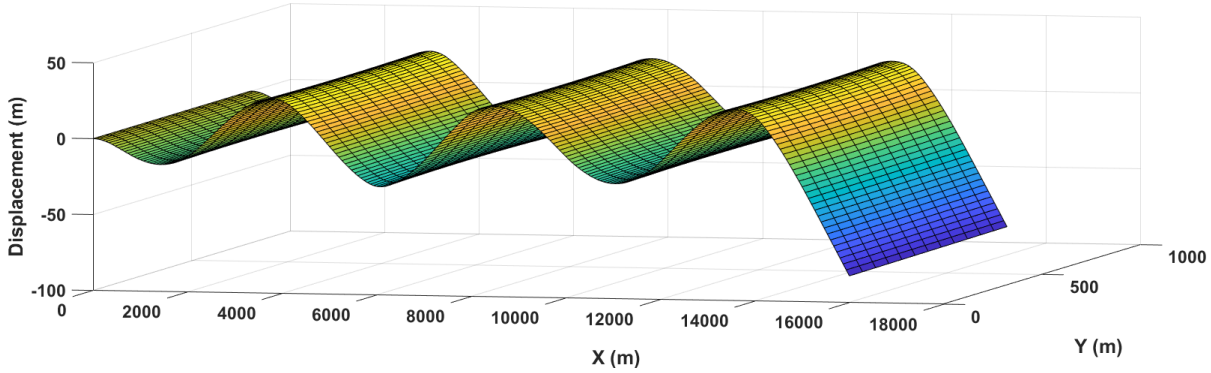

Fig. 14,c

Figure 14. Ice shelf vertical deflections result from the impact of the frontal incident wave. The periodicity of the forcing $\boldsymbol{T = 300s}$. The parameters of the model are **a)** $\boldsymbol{\alpha_1 = 0.6, \alpha_2 = 0.4}$; **b)** $\boldsymbol{\alpha_1 = 0.4, \alpha_2 = 0.6}$; **c)** $\boldsymbol{\alpha_1 = 0.0, \alpha_2 = 1.0}$.

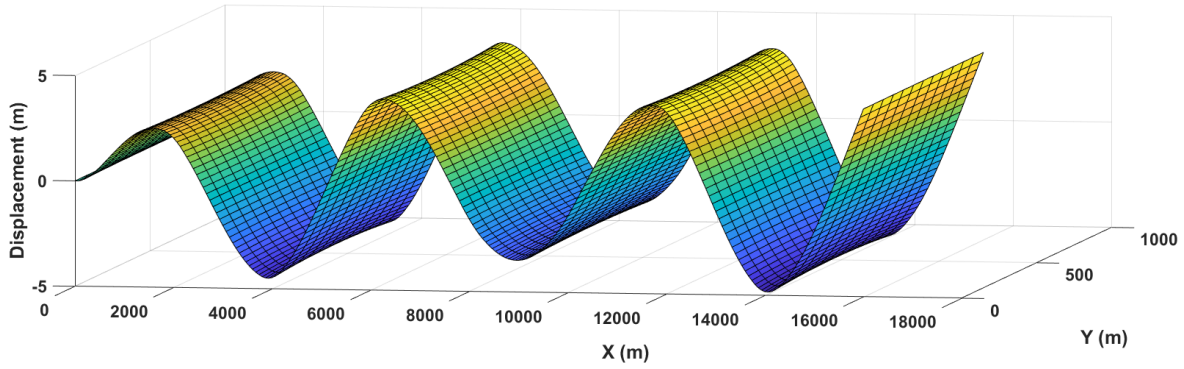

Fig. 15,a

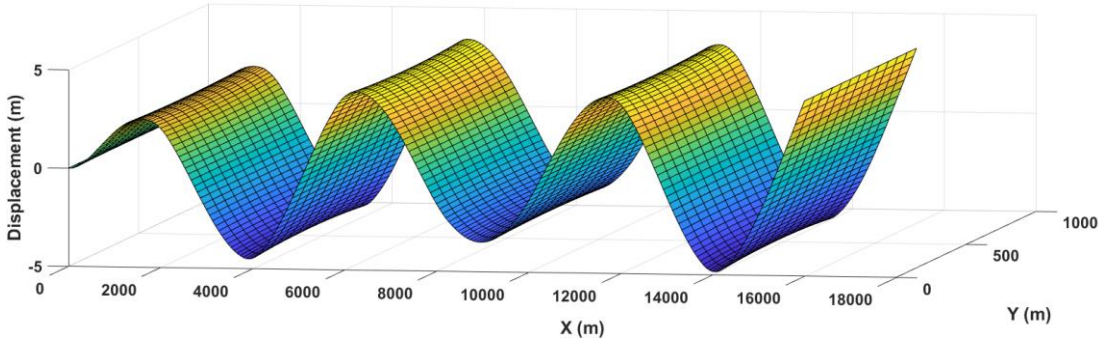

Fig. 15,b

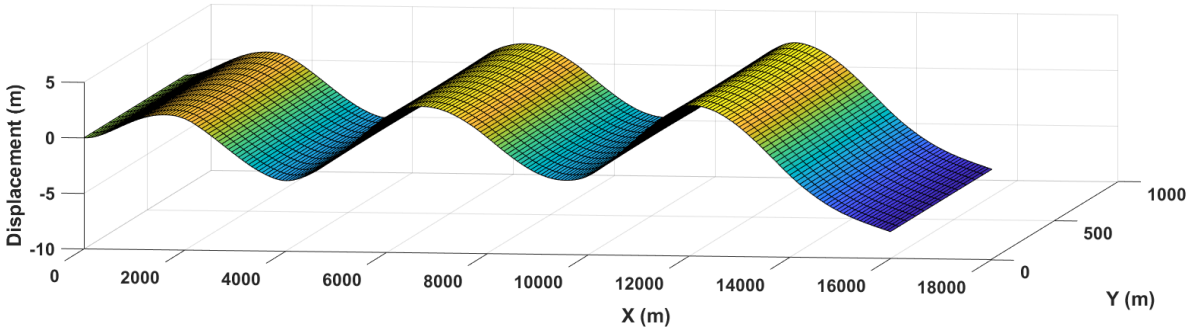

Fig. 15,c

Figure 15. Ice shelf vertical deflections result from the impact of the frontal incident wave. The periodicity of the forcing $\boldsymbol{T = 400s}$. The parameters of the model are **a)** $\boldsymbol{\alpha_1 = 0.6, \alpha_2 = 0.4}$; **b)** $\boldsymbol{\alpha_1 = 0.4, \alpha_2 = 0.6}$; **c)** $\boldsymbol{\alpha_1 = 0.0, \alpha_2 = 1.0}$.

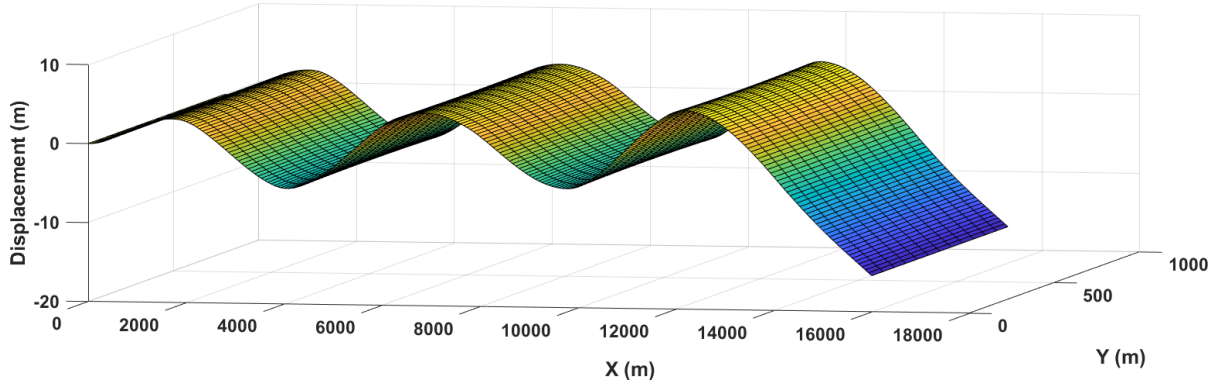

Fig. 16,a

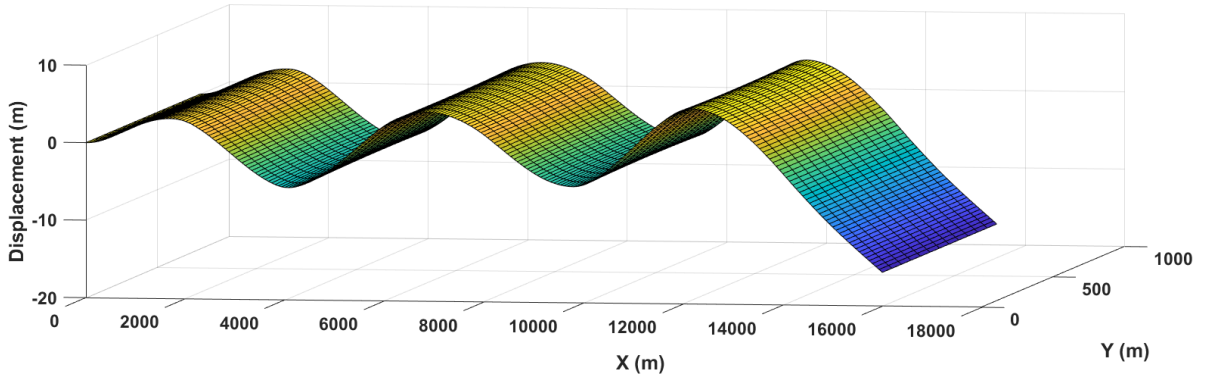

Fig. 16,b

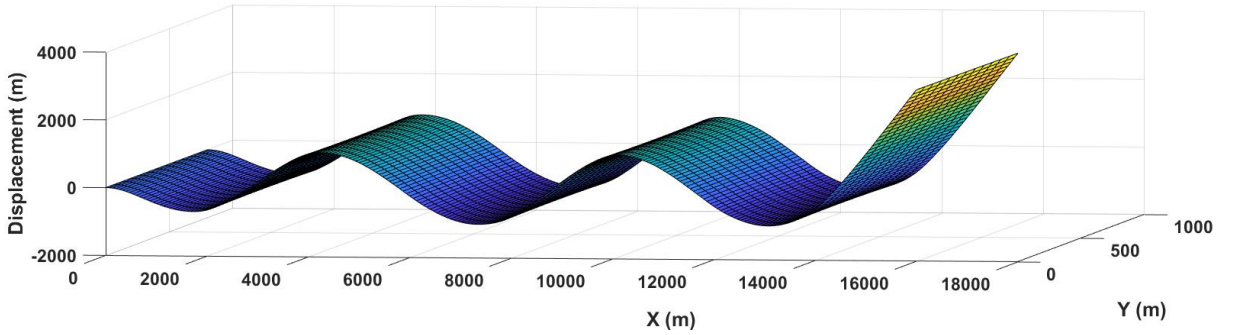

Fig. 16,c

Figure 16. Ice shelf vertical deflections result from the impact of the frontal incident wave. The periodicity of the forcing $\boldsymbol{T = 500s}$. The parameters of the model are **a)** $\boldsymbol{\alpha_1 = 0.6, \alpha_2 = 0.4}$; **b)** $\boldsymbol{\alpha_1 = 0.4, \alpha_2 = 0.6}$; **c)** $\boldsymbol{\alpha_1 = 0.0, \alpha_2 = 1.0}$.

2.2 Vertical deflections of the ice shelf were obtained with spatial periodicity of the crevasses $T_{cr} = 2.0\ km$ and with crevasse depth $D_{cr} = 40m$.

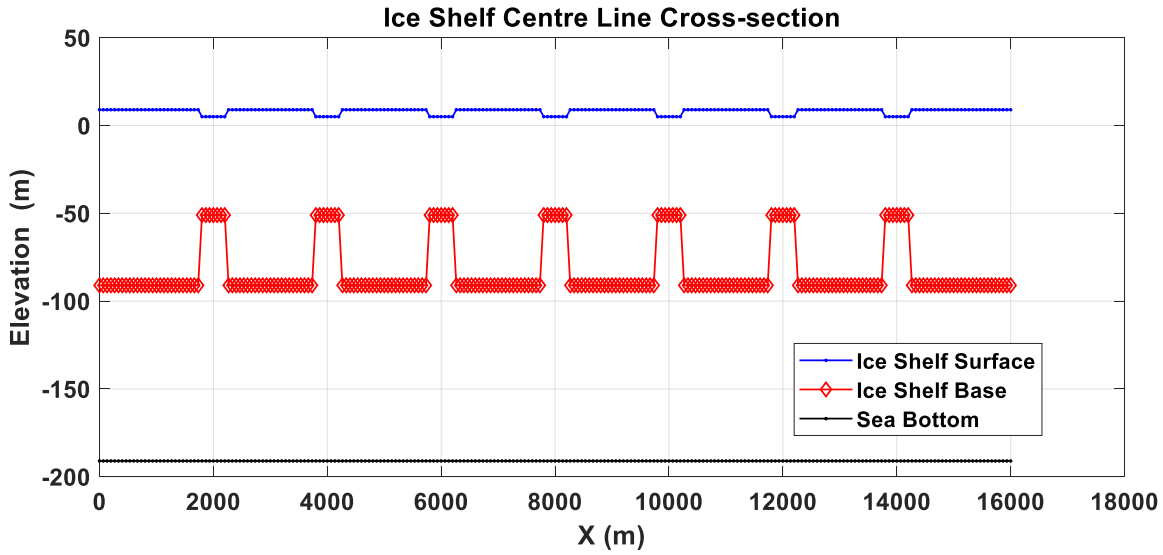

Figure 17. Ice shelf geometry. $T_{cr} = 2.0km$; $D_{cr} = 40m$.

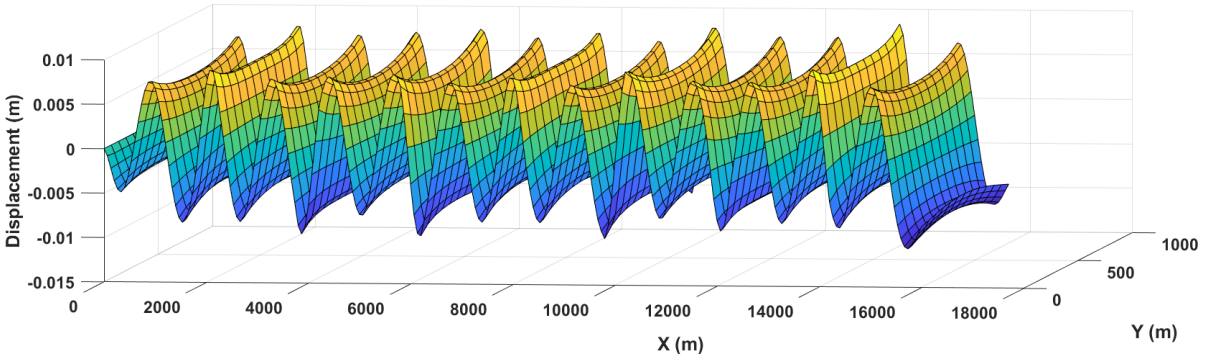

Fig. 18,a

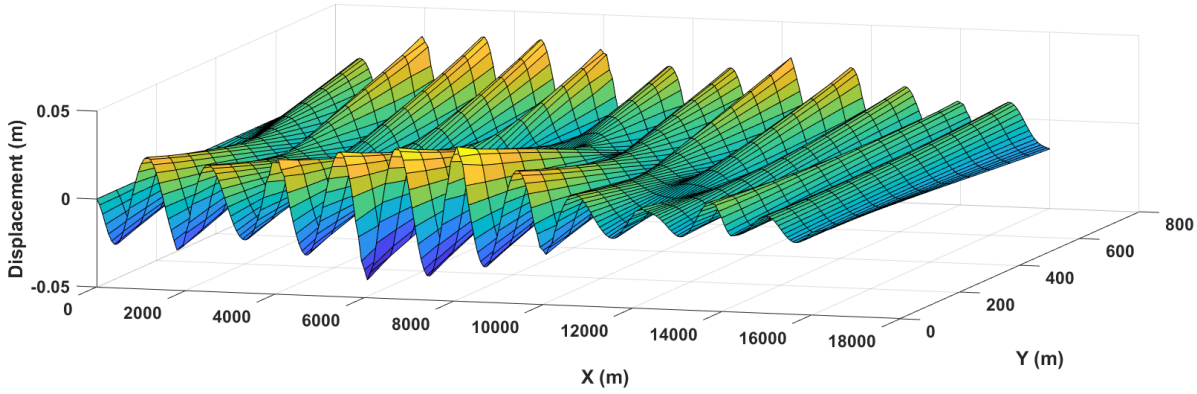

Fig. 18,b

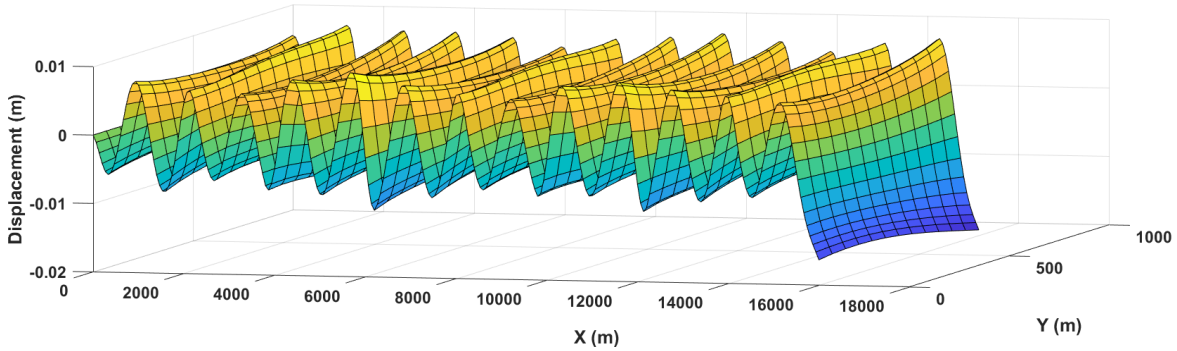

Fig. 18,c

Figure 18. Ice shelf vertical deflections result from the impact of the frontal incident wave. The periodicity of the forcing $\boldsymbol{T = 5s}$. The parameters of the model are **a)** $\boldsymbol{\alpha_1 = 0.6, \alpha_2 = 0.4}$; **b)** $\boldsymbol{\alpha_1 = 0.4, \alpha_2 = 0.6}$; **c)** $\boldsymbol{\alpha_1 = 0.0, \alpha_2 = 1.0}$.

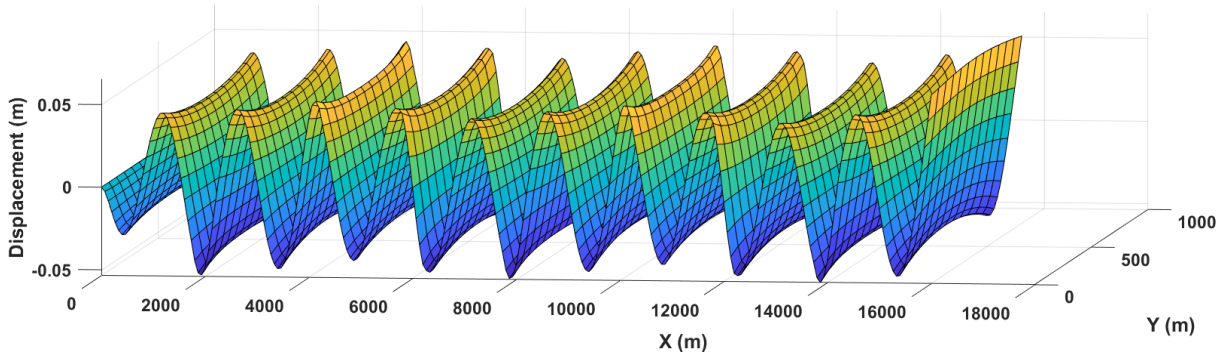

Fig. 19,a

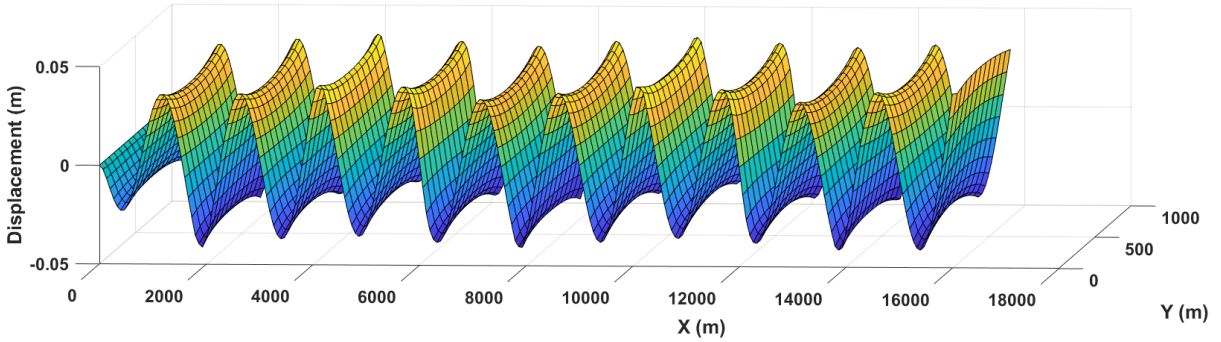

Fig. 19,b

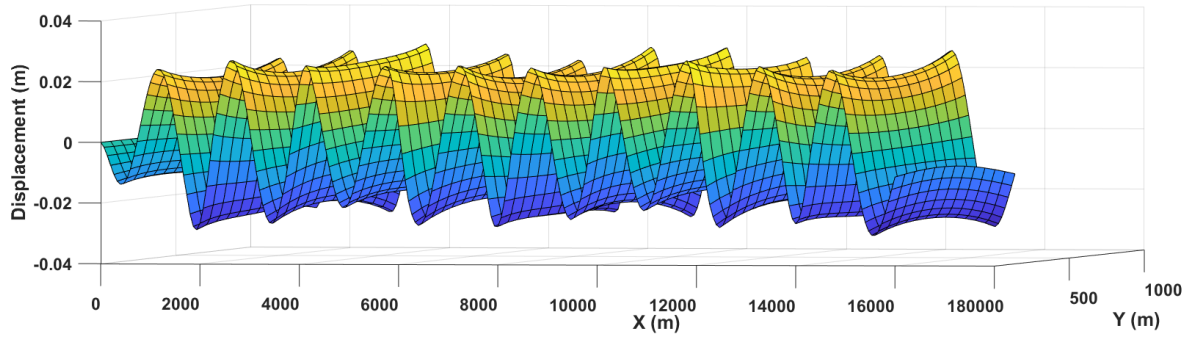

Fig. 19,c

Figure 19. Ice shelf vertical deflections result from the impact of the frontal incident wave. The periodicity of the forcing $\boldsymbol{T = 10s}$. The parameters of the model are **a)** $\boldsymbol{\alpha_1 = 0.6, \alpha_2 = 0.4}$; **b)** $\boldsymbol{\alpha_1 = 0.4, \alpha_2 = 0.6}$; **c)** $\boldsymbol{\alpha_1 = 0.0, \alpha_2 = 1.0}$.

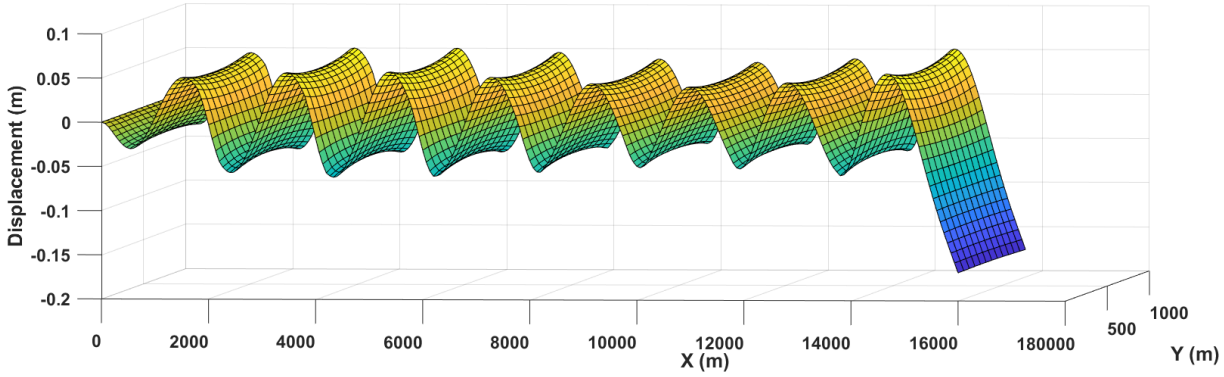

Fig. 20,a

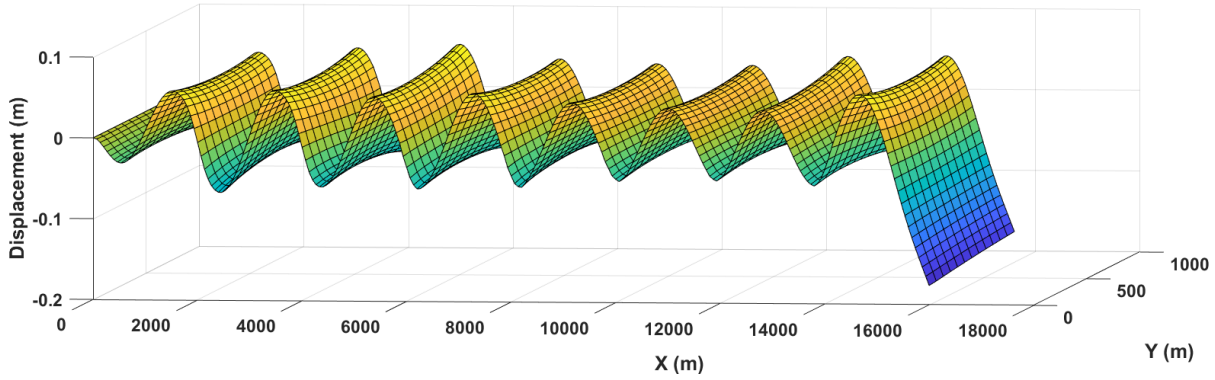

Fig. 20,b

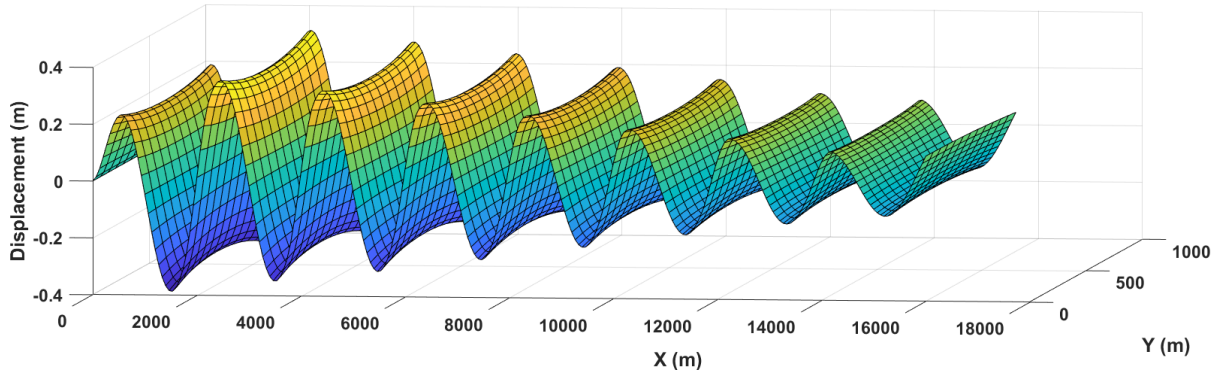

Fig. 20,c

Figure 20. Ice shelf vertical deflections result from the impact of the frontal incident wave. The periodicity of the forcing $\boldsymbol{T = 20s}$. The parameters of the model are **a)** $\boldsymbol{\alpha_1 = 0.6, \alpha_2 = 0.4}$; **b)** $\boldsymbol{\alpha_1 = 0.4, \alpha_2 = 0.6}$; **c)** $\boldsymbol{\alpha_1 = 0.0, \alpha_2 = 1.0}$.

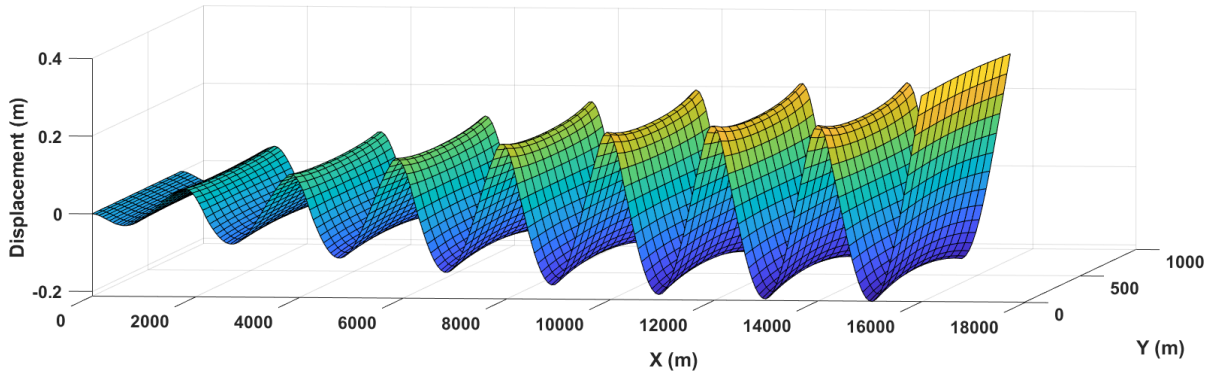

Fig. 21,a

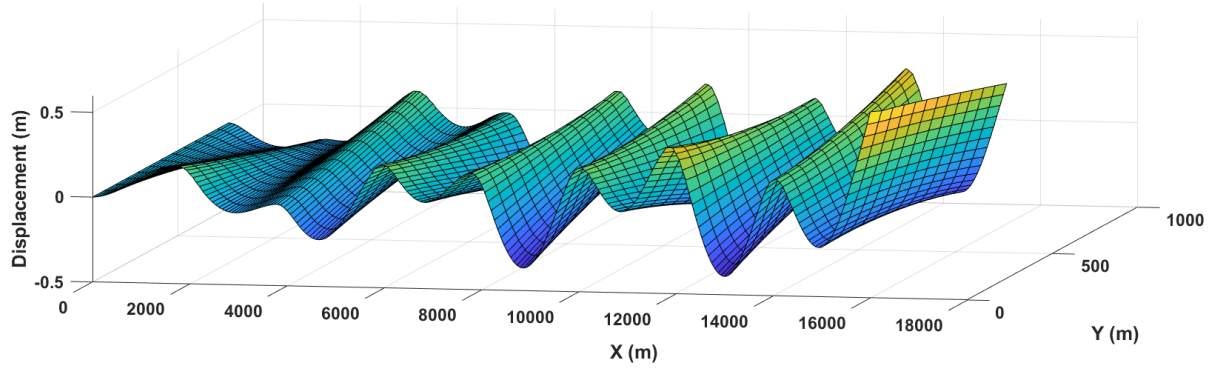

Fig. 21,b

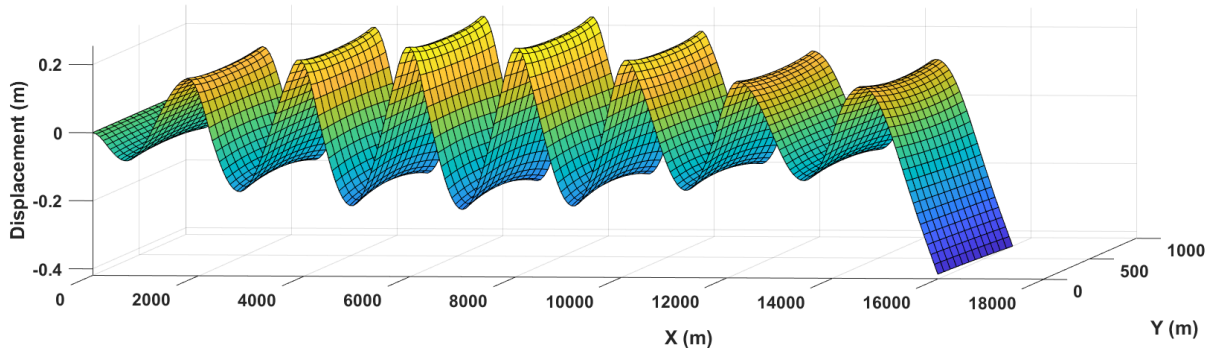

Fig. 21,c

Figure 21. Ice shelf vertical deflections result from the impact of the frontal incident wave. The periodicity of the forcing $\boldsymbol{T = 30s}$. The parameters of the model are **a)** $\boldsymbol{\alpha_1 = 0.6, \alpha_2 = 0.4}$; **b)** $\boldsymbol{\alpha_1 = 0.4, \alpha_2 = 0.6}$; **c)** $\boldsymbol{\alpha_1 = 0.0, \alpha_2 = 1.0}$.

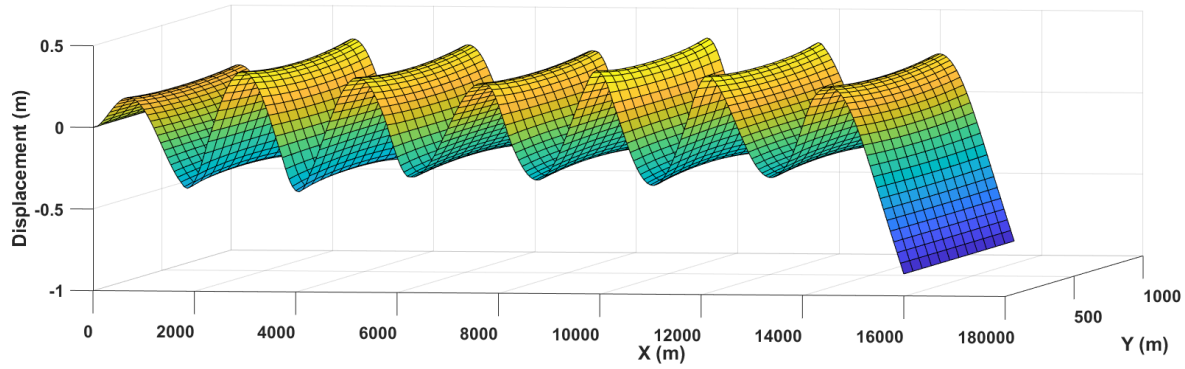

Fig. 22,a

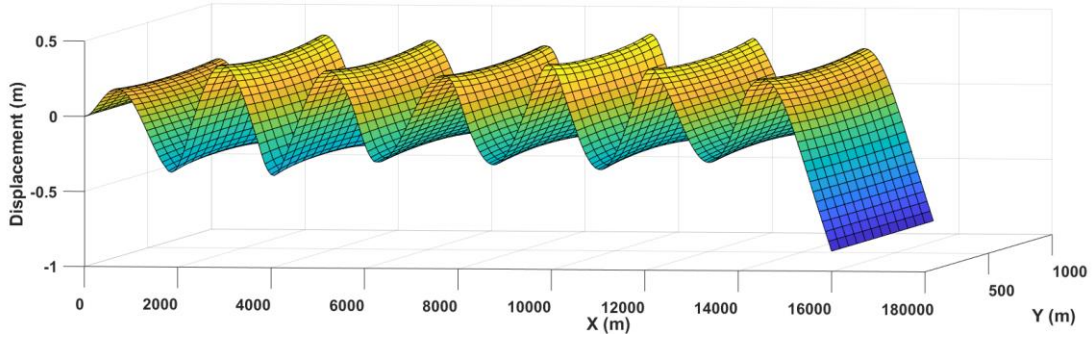

Fig. 22,b

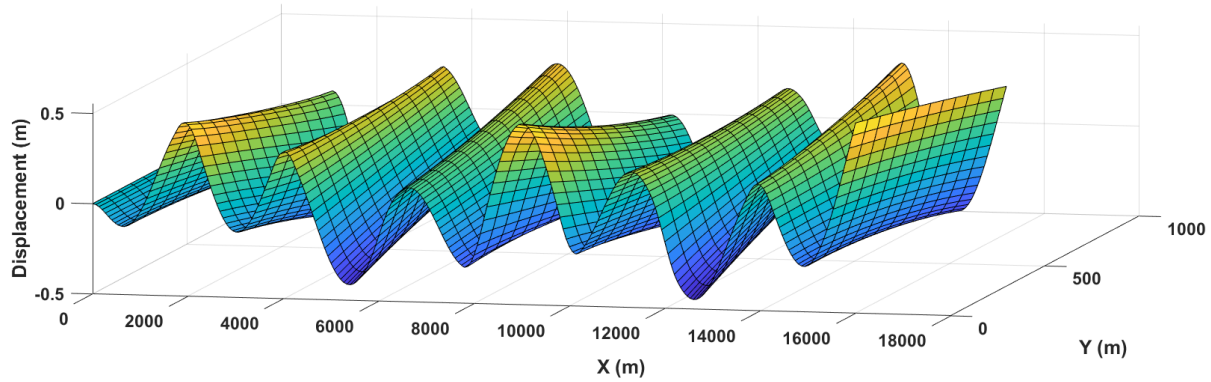

Fig. 22,c

Figure 22. Ice shelf vertical deflections result from the impact of the frontal incident wave. The periodicity of the forcing $\boldsymbol{T = 40s}$. The parameters of the model are **a)** $\boldsymbol{\alpha_1 = 0.6, \alpha_2 = 0.4}$; **b)** $\boldsymbol{\alpha_1 = 0.4, \alpha_2 = 0.6}$; **c)** $\boldsymbol{\alpha_1 = 0.0, \alpha_2 = 1.0}$.

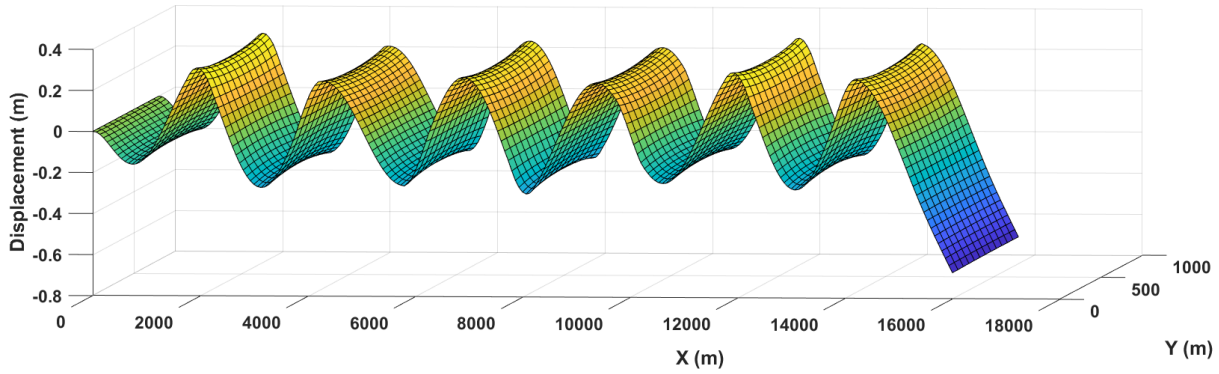

Fig. 23,a

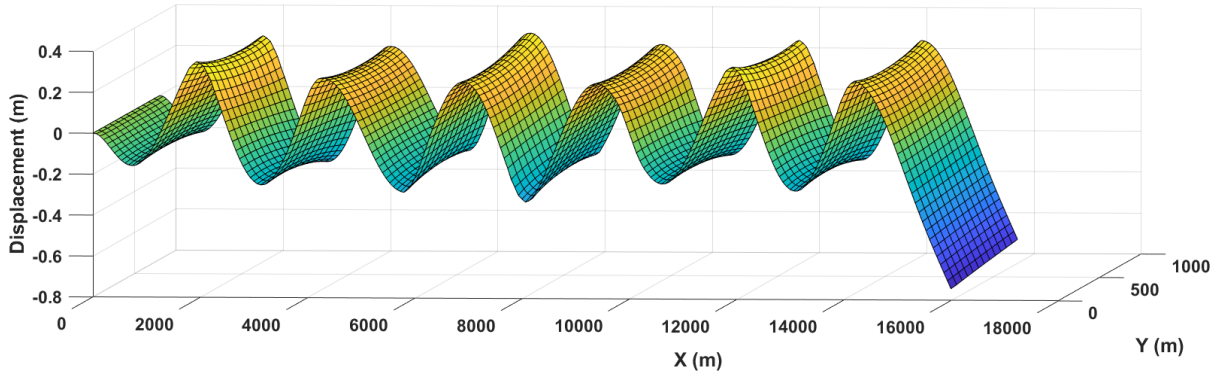

Fig. 23,b

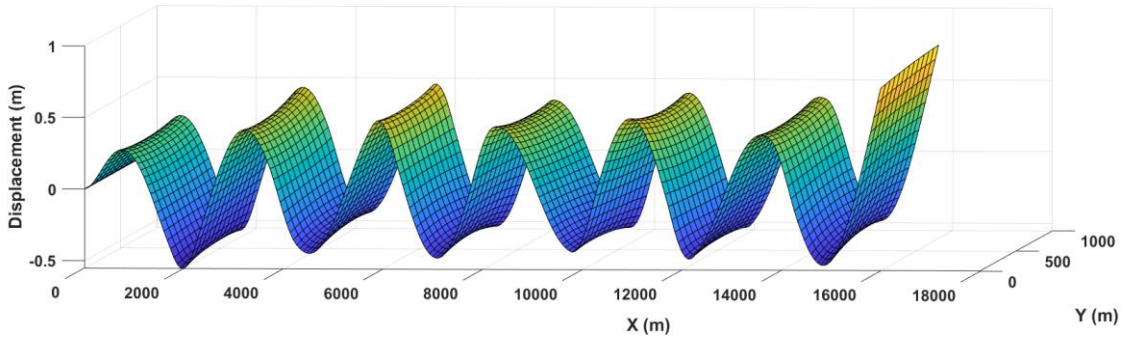

Fig. 23,c

Figure 23. Ice shelf vertical deflections result from the impact of the frontal incident wave. The periodicity of the forcing $\boldsymbol{T = 50s}$. The parameters of the model are **a)** $\boldsymbol{\alpha_1 = 0.6, \alpha_2 = 0.4}$; **b)** $\boldsymbol{\alpha_1 = 0.4, \alpha_2 = 0.6}$; **c)** $\boldsymbol{\alpha_1 = 0.0, \alpha_2 = 1.0}$.

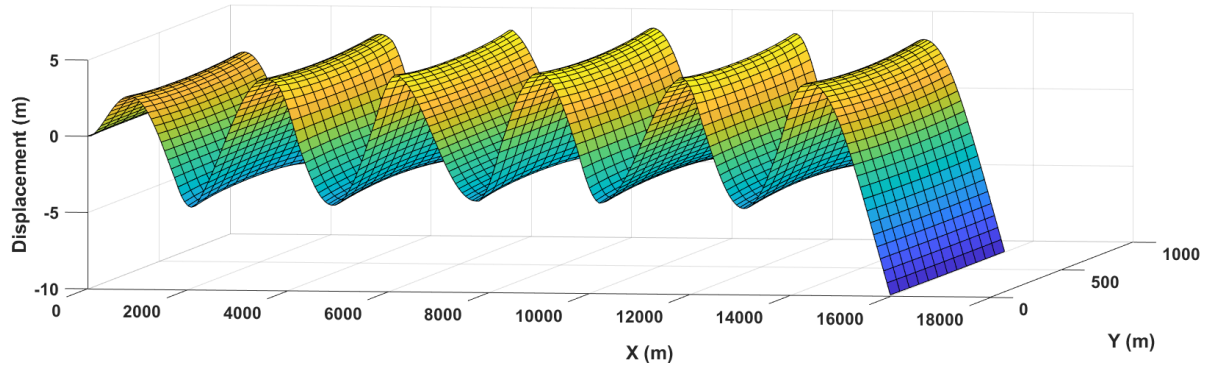

Fig. 24,a

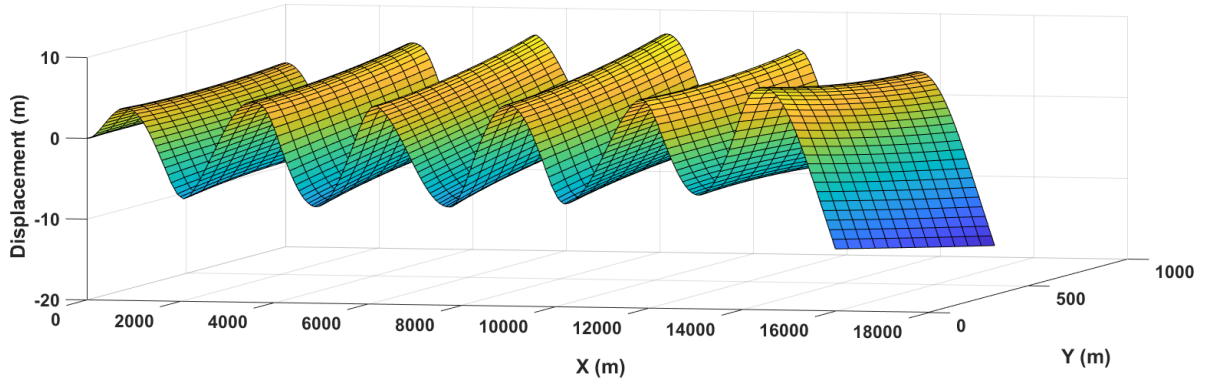

Fig. 24,b

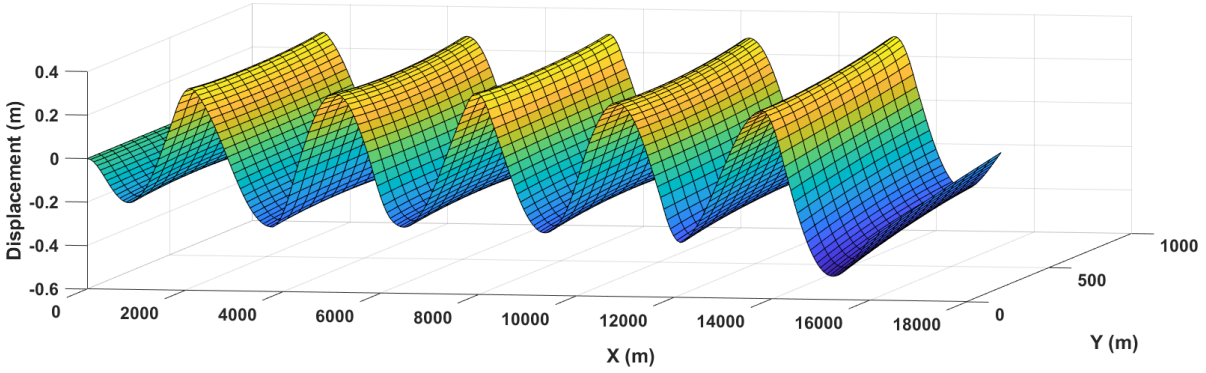

Fig. 24,c

Figure 24. Ice shelf vertical deflections result from the impact of the frontal incident wave. The periodicity of the forcing $\boldsymbol{T = 70s}$. The parameters of the model are **a)** $\boldsymbol{\alpha_1 = 0.6, \alpha_2 = 0.4}$; **b)** $\boldsymbol{\alpha_1 = 0.4, \alpha_2 = 0.6}$; **c)** $\boldsymbol{\alpha_1 = 0.0, \alpha_2 = 1.0}$.

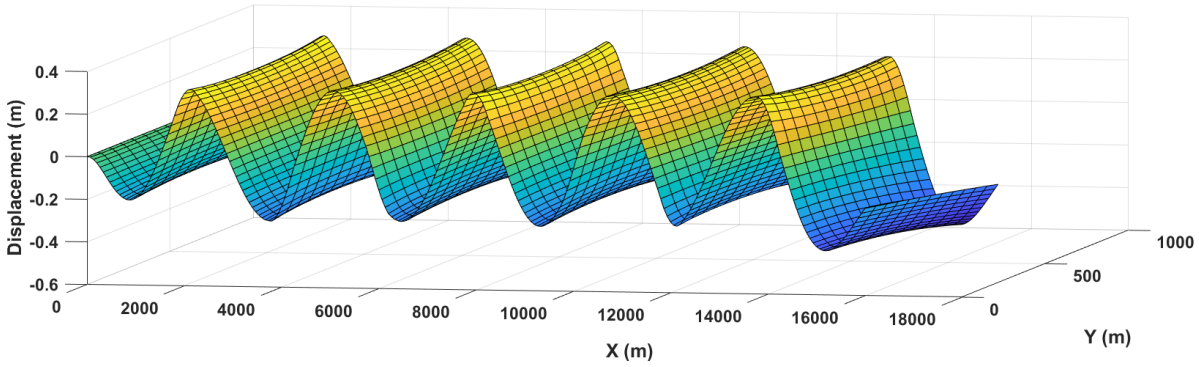

Fig. 25,a

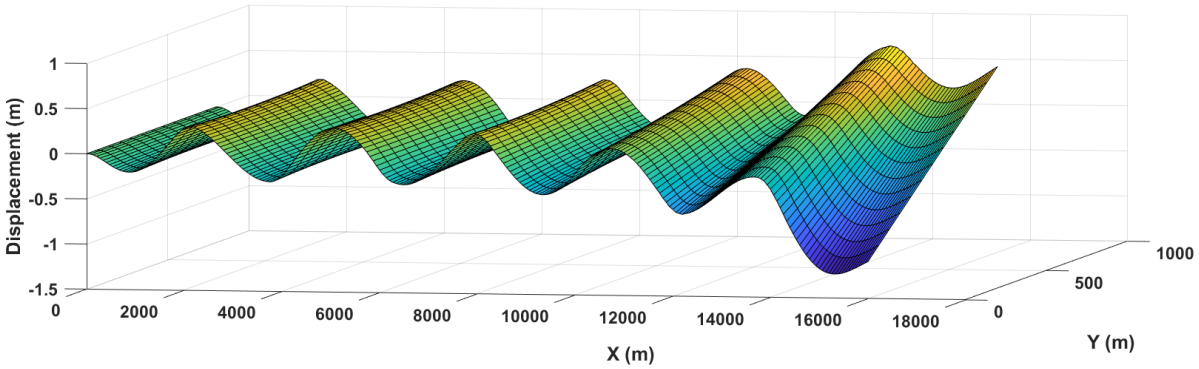

Fig. 25,b

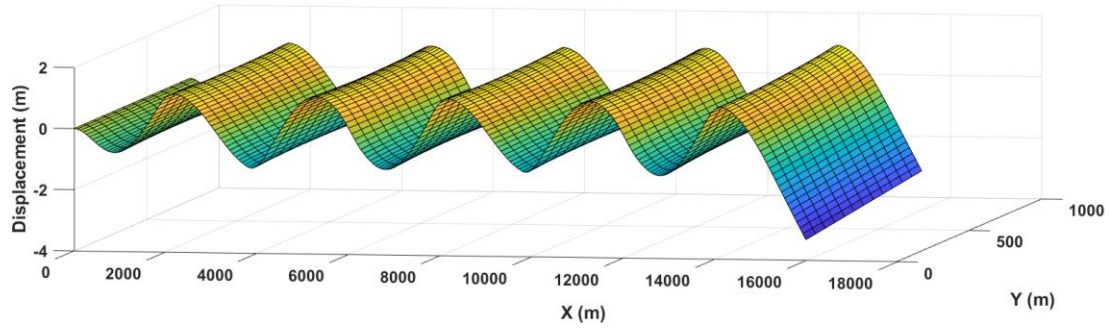

Fig. 25,c

Figure 25. Ice shelf vertical deflections result from the impact of the frontal incident wave. The periodicity of the forcing $\boldsymbol{T = 80s}$. The parameters of the model are **a)** $\boldsymbol{\alpha_1 = 0.6, \alpha_2 = 0.4}$; **b)** $\boldsymbol{\alpha_1 = 0.4, \alpha_2 = 0.6}$; **c)** $\boldsymbol{\alpha_1 = 0.0, \alpha_2 = 1.0}$.

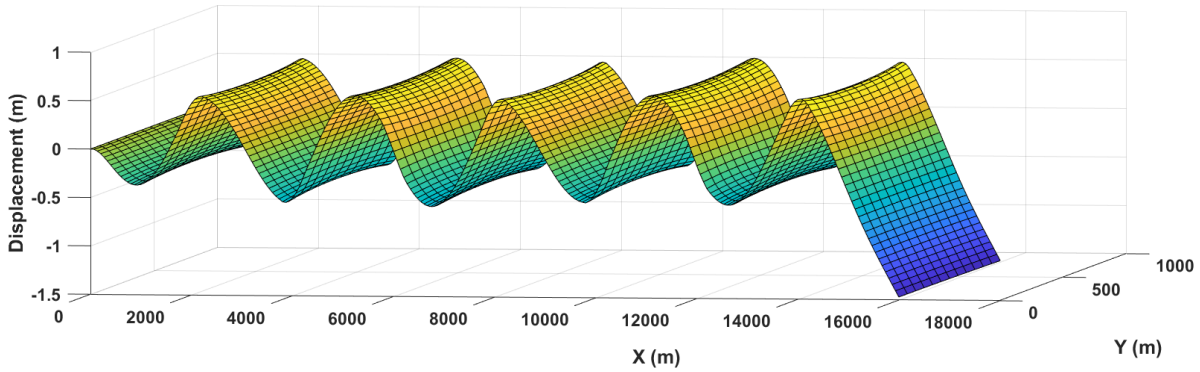

Fig. 26,a

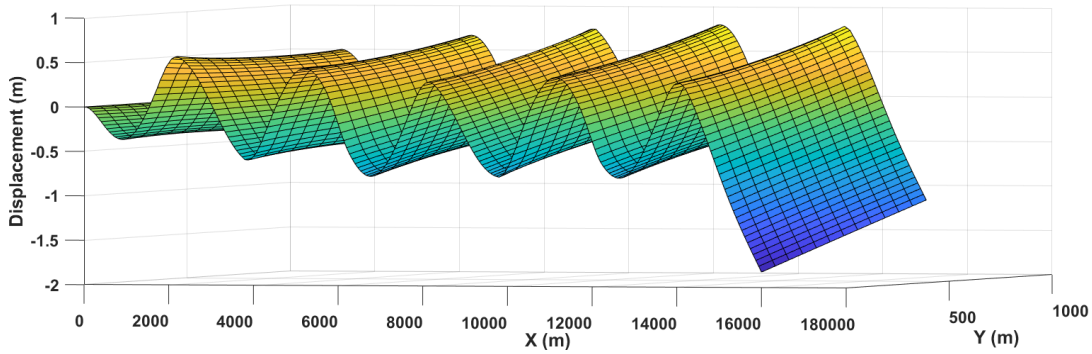

Fig. 26,b

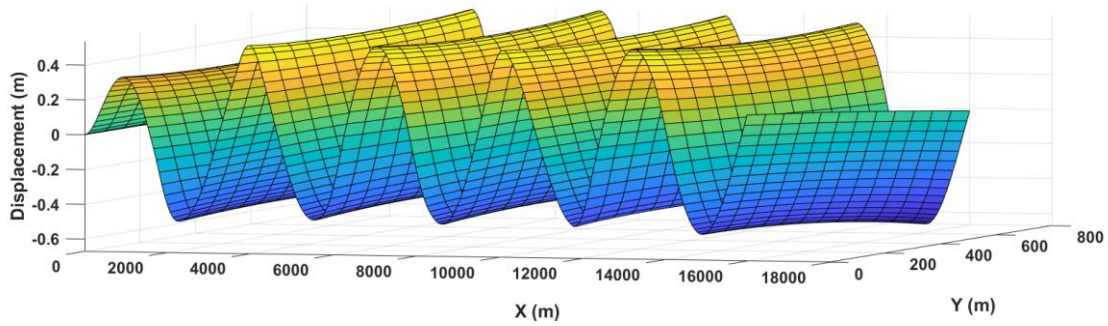

Fig. 26,c

Figure 26. Ice shelf vertical deflections result from the impact of the frontal incident wave. The periodicity of the forcing $\boldsymbol{T = 90s}$. The parameters of the model are **a)** $\boldsymbol{\alpha_1 = 0.6, \alpha_2 = 0.4}$; **b)** $\boldsymbol{\alpha_1 = 0.4, \alpha_2 = 0.6}$; **c)** $\boldsymbol{\alpha_1 = 0.0, \alpha_2 = 1.0}$.

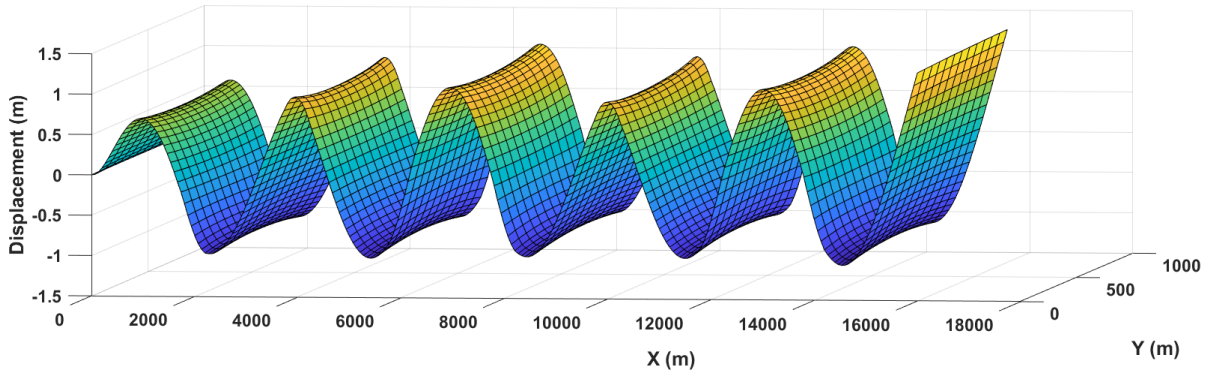

Fig. 27,a

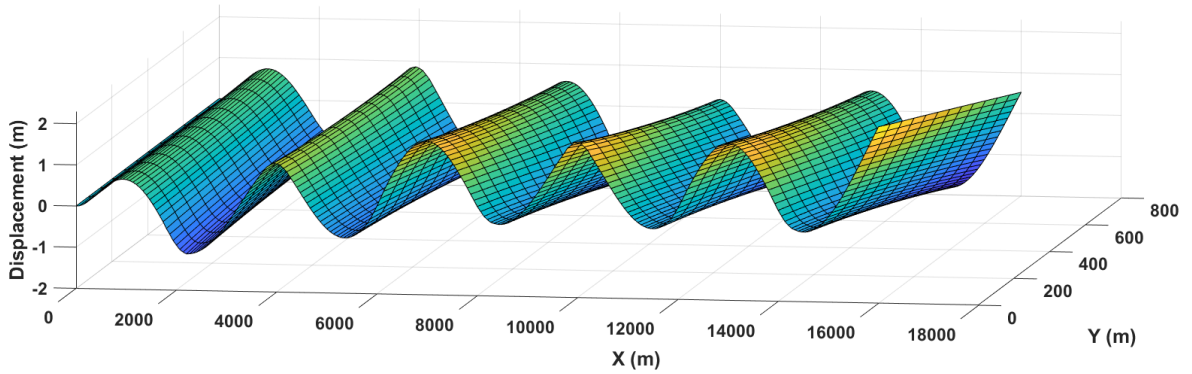

Fig. 27,b

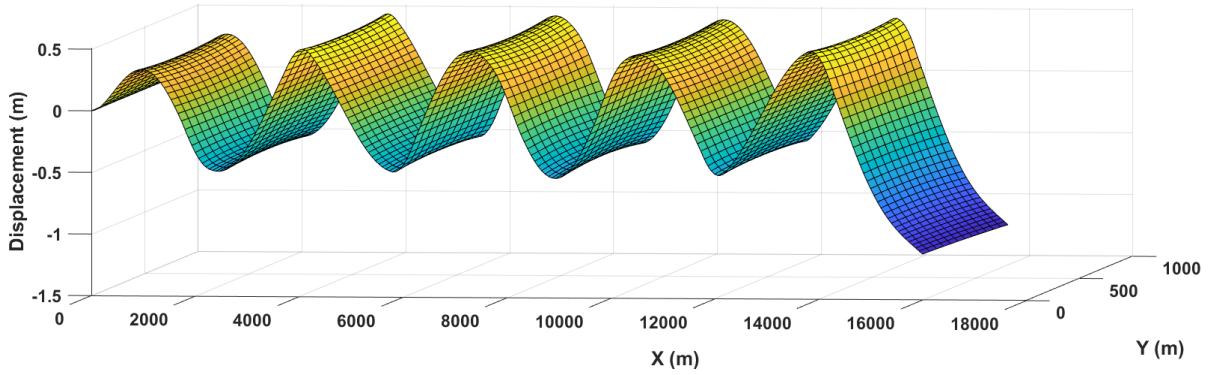

Fig. 27,c

Figure 27. Ice shelf vertical deflections result from the impact of the frontal incident wave. The periodicity of the forcing $\boldsymbol{T = 100s}$. The parameters of the model are **a)** $\boldsymbol{\alpha_1 = 0.6, \alpha_2 = 0.4}$; **b)** $\boldsymbol{\alpha_1 = 0.4, \alpha_2 = 0.6}$; **c)** $\boldsymbol{\alpha_1 = 0.0, \alpha_2 = 1.0}$.

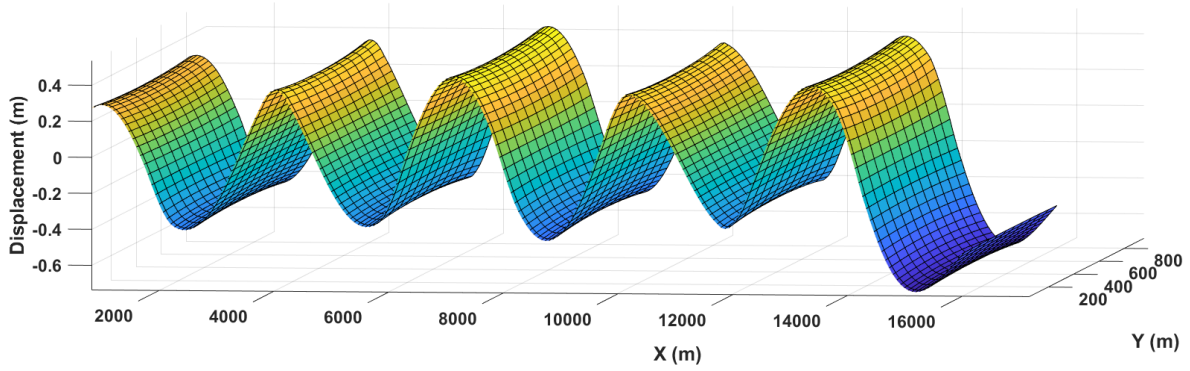

Fig. 28,a

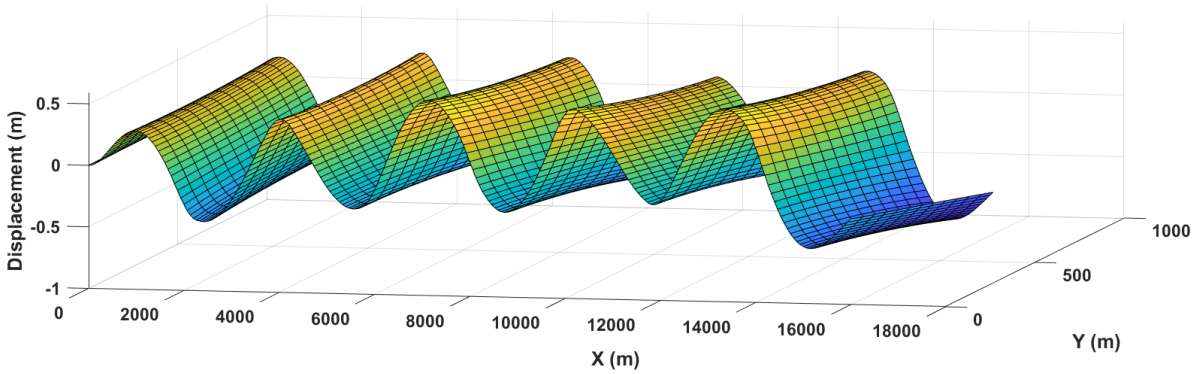

Fig. 28,b

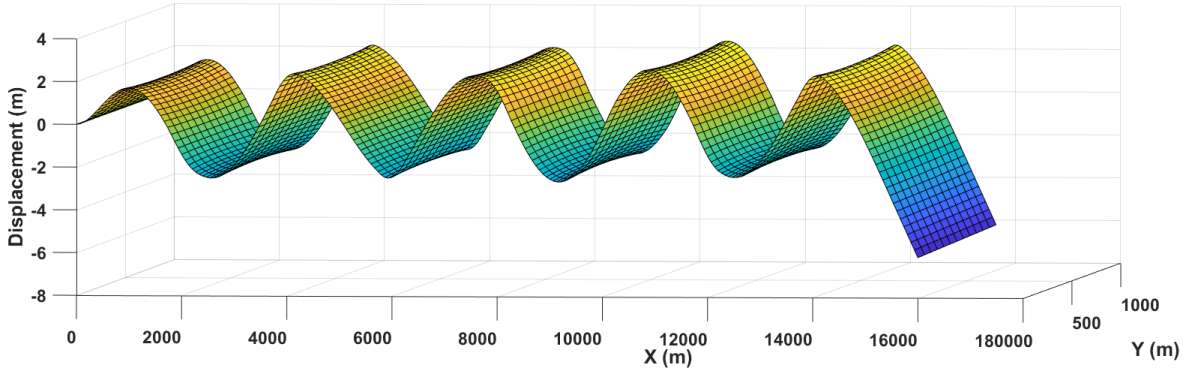

Fig. 28,c

Figure 28. Ice shelf vertical deflections result from the impact of the frontal incident wave. The periodicity of the forcing $\boldsymbol{T = 110s}$. The parameters of the model are **a)** $\boldsymbol{\alpha_1 = 0.6, \alpha_2 = 0.4}$; **b)** $\boldsymbol{\alpha_1 = 0.4, \alpha_2 = 0.6}$; **c)** $\boldsymbol{\alpha_1 = 0.0, \alpha_2 = 1.0}$.

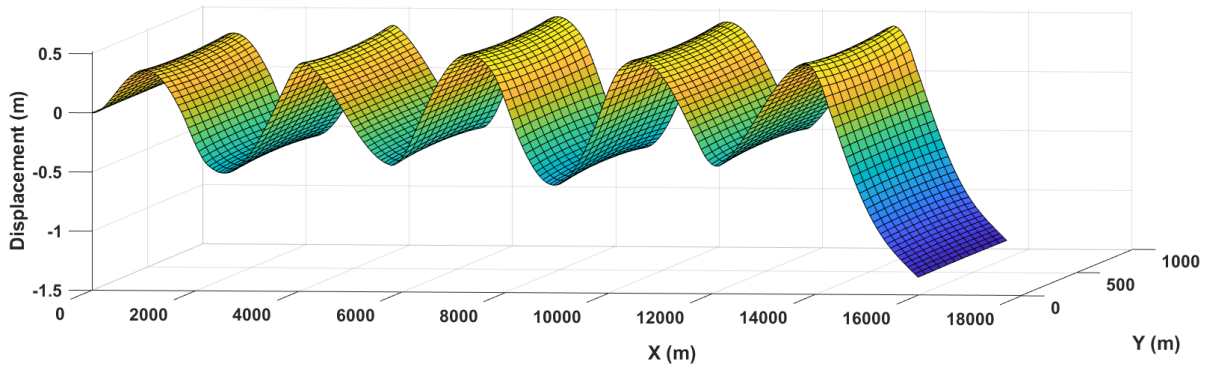

Fig. 29,a

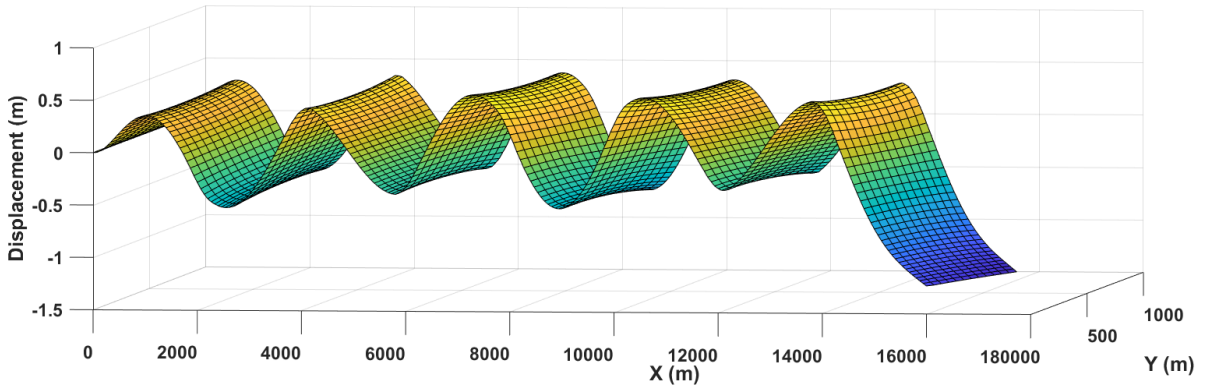

Fig. 29,b

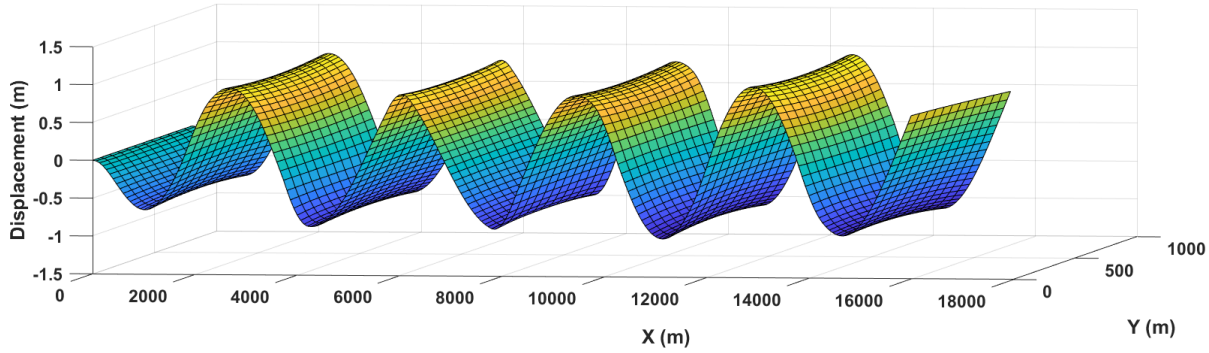

Fig. 29,c

Figure 29. Ice shelf vertical deflections result from the impact of the frontal incident wave. The periodicity of the forcing $\boldsymbol{T = 120s}$. The parameters of the model are **a)** $\boldsymbol{\alpha_1 = 0.6, \alpha_2 = 0.4}$; **b)** $\boldsymbol{\alpha_1 = 0.4, \alpha_2 = 0.6}$; **c)** $\boldsymbol{\alpha_1 = 0.0, \alpha_2 = 1.0}$.

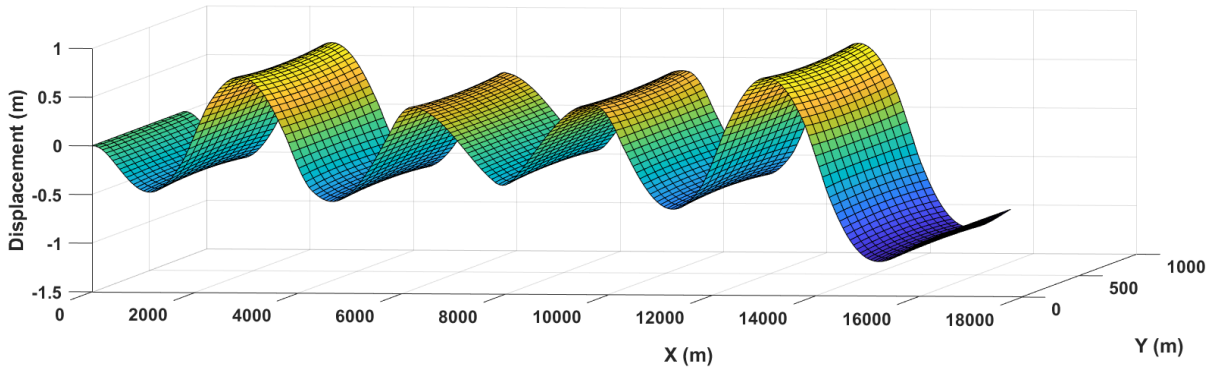

Fig. 30,a

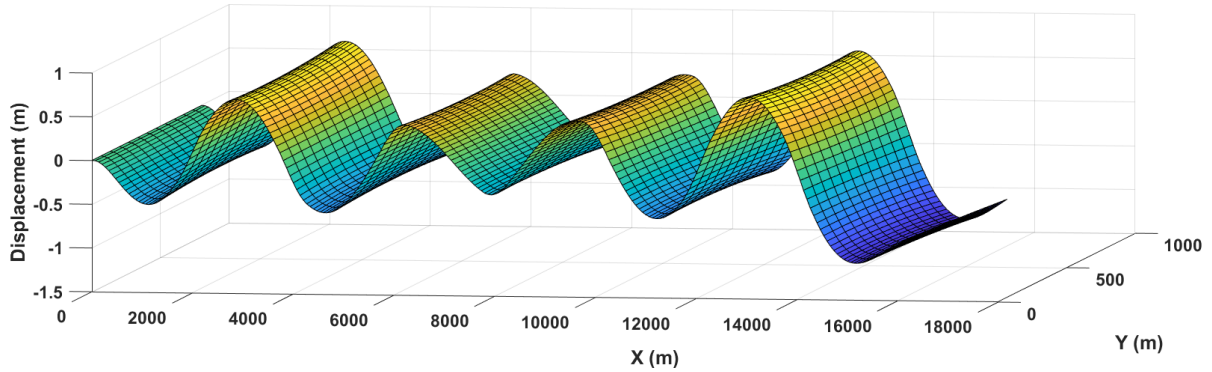

Fig. 30,b

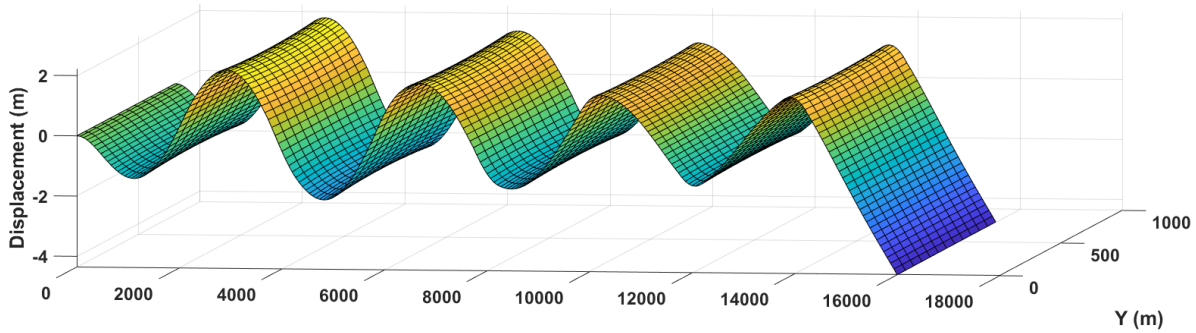

Fig. 30,c

Figure 30. Ice shelf vertical deflections result from the impact of the frontal incident wave. The periodicity of the forcing $\boldsymbol{T = 150s}$. The parameters of the model are **a)** $\boldsymbol{\alpha_1 = 0.6, \alpha_2 = 0.4}$; **b)** $\boldsymbol{\alpha_1 = 0.4, \alpha_2 = 0.6}$; **c)** $\boldsymbol{\alpha_1 = 0.0, \alpha_2 = 1.0}$.

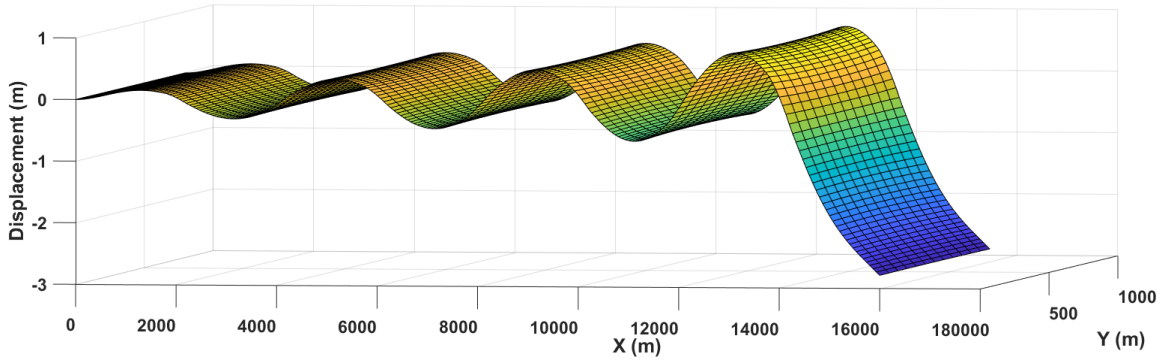

Fig. 31,a

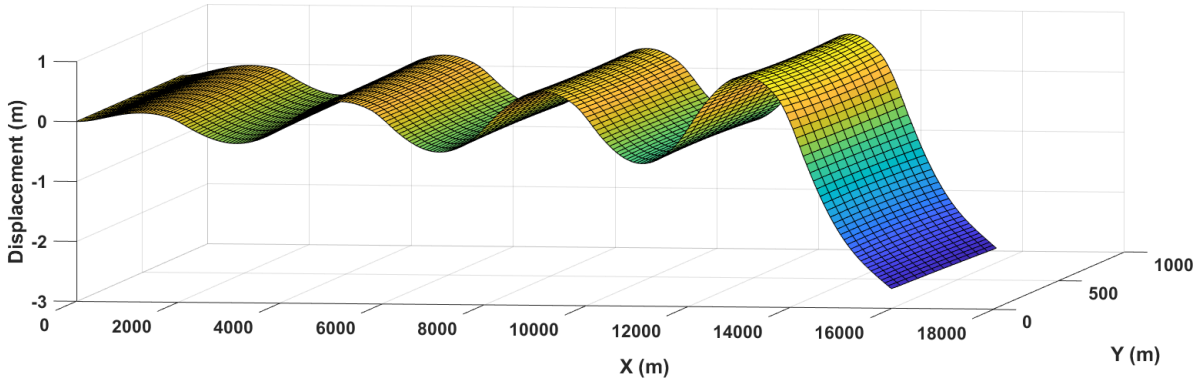

Fig. 31,b

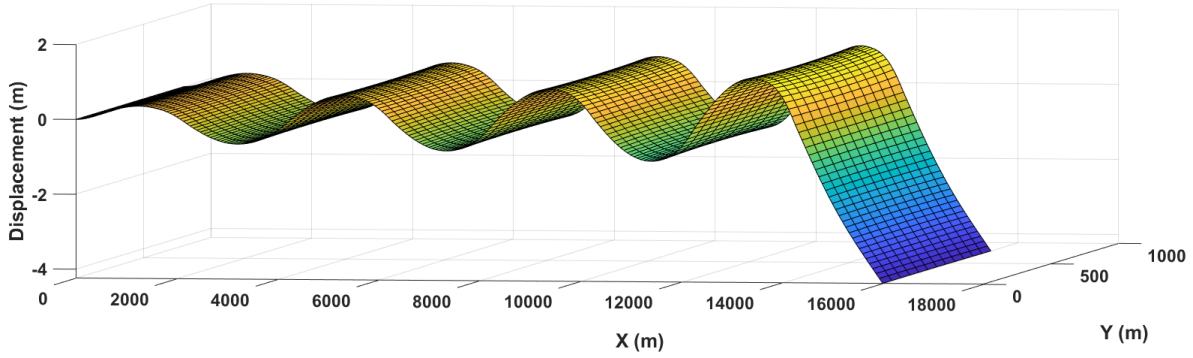

Fig. 31,c

Figure 31. Ice shelf vertical deflections result from the impact of the frontal incident wave. The periodicity of the forcing $\boldsymbol{T = 200s}$. The parameters of the model are **a)** $\boldsymbol{\alpha_1 = 0.6, \alpha_2 = 0.4}$; **b)** $\boldsymbol{\alpha_1 = 0.4, \alpha_2 = 0.6}$; **c)** $\boldsymbol{\alpha_1 = 0.0, \alpha_2 = 1.0}$.

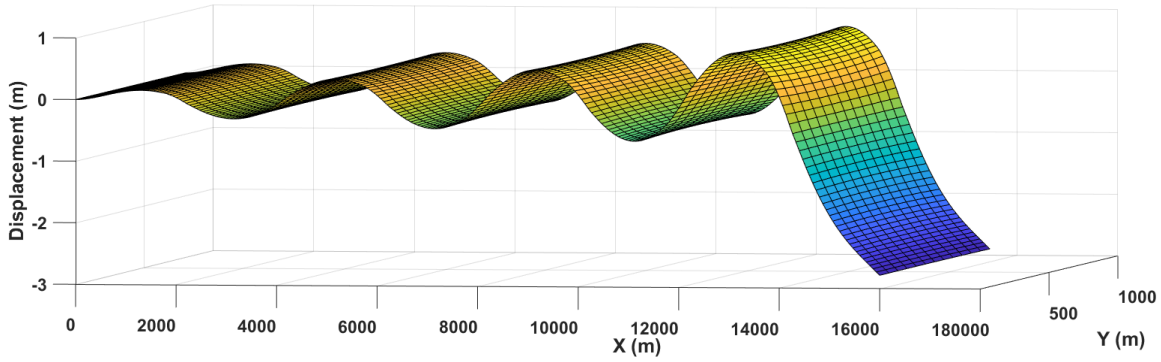

Fig. 31,a

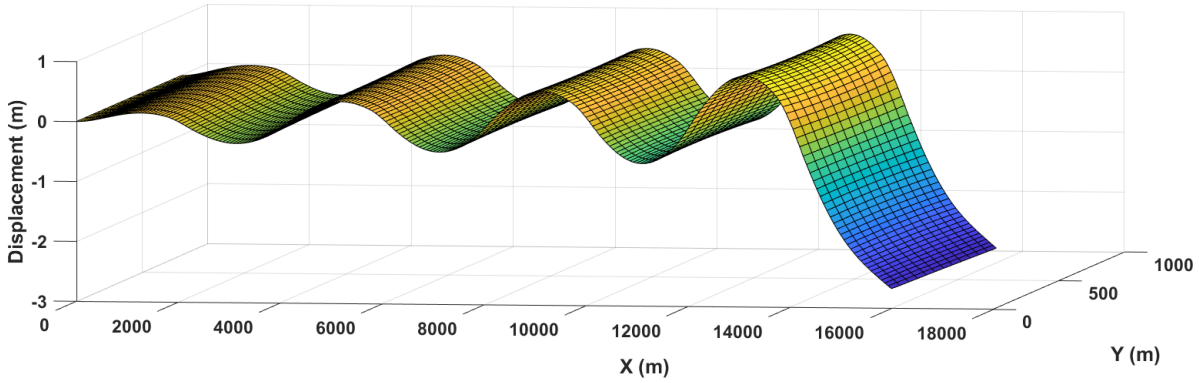

Fig. 31,b

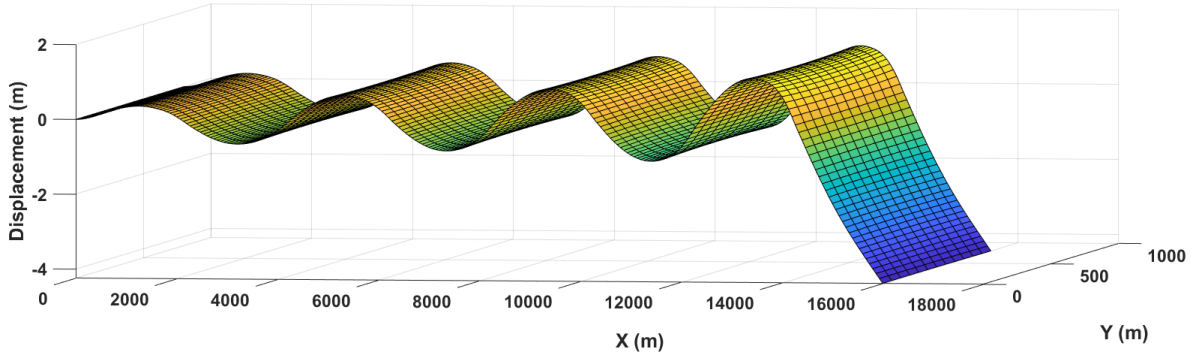

Fig. 31,c

Figure 31. Ice shelf vertical deflections result from the impact of the frontal incident wave. The periodicity of the forcing $\boldsymbol{T = 200s}$. The parameters of the model are **a)** $\boldsymbol{\alpha_1 = 0.6, \alpha_2 = 0.4}$; **b)** $\boldsymbol{\alpha_1 = 0.4, \alpha_2 = 0.6}$; **c)** $\boldsymbol{\alpha_1 = 0.0, \alpha_2 = 1.0}$.

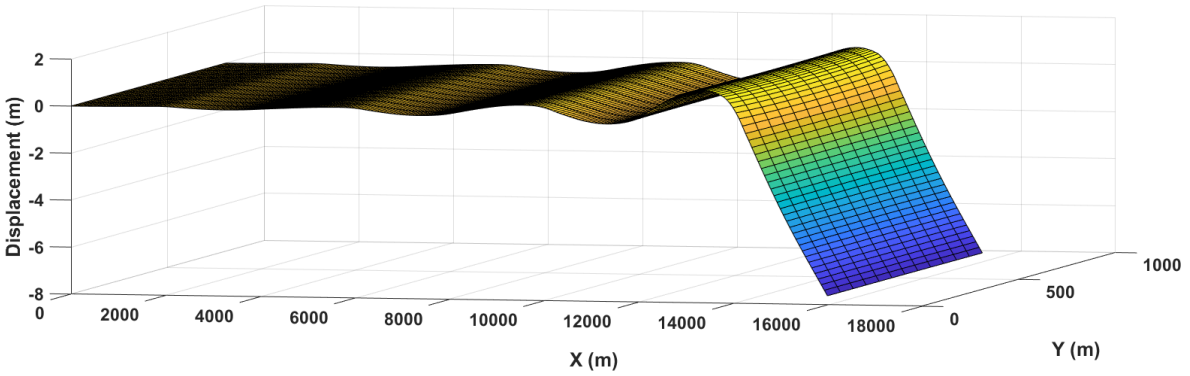

Fig. 32,a

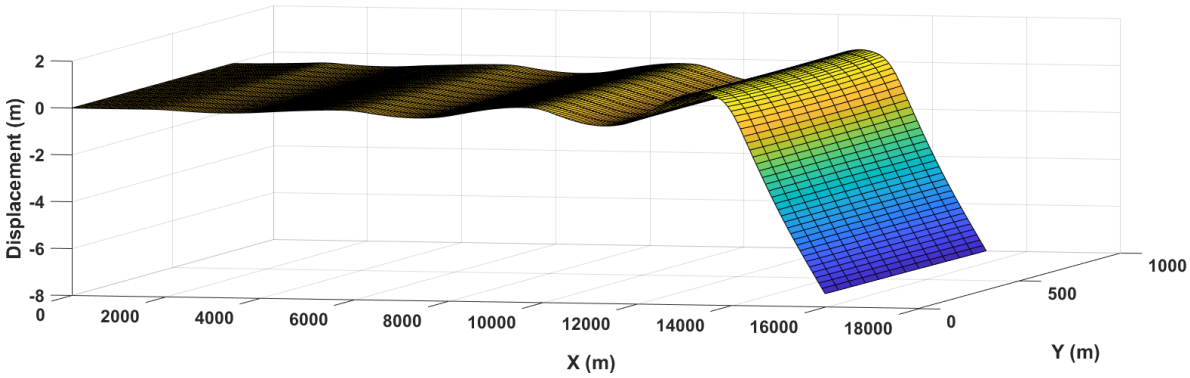

Fig. 32,b

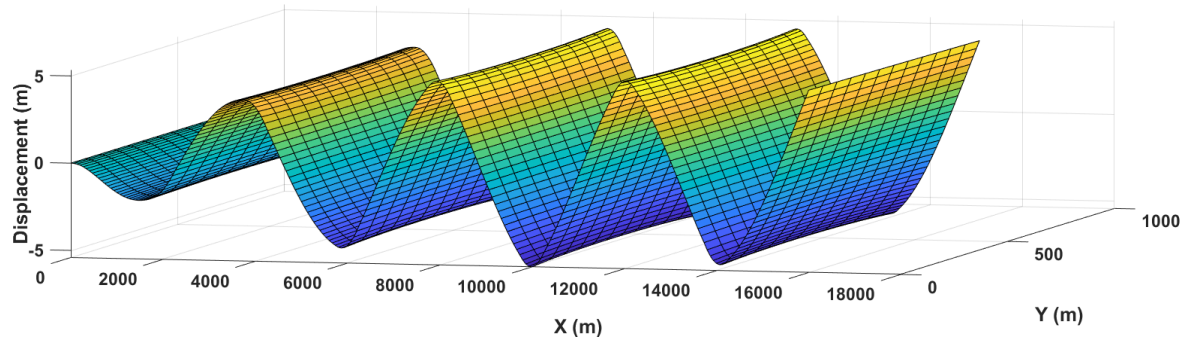

Fig. 32,c

Figure 32. Ice shelf vertical deflections result from the impact of the frontal incident wave. The periodicity of the forcing $\boldsymbol{T = 300s}$. The parameters of the model are **a)** $\boldsymbol{\alpha_1 = 0.6, \alpha_2 = 0.4}$; **b)** $\boldsymbol{\alpha_1 = 0.4, \alpha_2 = 0.6}$; **c)** $\boldsymbol{\alpha_1 = 0.0, \alpha_2 = 1.0}$.

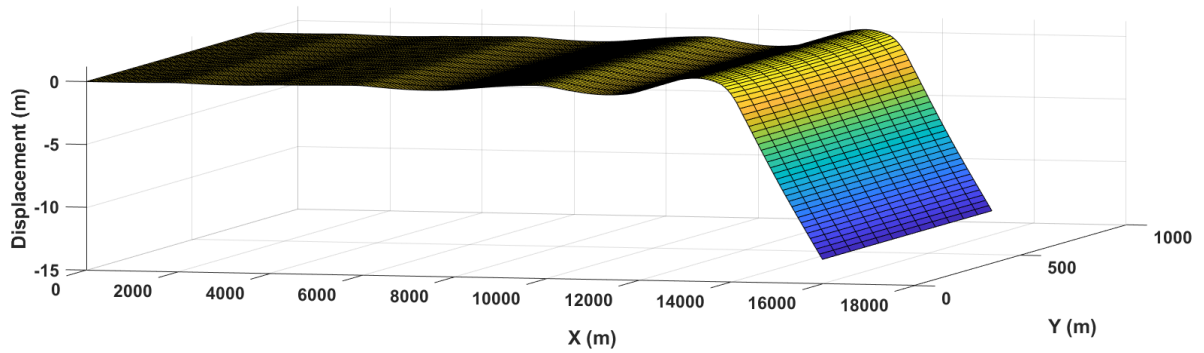

Fig. 33,a

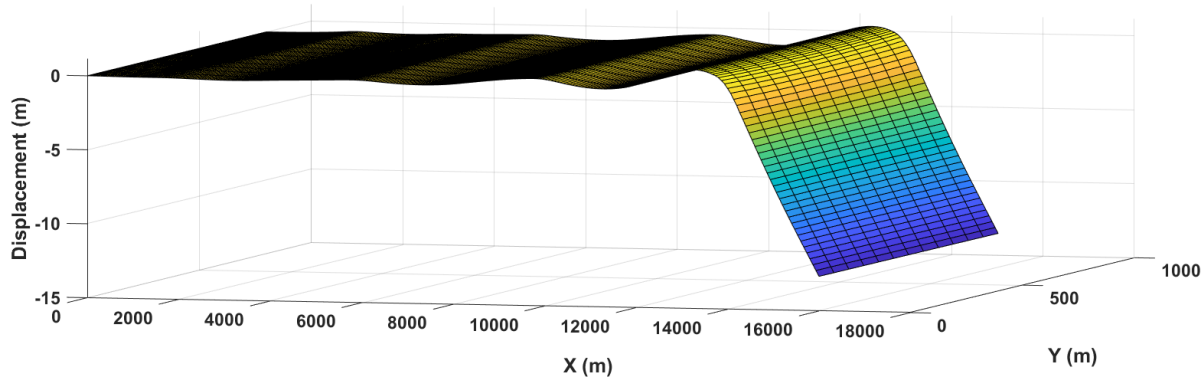

Fig. 33,b

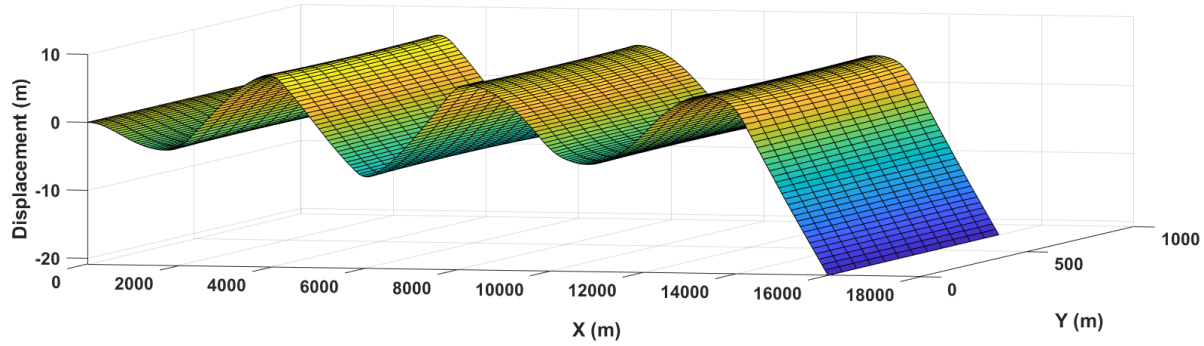

Fig. 33,c

Figure 33. Ice shelf vertical deflections result from the impact of the frontal incident wave. The periodicity of the forcing $\boldsymbol{T = 400s}$. The parameters of the model are **a)** $\boldsymbol{\alpha_1 = 0.6, \alpha_2 = 0.4}$; **b)** $\boldsymbol{\alpha_1 = 0.4, \alpha_2 = 0.6}$; **c)** $\boldsymbol{\alpha_1 = 0.0, \alpha_2 = 1.0}$.

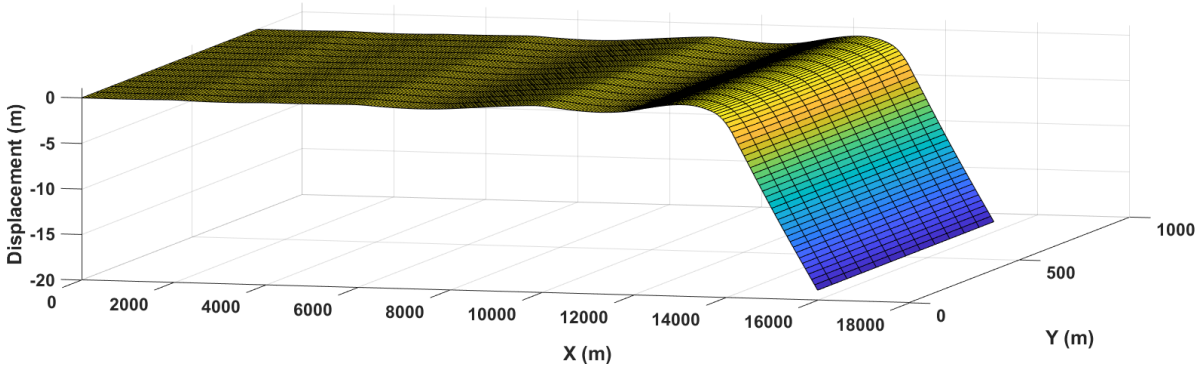

Fig. 34,a

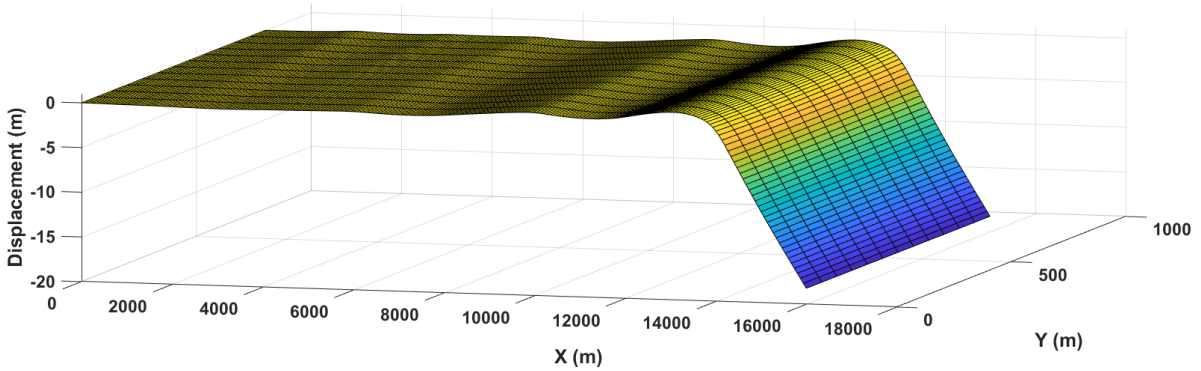

Fig. 34,b

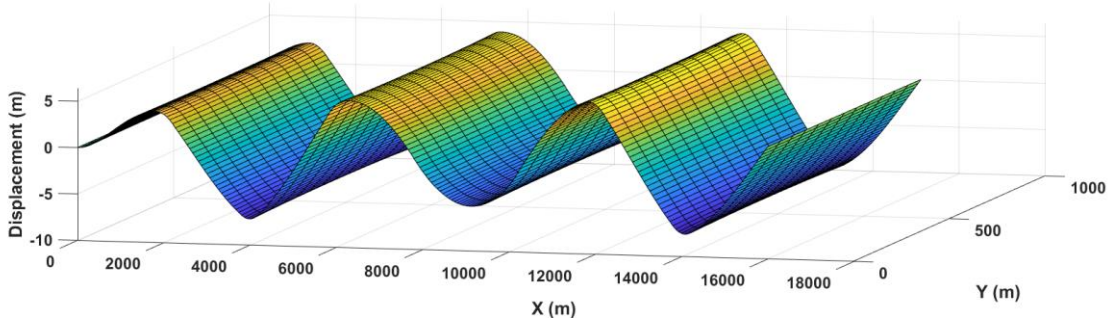

Fig. 34,c

Figure 34. Ice shelf vertical deflections result from the impact of the frontal incident wave. The periodicity of the forcing $\boldsymbol{T = 500s}$. The parameters of the model are **a)** $\boldsymbol{\alpha_1 = 0.6, \alpha_2 = 0.4}$; **b)** $\boldsymbol{\alpha_1 = 0.4, \alpha_2 = 0.6}$; **c)** $\boldsymbol{\alpha_1 = 0.0, \alpha_2 = 1.0}$.

2.3 Vertical deflections of the ice shelf were obtained with spatial periodicity of the crevasses $T_{cr} = 1.5\ km$ and with crevasse depth $D_{cr} = 20m$.

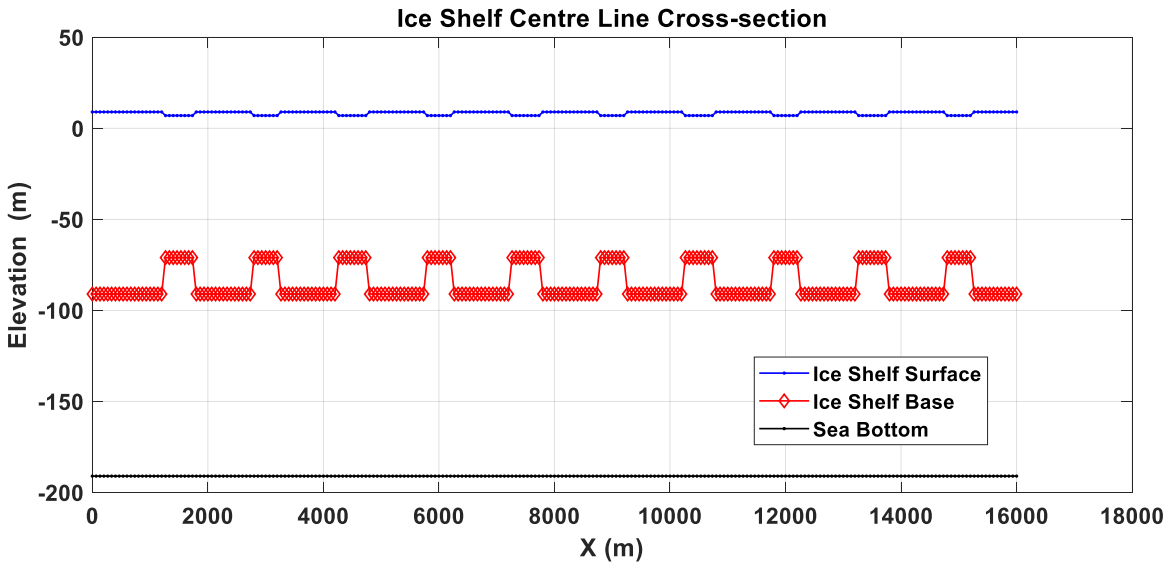

Figure 35. Ice shelf geometry. $T_{cr} = 1.5\ km$; $D_{cr} = 20m$.

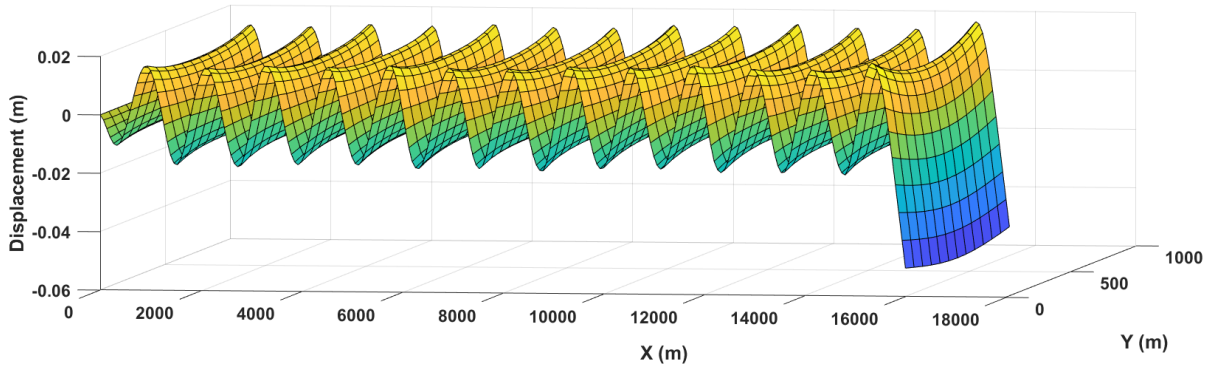

Fig. 36,a

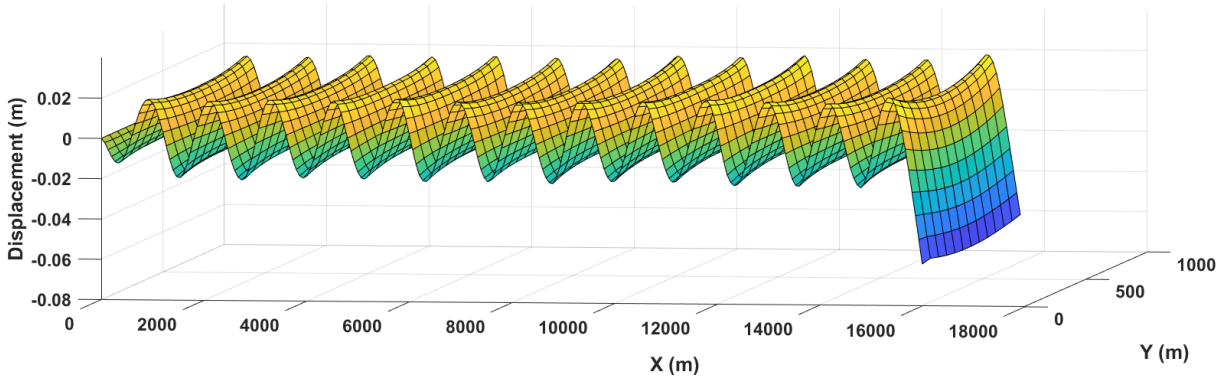

Fig. 36,b

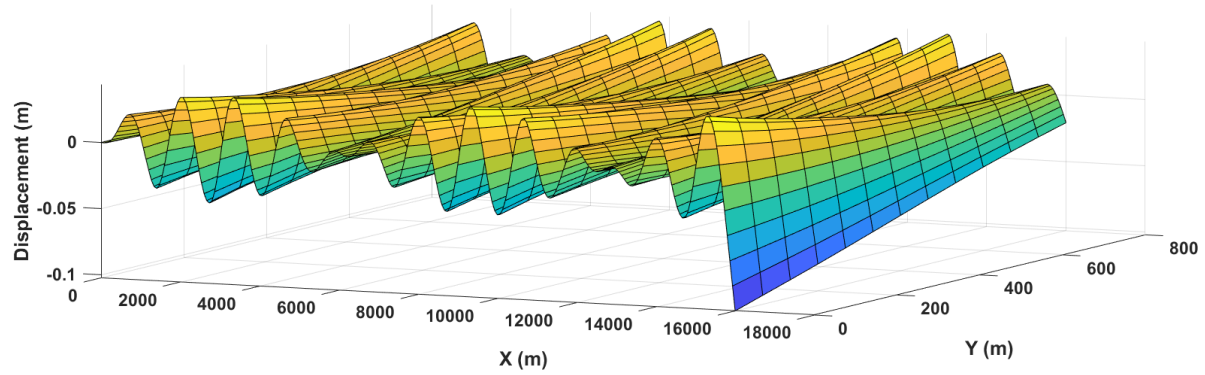

Fig. 36,c

Figure 36. Ice shelf vertical deflections result from the impact of the frontal incident wave. The periodicity of the forcing $\boldsymbol{T = 5s}$. The parameters of the model are **a)** $\boldsymbol{\alpha_1 = 0.6, \alpha_2 = 0.4}$; **b)** $\boldsymbol{\alpha_1 = 0.4, \alpha_2 = 0.6}$; **c)** $\boldsymbol{\alpha_1 = 0.0, \alpha_2 = 1.0}$.

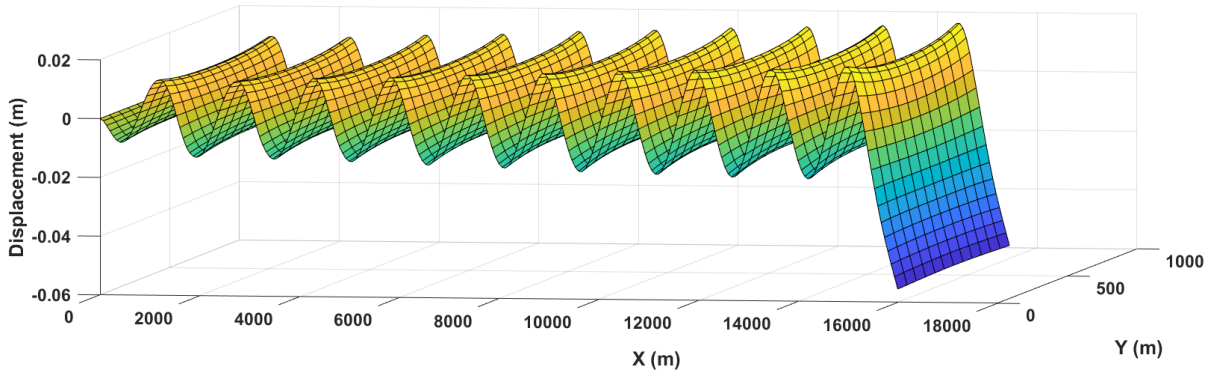

Fig. 37,a

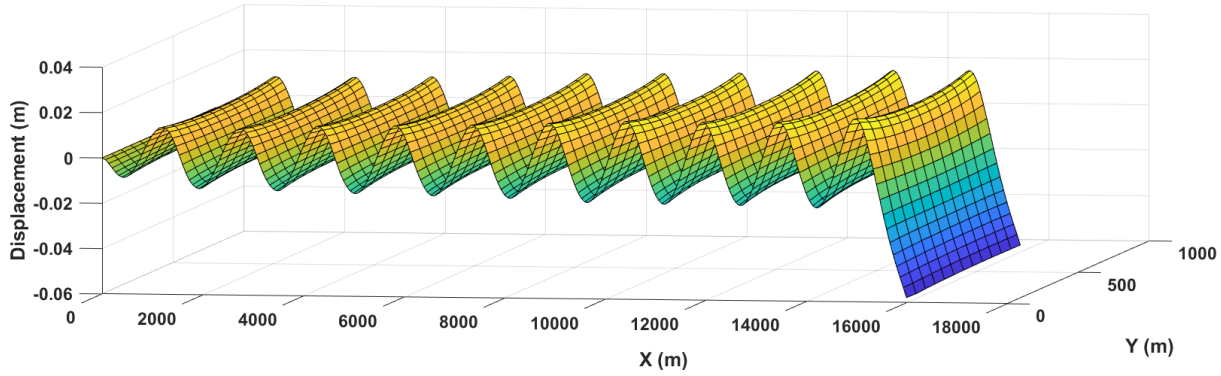

Fig. 37,b

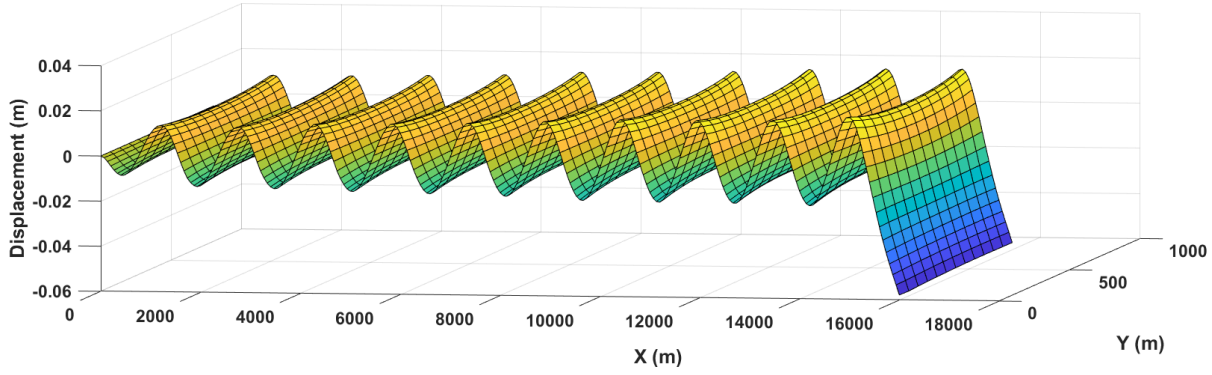

Fig. 37,c

Figure 37. Ice shelf vertical deflections result from the impact of the frontal incident wave. The periodicity of the forcing $\boldsymbol{T = 10s}$. The parameters of the model are **a)** $\boldsymbol{\alpha_1 = 0.6, \alpha_2 = 0.4}$; **b)** $\boldsymbol{\alpha_1 = 0.4, \alpha_2 = 0.6}$; **c)** $\boldsymbol{\alpha_1 = 0.0, \alpha_2 = 1.0}$.

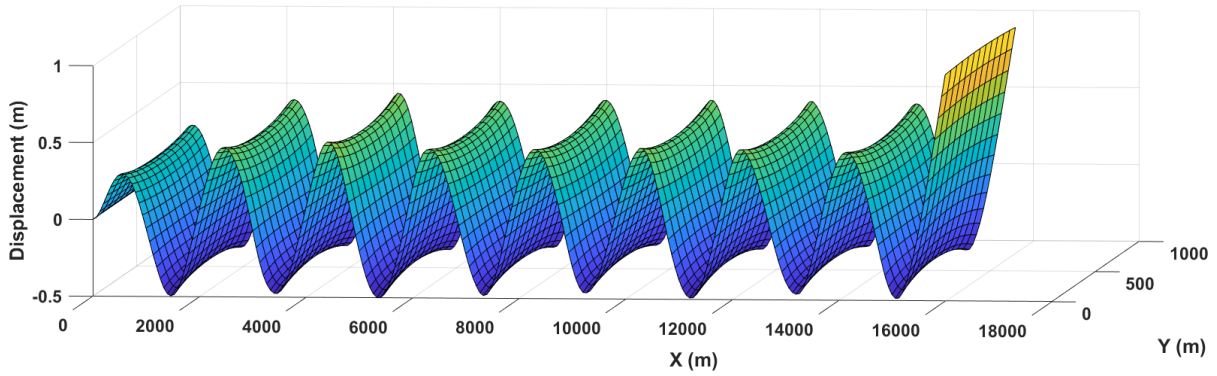

Fig. 38,a

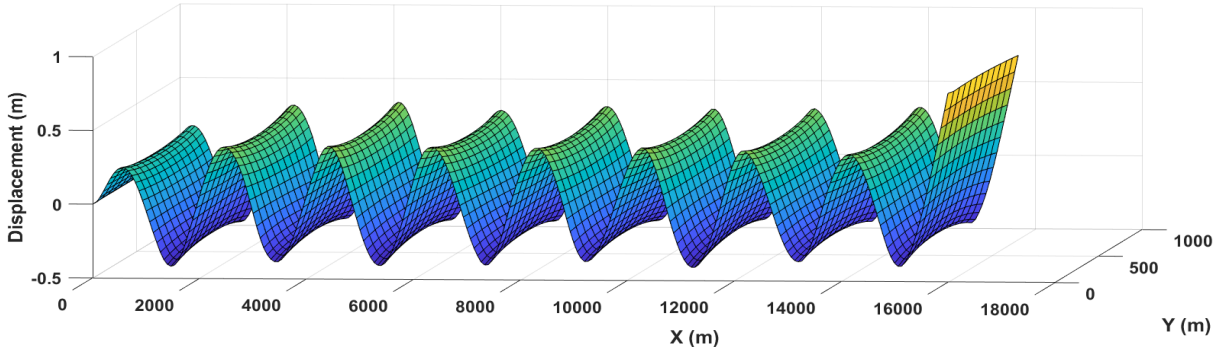

Fig. 38,b

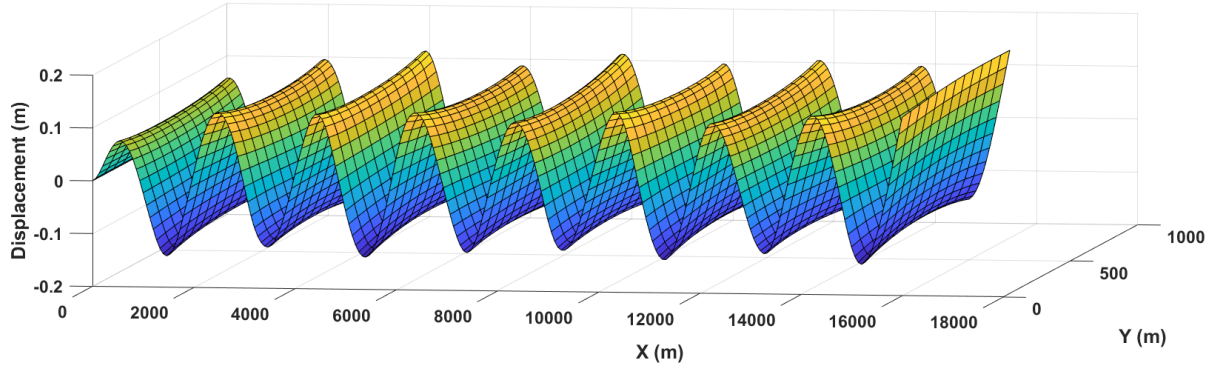

Fig. 38,c

Figure 38. Ice shelf vertical deflections result from the impact of the frontal incident wave. The periodicity of the forcing $\boldsymbol{T = 20s}$. The parameters of the model are **a)** $\boldsymbol{\alpha_1 = 0.6, \alpha_2 = 0.4}$; **b)** $\boldsymbol{\alpha_1 = 0.4, \alpha_2 = 0.6}$; **c)** $\boldsymbol{\alpha_1 = 0.0, \alpha_2 = 1.0}$.

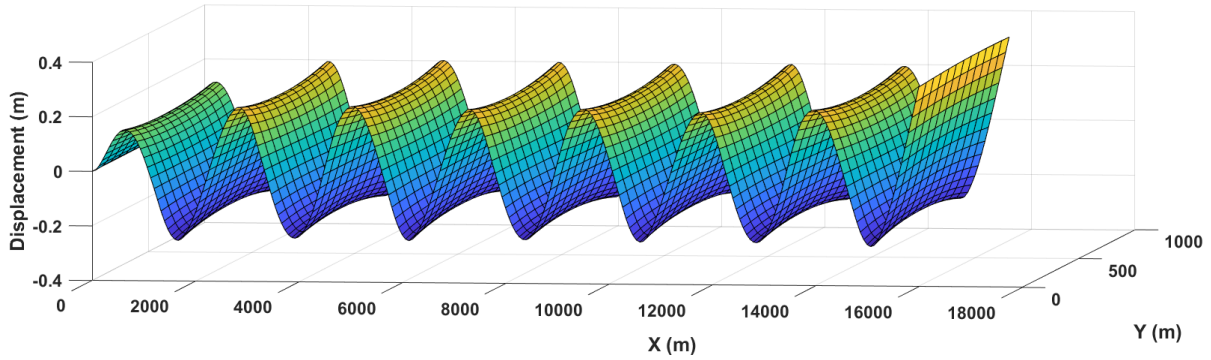

Fig. 39,a

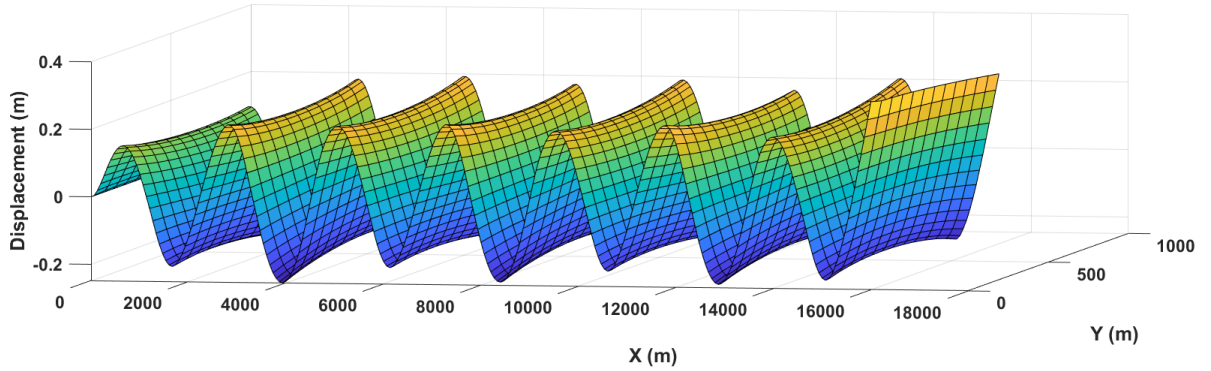

Fig. 39,b

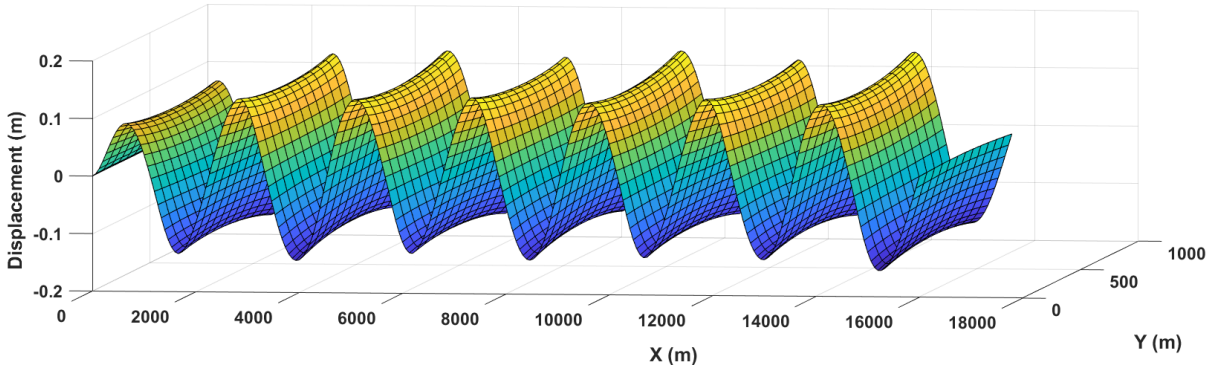

Fig. 39,c

Figure 39. Ice shelf vertical deflections result from the impact of the frontal incident wave. The periodicity of the forcing $\boldsymbol{T = 30s}$. The parameters of the model are **a)** $\boldsymbol{\alpha_1 = 0.6, \alpha_2 = 0.4}$; **b)** $\boldsymbol{\alpha_1 = 0.4, \alpha_2 = 0.6}$; **c)** $\boldsymbol{\alpha_1 = 0.0, \alpha_2 = 1.0}$.

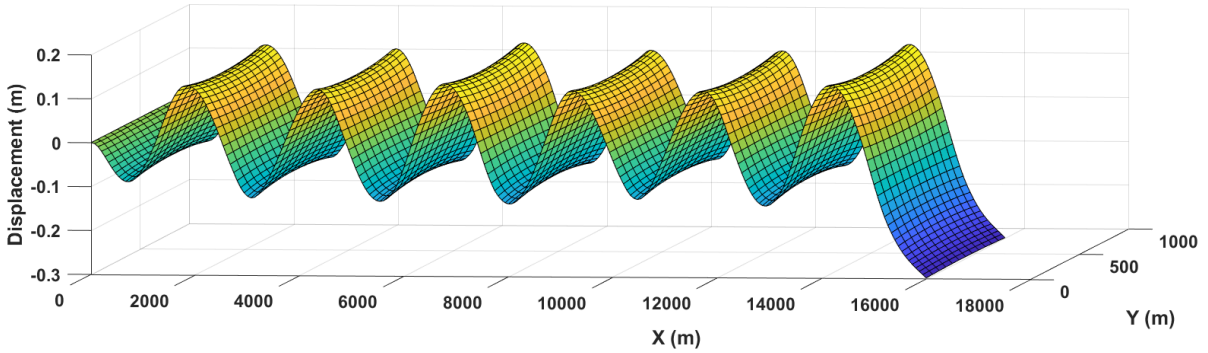

Fig. 40,a

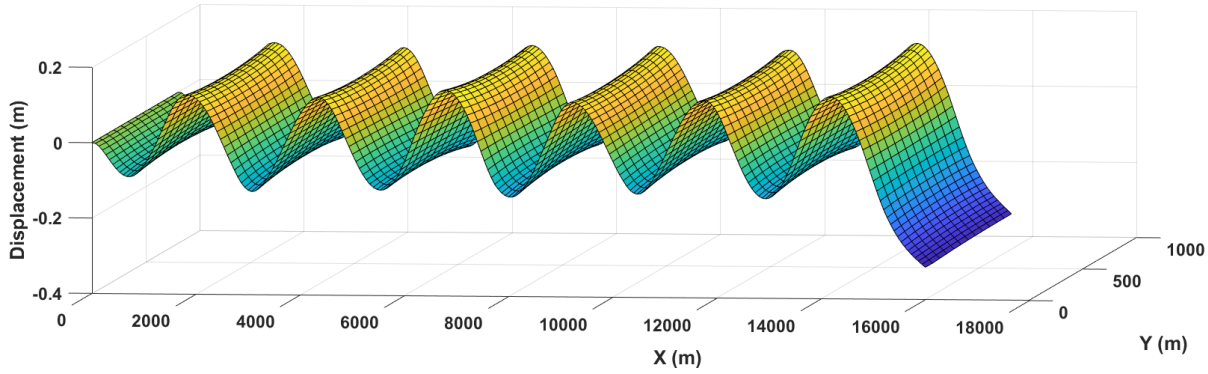

Fig. 40,b

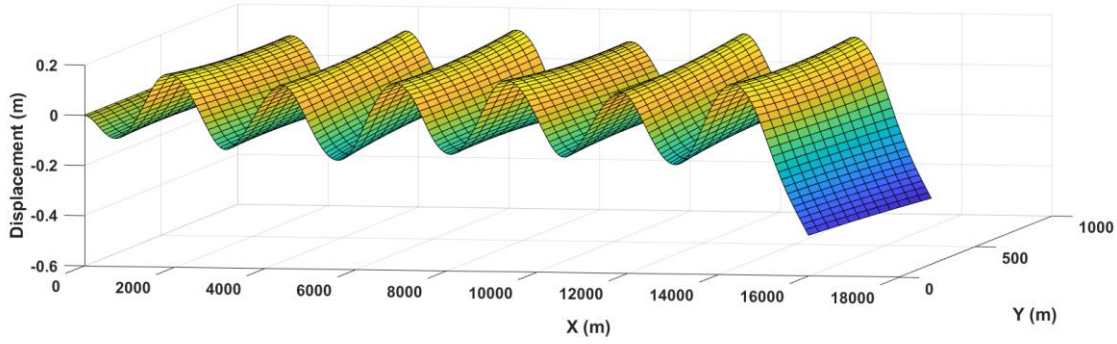

Fig. 40,c

Figure 40. Ice shelf vertical deflections result from the impact of the frontal incident wave. The periodicity of the forcing $\boldsymbol{T = 40s}$. The parameters of the model are **a)** $\boldsymbol{\alpha_1 = 0.6, \alpha_2 = 0.4}$; **b)** $\boldsymbol{\alpha_1 = 0.4, \alpha_2 = 0.6}$; **c)** $\boldsymbol{\alpha_1 = 0.0, \alpha_2 = 1.0}$.

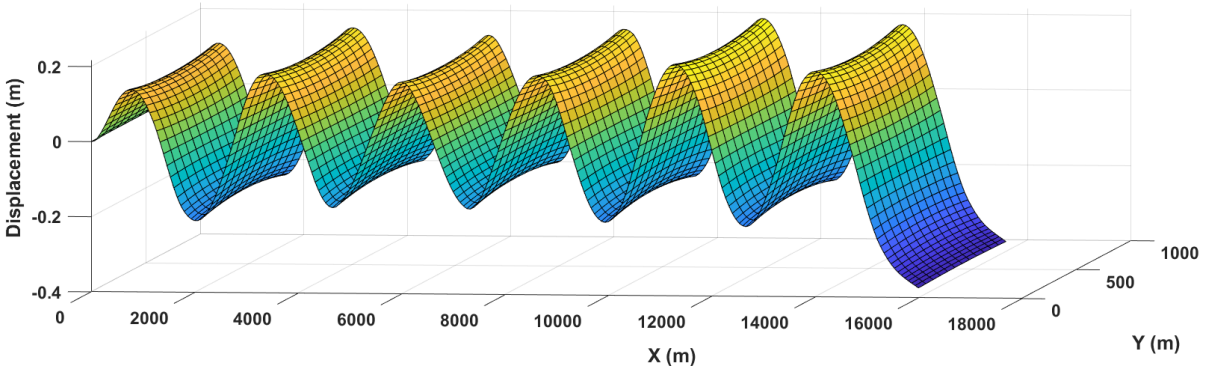

Fig. 41,a

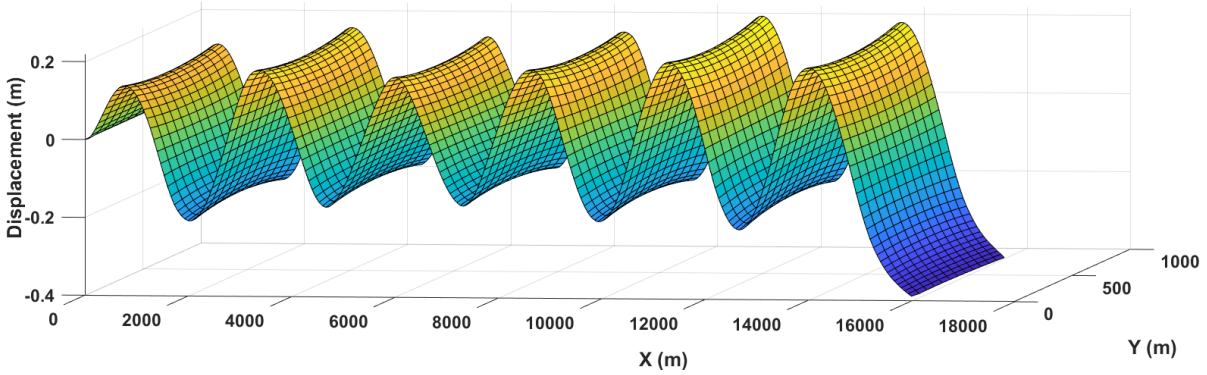

Fig. 41,b

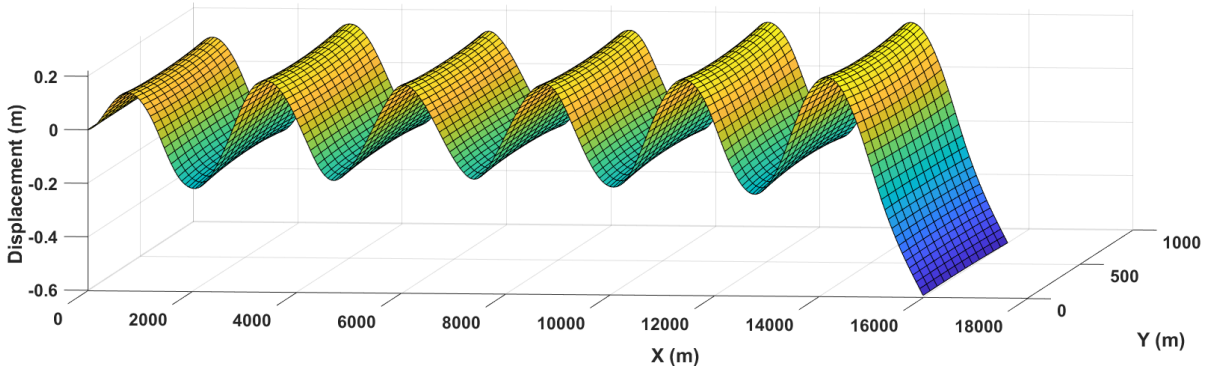

Fig. 41,c

Figure 41. Ice shelf vertical deflections result from the impact of the frontal incident wave. The periodicity of the forcing $\boldsymbol{T = 50s}$. The parameters of the model are **a)** $\boldsymbol{\alpha_1 = 0.6, \alpha_2 = 0.4}$; **b)** $\boldsymbol{\alpha_1 = 0.4, \alpha_2 = 0.6}$; **c)** $\boldsymbol{\alpha_1 = 0.0, \alpha_2 = 1.0}$.

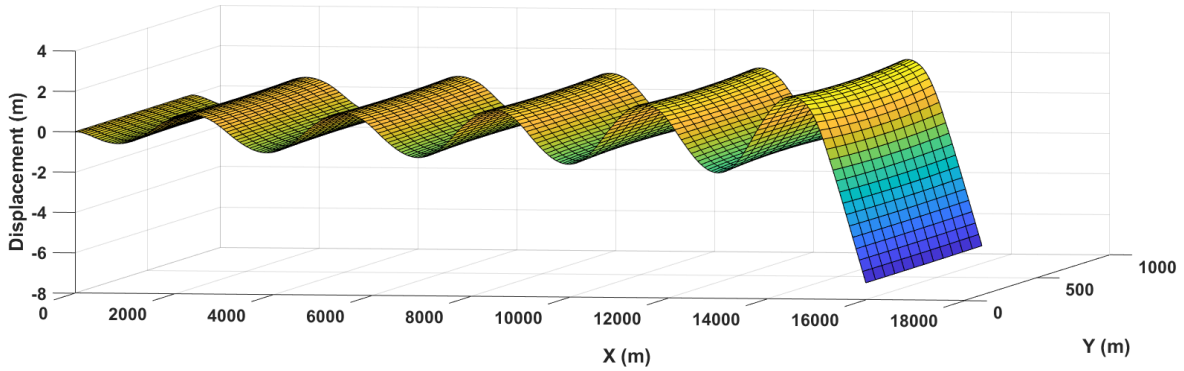

Fig. 42,a

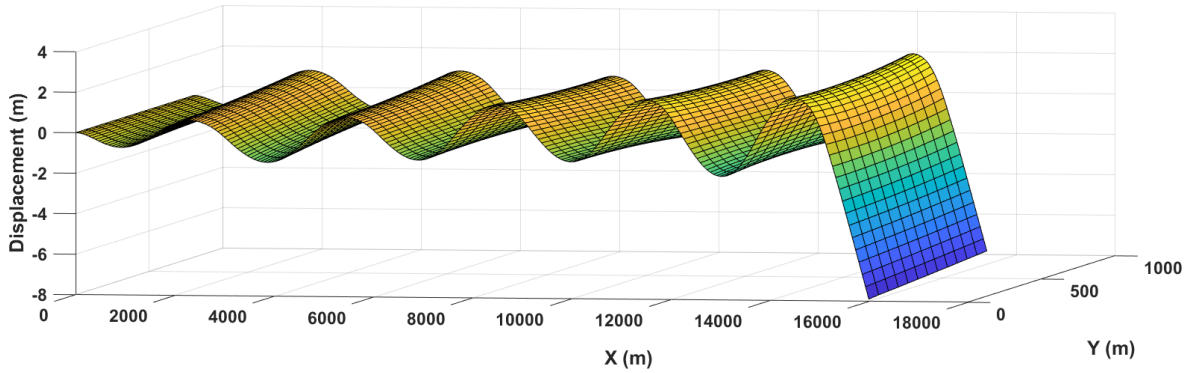

Fig. 42,b

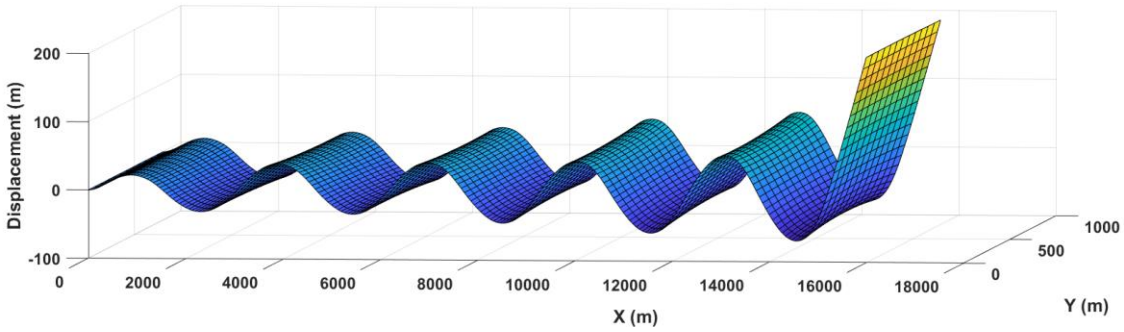

Fig. 42,c

Figure 42. Ice shelf vertical deflections result from the impact of the frontal incident wave. The periodicity of the forcing $\boldsymbol{T = 70s}$. The parameters of the model are **a)** $\boldsymbol{\alpha_1 = 0.6, \alpha_2 = 0.4}$; **b)** $\boldsymbol{\alpha_1 = 0.4, \alpha_2 = 0.6}$; **c)** $\boldsymbol{\alpha_1 = 0.0, \alpha_2 = 1.0}$.

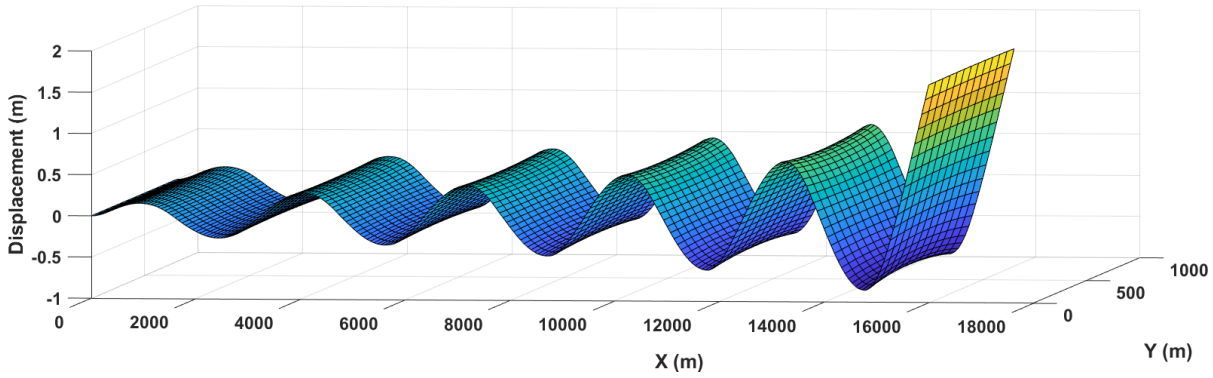

Fig. 43,a

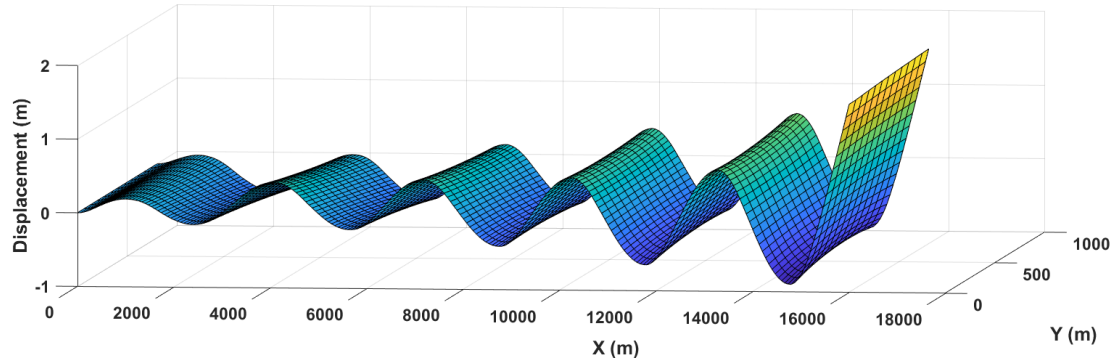

Fig. 43,b

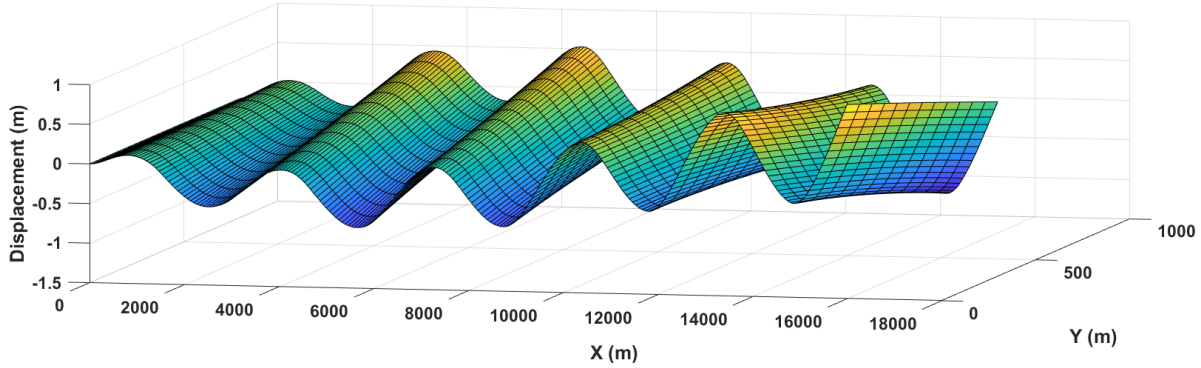

Fig. 43,c

Figure 43. Ice shelf vertical deflections result from the impact of the frontal incident wave. The periodicity of the forcing $\boldsymbol{T = 80s}$. The parameters of the model are **a)** $\boldsymbol{\alpha_1 = 0.6, \alpha_2 = 0.4}$; **b)** $\boldsymbol{\alpha_1 = 0.4, \alpha_2 = 0.6}$; **c)** $\boldsymbol{\alpha_1 = 0.0, \alpha_2 = 1.0}$.

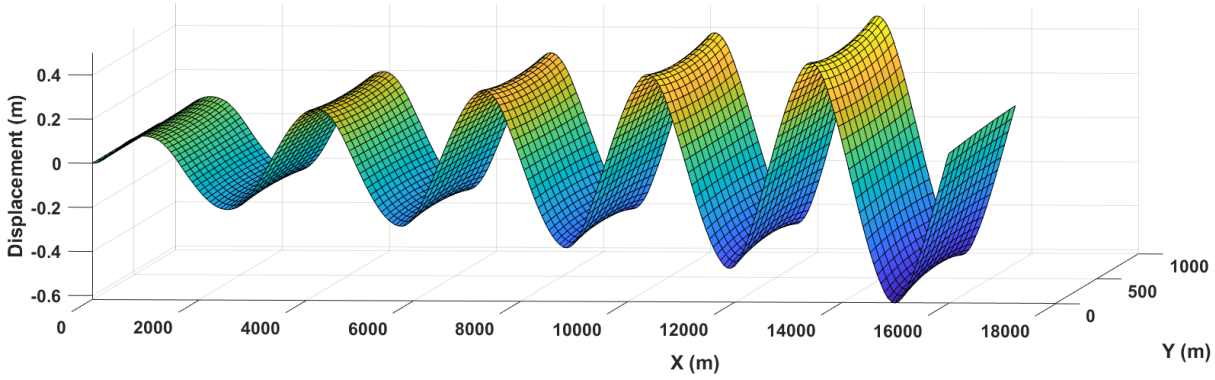

Fig. 44,a

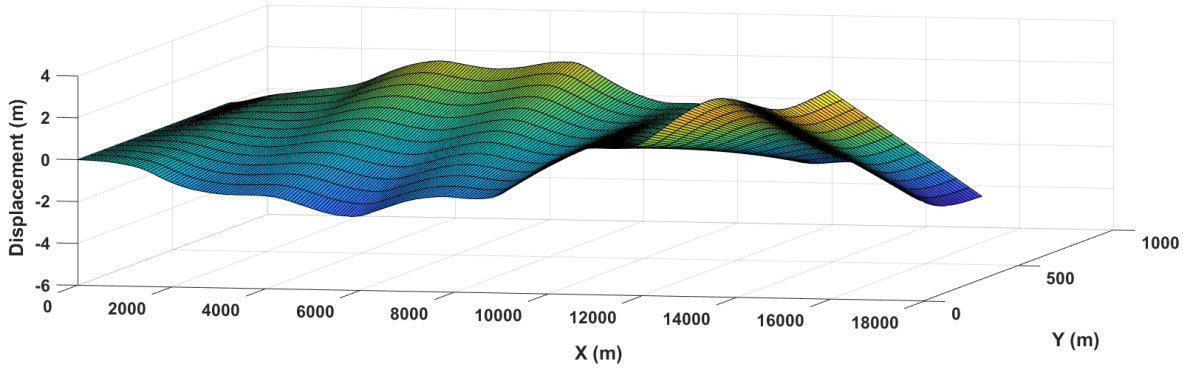

Fig. 44,b

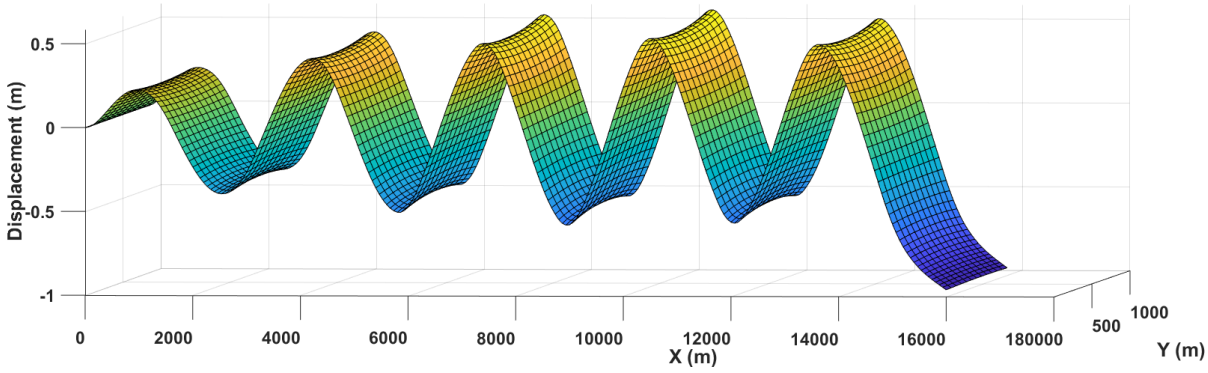

Fig. 44,c

Figure 44. Ice shelf vertical deflections result from the impact of the frontal incident wave. The periodicity of the forcing $\boldsymbol{T = 90s}$. The parameters of the model are **a)** $\boldsymbol{\alpha_1 = 0.6, \alpha_2 = 0.4}$; **b)** $\boldsymbol{\alpha_1 = 0.4, \alpha_2 = 0.6}$; **c)** $\boldsymbol{\alpha_1 = 0.0, \alpha_2 = 1.0}$.

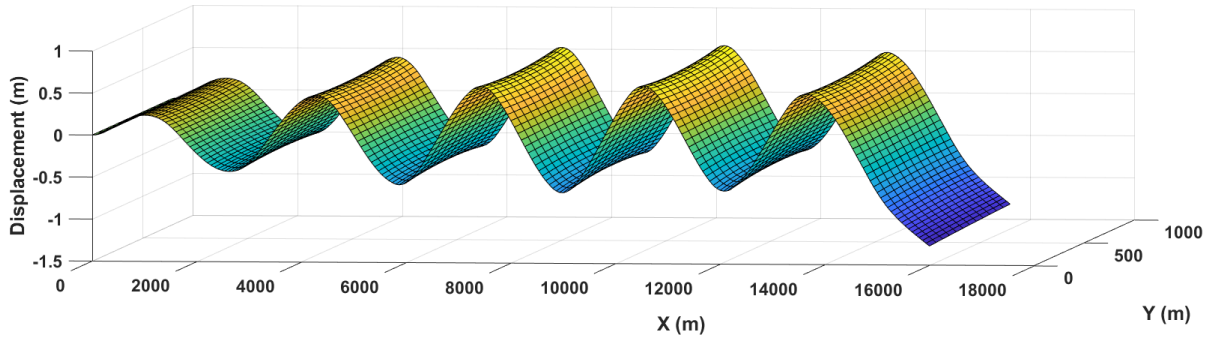

Fig. 45,a

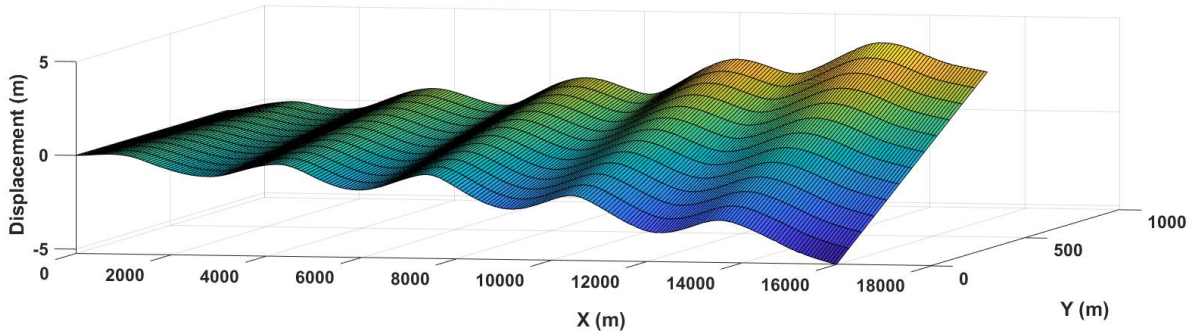

Fig. 45,b

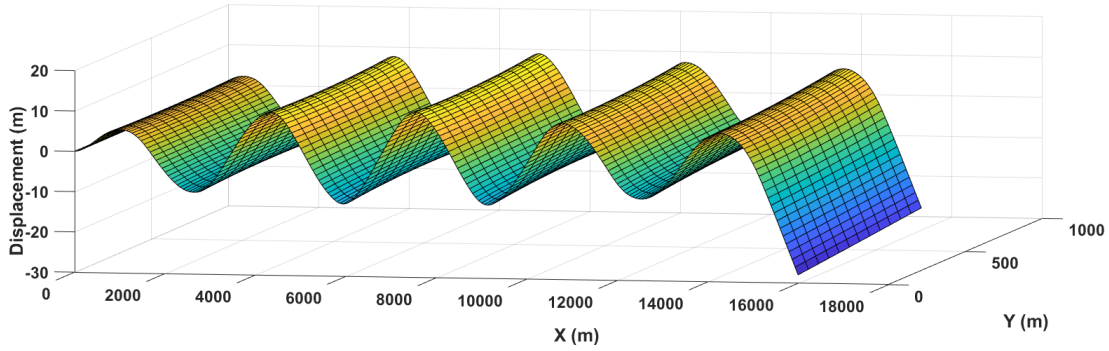

Fig. 45,c

Figure 45. Ice shelf vertical deflections result from the impact of the frontal incident wave. The periodicity of the forcing $\boldsymbol{T = 100s}$. The parameters of the model are **a)** $\boldsymbol{\alpha_1 = 0.6, \alpha_2 = 0.4}$; **b)** $\boldsymbol{\alpha_1 = 0.4, \alpha_2 = 0.6}$; **c)** $\boldsymbol{\alpha_1 = 0.0, \alpha_2 = 1.0}$.

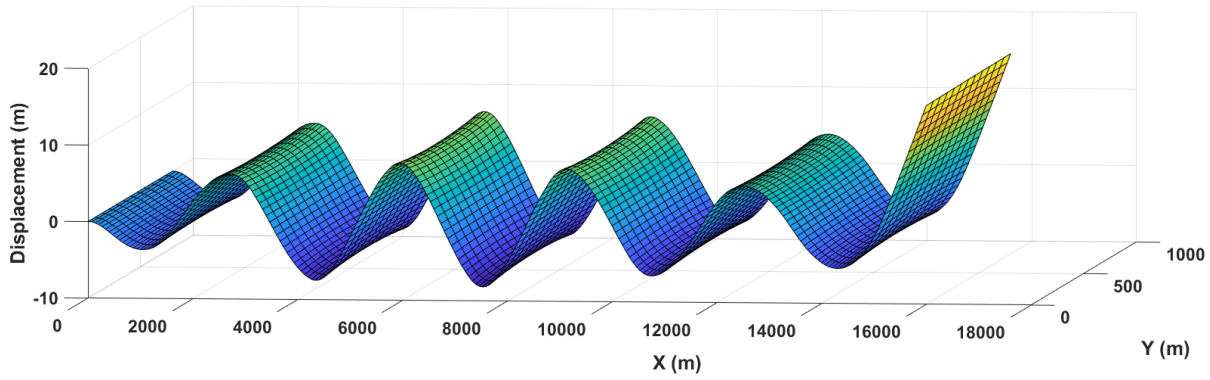

Fig. 46,a

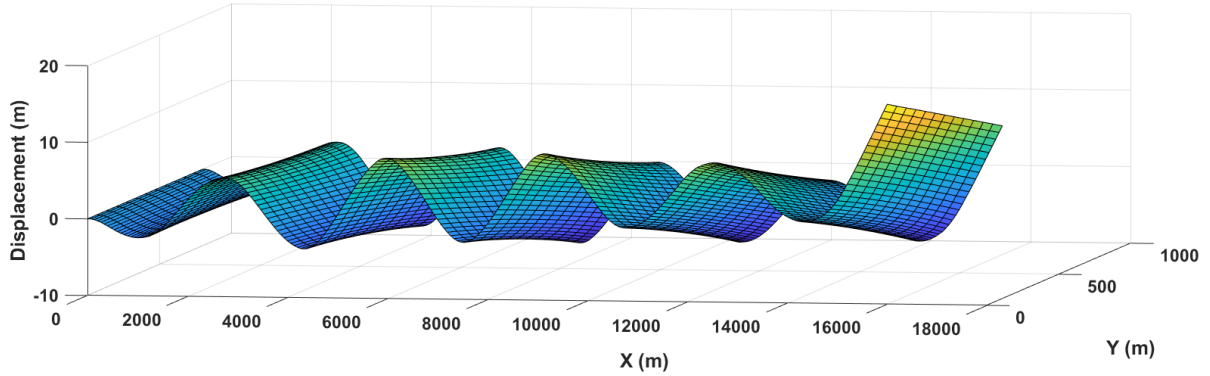

Fig. 46,b

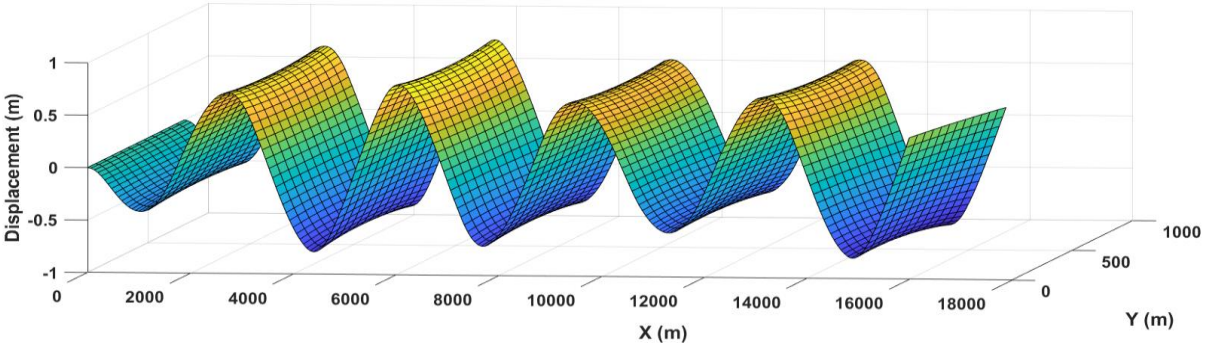

Fig. 46,c

Figure 46. Ice shelf vertical deflections result from the impact of the frontal incident wave. The periodicity of the forcing $\boldsymbol{T = 110s}$. The parameters of the model are **a)** $\boldsymbol{\alpha_1 = 0.6, \alpha_2 = 0.4}$; **b)** $\boldsymbol{\alpha_1 = 0.4, \alpha_2 = 0.6}$; **c)** $\boldsymbol{\alpha_1 = 0.0, \alpha_2 = 1.0}$.

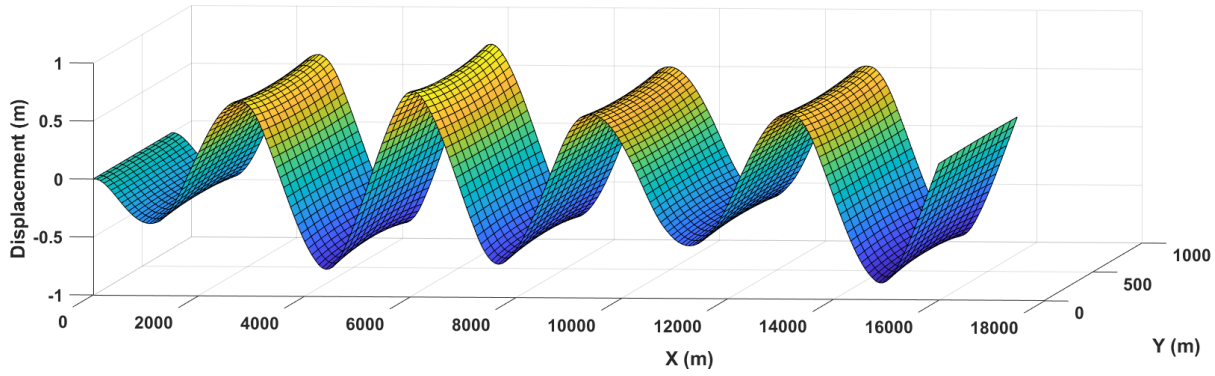

Fig. 47,a

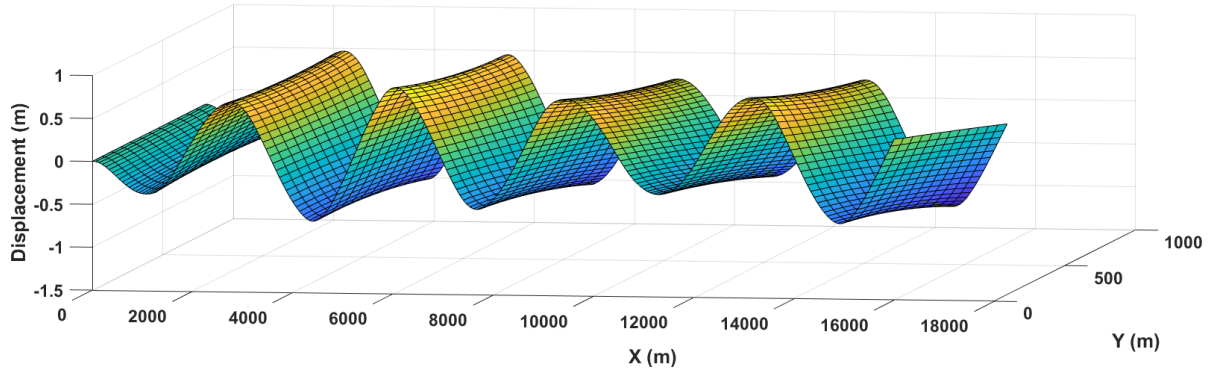

Fig. 47,b

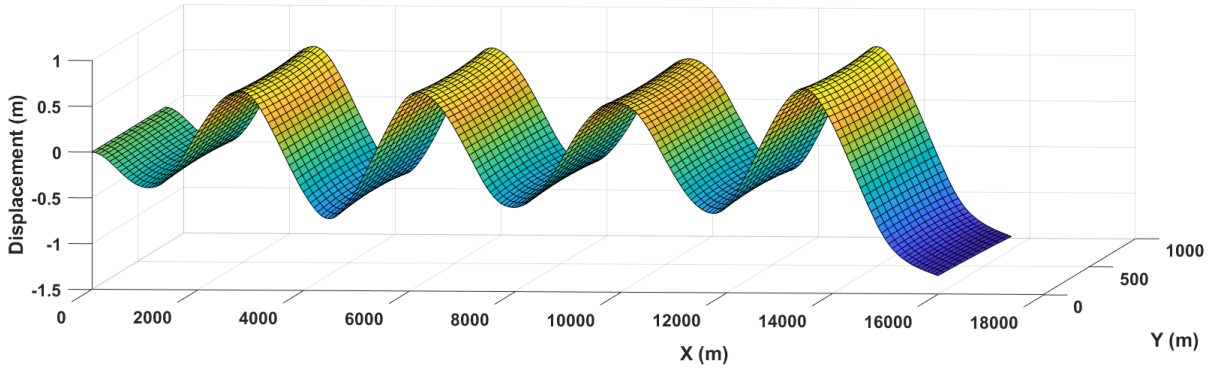

Fig. 47,c

Figure 47. Ice shelf vertical deflections result from the impact of the frontal incident wave. The periodicity of the forcing $\boldsymbol{T = 120s}$. The parameters of the model are **a)** $\boldsymbol{\alpha_1 = 0.6, \alpha_2 = 0.4}$; **b)** $\boldsymbol{\alpha_1 = 0.4, \alpha_2 = 0.6}$; **c)** $\boldsymbol{\alpha_1 = 0.0, \alpha_2 = 1.0}$.

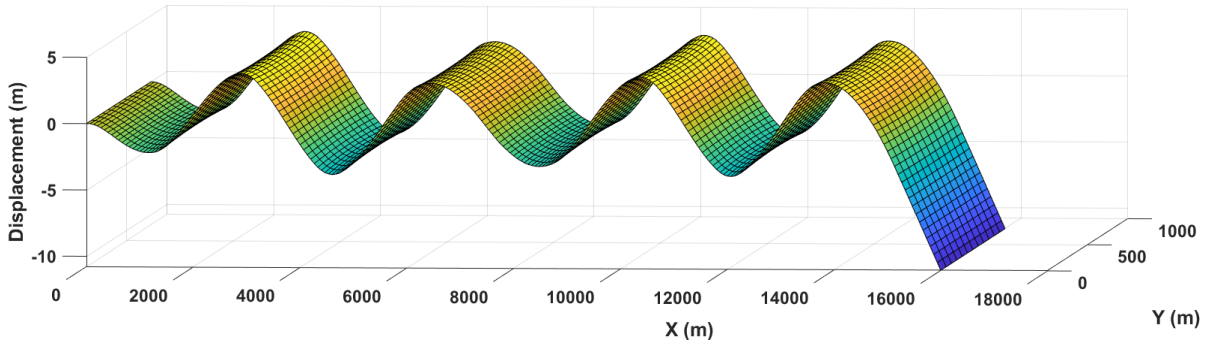

Fig. 48,a

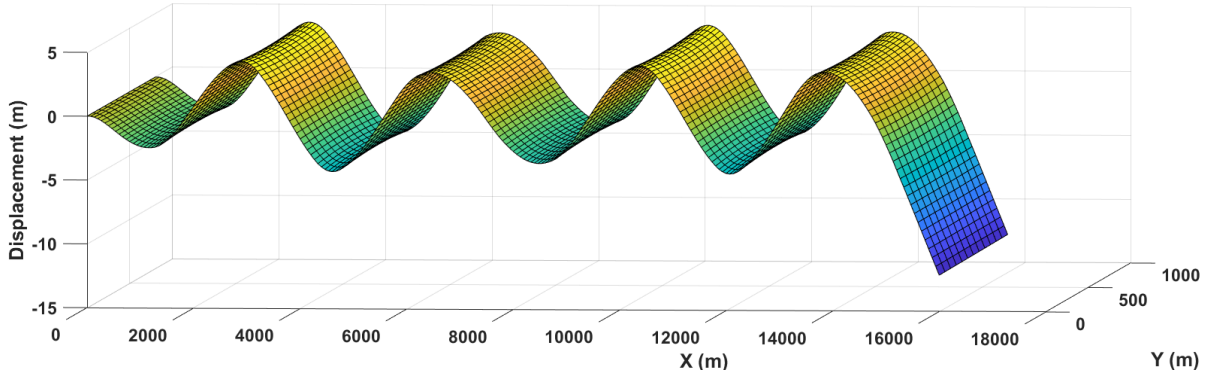

Fig. 48,b

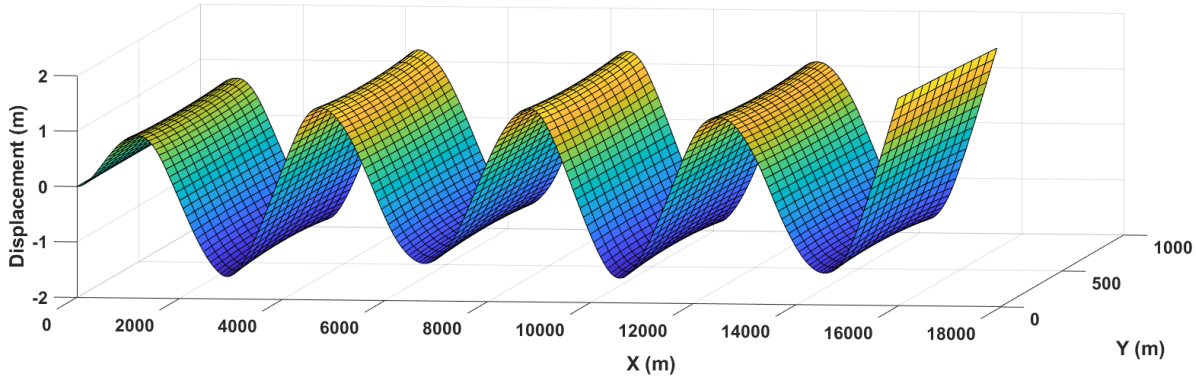

Fig. 48,c

Figure 48. Ice shelf vertical deflections result from the impact of the frontal incident wave. The periodicity of the forcing $\boldsymbol{T = 150s}$. The parameters of the model are **a)** $\boldsymbol{\alpha_1 = 0.6, \alpha_2 = 0.4}$; **b)** $\boldsymbol{\alpha_1 = 0.4, \alpha_2 = 0.6}$; **c)** $\boldsymbol{\alpha_1 = 0.0, \alpha_2 = 1.0}$.

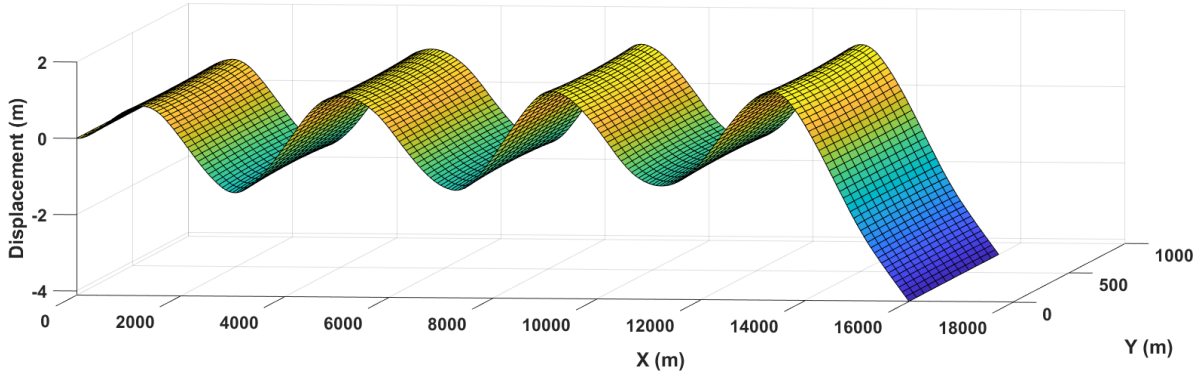

Fig. 49,a

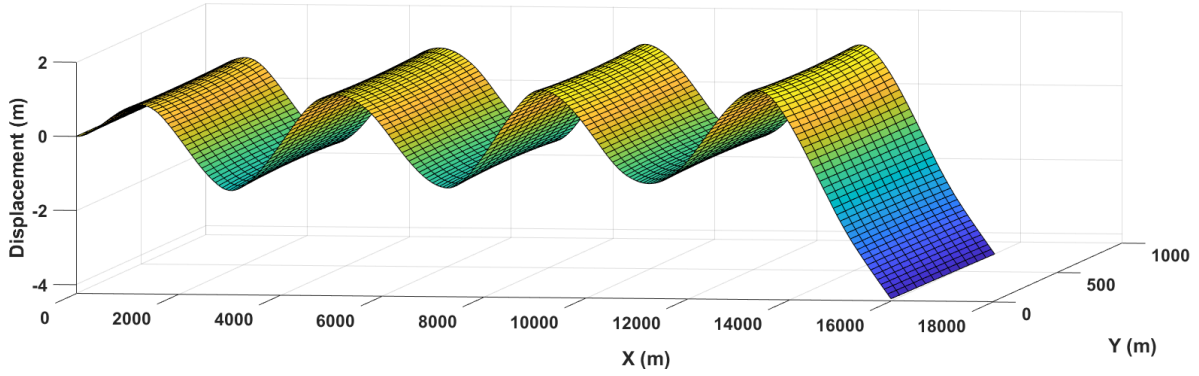

Fig. 49,b

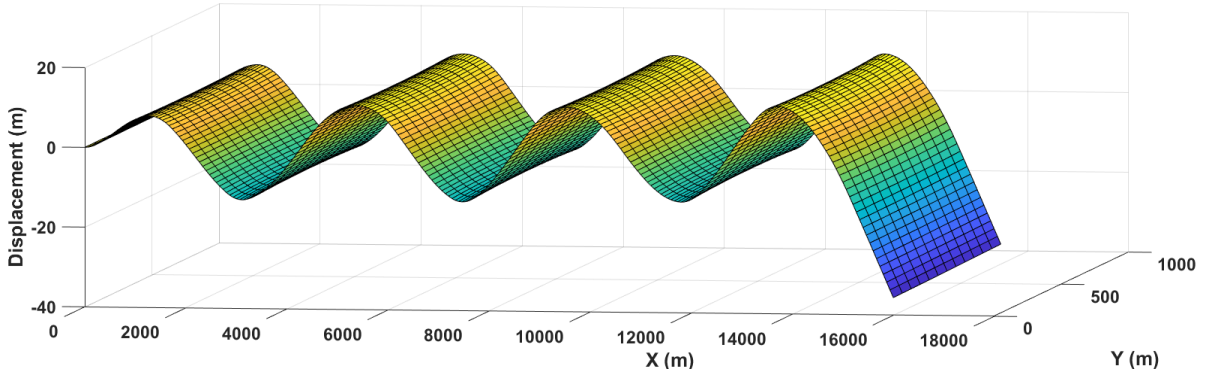

Fig. 49,c

Figure 49. Ice shelf vertical deflections result from the impact of the frontal incident wave. The periodicity of the forcing $\boldsymbol{T = 200s}$. The parameters of the model are **a)** $\boldsymbol{\alpha_1 = 0.6, \alpha_2 = 0.4}$; **b)** $\boldsymbol{\alpha_1 = 0.4, \alpha_2 = 0.6}$; **c)** $\boldsymbol{\alpha_1 = 0.0, \alpha_2 = 1.0}$.

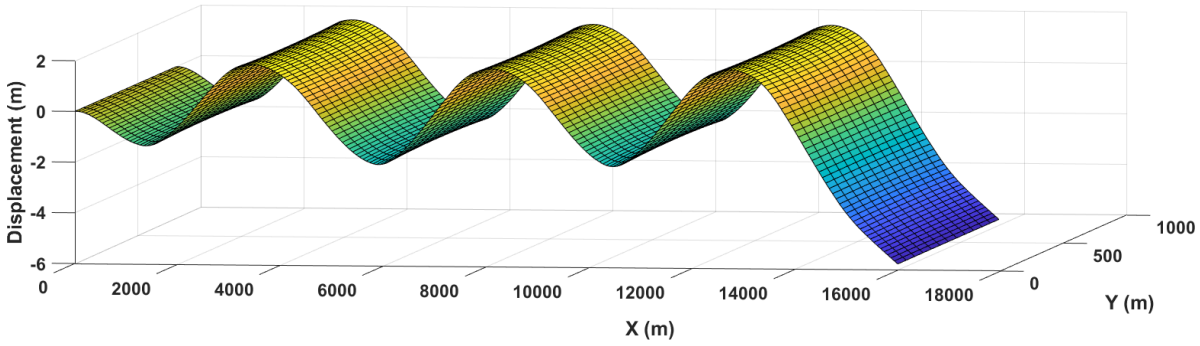

Fig. 50,a

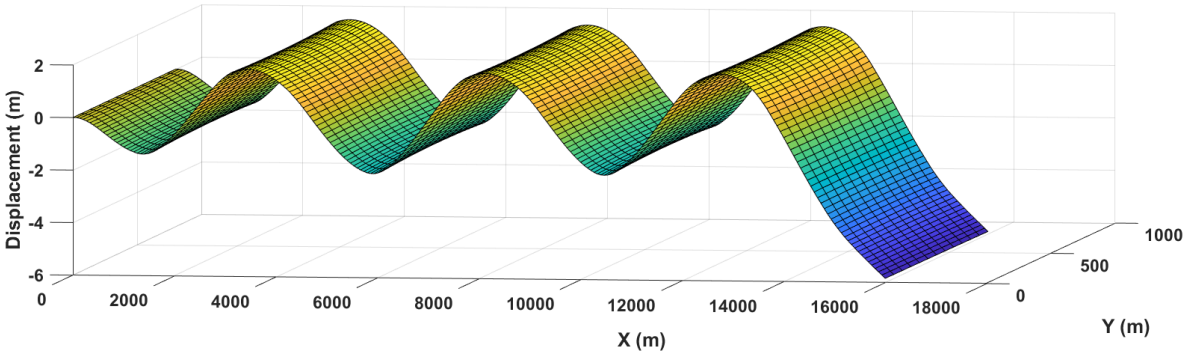

Fig. 50,b

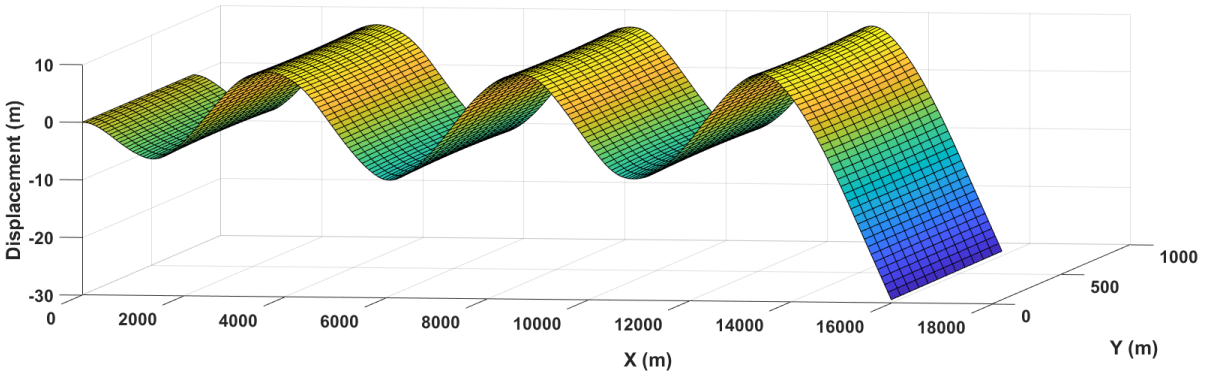

Fig. 50,c

Figure 50. Ice shelf vertical deflections result from the impact of the frontal incident wave. The periodicity of the forcing $\boldsymbol{T = 300s}$. The parameters of the model are **a)** $\boldsymbol{\alpha_1 = 0.6, \alpha_2 = 0.4}$; **b)** $\boldsymbol{\alpha_1 = 0.4, \alpha_2 = 0.6}$; **c)** $\boldsymbol{\alpha_1 = 0.0, \alpha_2 = 1.0}$.

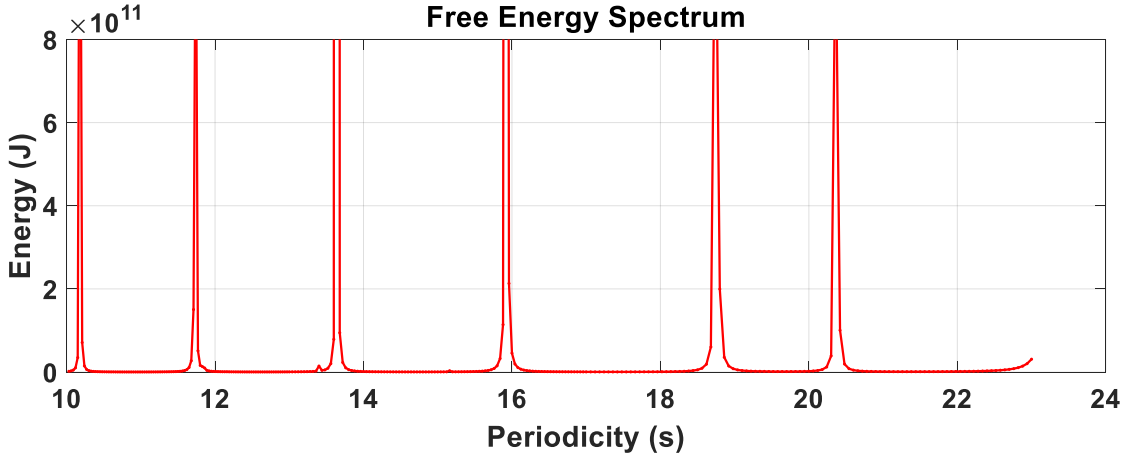

Fig. 51,a

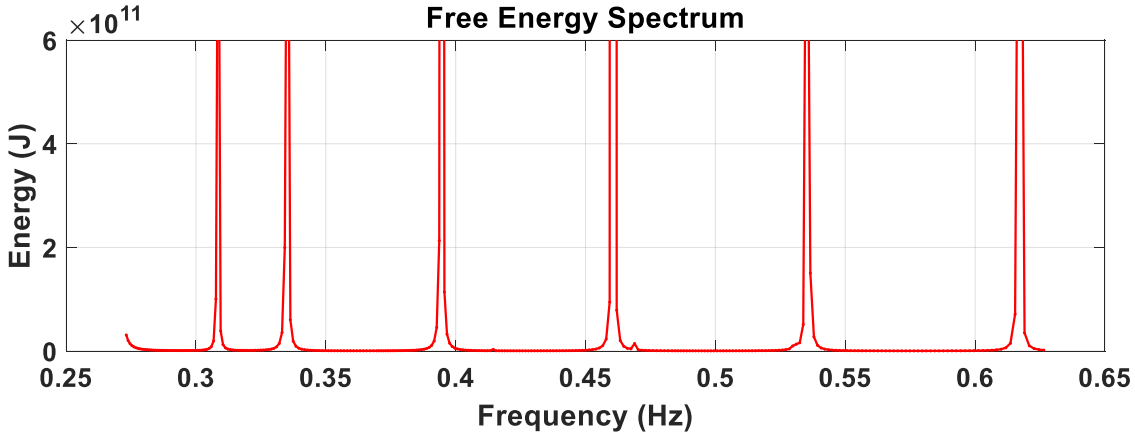

Fig. 51,b

Figure 51. Free energy of the ice shelf depending on the **(a)** periodicity/ **(b)** frequency of the forcing. The parameters of the model are $\boldsymbol{\alpha_1 = 0, \alpha_2 = 1.\ T_{cr} = 2\ km; D_{cr} = 20m.}$

References

1. Lamb, H.: Hydrodynamics. (6th ed.). Cambridge: Cambridge University Press, 1994.
2. Landau, L.D., Lifshitz, E.M.: Fluid Mechanics (Vol. 6). Pergamon Press., New York, USA, 1987
3. Landau, L.D., E.M. Lifshitz: Theory of Elasticity. (3rd ed.). Oxford: Butterworth-Heinemann, (Vol. 7), 1986.
4. Lurie, A.I.: Theory of Elasticity. Berlin: Springer, (Foundations of Engineering Mechanics), 2005.
5. Holdsworth, G. & J. Glynn: Iceberg calving from floating glaciers by a vibrating mechanism. Nature, 274, 464-466, 1978.
6. Konovalov Y.V. (2019) Ice-shelf vibrations modeled by a full 3-D elastic model. *Annals of Glaciology,* 60(79), 68-74. doi:10.1017/aog.2019.9 (http://dx.doi.org/10.1017/aog.2019.9)
7. Tikhonov, A.N., Samarskii, A.A.: Equations of Mathematical Physics. Pergamon Press Ltd., USA, 1963
8. Freed-Brown, J., Amundson J., MacAyeal, D., & Zhang, W.: Blocking a wave: Frequency band gaps in ice shelves with periodic crevasses. Ann. Glaciol., 53(60), 85-89, doi: 10.3189/2012AoG60A120, 2012
9. Konovalov Y.V. Modeling of Ocean Wave Impacts on Crevassed Ice Shelves. *Seismological Research Letters* 2023; 94 (3): 1526–1535. doi: https://doi.org/10.1785/0220220263
10. Ashcroft, N.W., & Mermin, N.D.: Solid state physics. Books Cole, Belmont, CA, 1976

11. Balmforth, N.J., & Craster, R.V.: Ocean waves and ice sheets. J. Fluid Mech., 395, 89-124, doi: 10.1017/S0022112099005145, 1999
12. Bassis, J.N., Fricker, H.A., Coleman, R., Minster, J.-B.: An investigation into the forces that drive ice-shelf rift propagation on the Amery Ice Shelf, East Antarctica. J. Glaciol., 54 (184), 17-27, doi: 10.3189/002214308784409116, 2008
13. Bennetts, L.G., Biggs, N.R.T., Porter, D.: The interaction of flexural-gravity waves with periodic geometries. Wave Motion, 46 (1), 57-73, doi.org/10.1016/j.wavemoti.2008.08.002, 2009
14. Bennets, L., Squire, V.: Wave scattering by multiple rows of circular ice floes. J. Fluid Mech., 639, 213-238. doi:10.1017/S0022112009991017, 2009
15. Bennets, L., Williams, T.: Wave scattering by ice floes and polynyas of arbitrary shape. J Fluid Mech., 662, 5-35. doi:10.1017/S0022112010004039, 2010
16. Bennetts, L.G., Squire V.A.: On the calculation of an attenuation coefficient for transects of ice-covered ocean. Proc. R. Soc. A., 468, 136–162, doi:10.1098/rspa.2011.0155, 2012
17. Bromirski, P.D., Sergienko, O.V., MacAyeal, D.R.: Transoceanic infragravity waves impacting Antarctic ice shelves. Geophys. Res. Lett., 37, L02502. doi:10.1029/2009GL041488, 2009
18. Bromirski, P., Stephen, R.: Response of the Ross Ice Shelf, Antarctica, to ocean gravity-wave forcing. Ann. Glaciol., 53(60), 163-172. doi:10.3189/2012AoG60A058, 2012
19. Bromirski, P. D., Diez, A., Gerstoft, P., Stephen, R. A., Bolmer, T., Wiens, D. A., Aster, R. C., and Nyblade, A.: Ross ice shelf vibrations. Geophys. Res. Lett., 42, 7589–7597, doi:10.1002/2015GL065284, 2015
20. Gerstoft P., Bromirski P., Chen Z., Stephen R.A, Aster R.C., Wiens D.A., Nyblade, A.: Tsunami excitation of the Ross Ice Shelf, Antarctica. The Journal of the Acoustical Society of America, 141(5), 3526, doi:10.1121/1.4987434, 2017

21. Chen, Z., Bromirski, P., Gerstoft, P., Stephen, R., Wiens, D., Aster, R., & Nyblade, A.: Ocean-excited plate waves in the Ross and Pine Island Glacier ice shelves. J. Glaciol., 64(247), 730-744, doi:10.1017/jog.2018.66, 2018
22. Chen, Z., Bromirski, P., D, Gerstoft, P., Stephen, R. A., Lee, W. S., Yun, S., Olinger, S.D., Aster R.C., Wiens D.A., Nyblade A.A.: Ross Ice Shelf icequakes associated with ocean gravity wave activity. Geophys. Res. Lett., 46, 8893– 8902, doi:10.1029/2019GL084123, 2019
23. Chou, T.: Band structure of surface flexural-gravity waves along periodic interfaces. J. Fluid Mech., 369, 333-350, 1998.
24. Gerstoft, P., Bromirski, P., Chen, Z., Stephen, R.A, Aster, R.C., Wiens, D.A., Nyblade, A.: Tsunami excitation of the Ross Ice Shelf, Antarctica. The Journal of the Acoustical Society of America, 141(5), 3526, doi:10.1121/1.4987434, 2017
25. Godin, O. A, Zabotin, N. A.: Resonance vibrations of the Ross Ice Shelf and observations of persistent atmospheric waves. J. Geophys. Res. Space Phys., 121, 10157-10171, doi:10.1002/2016JA023226, 2016
26. Goodman, D.J., Wadhams, P., & Squire, V.A.: The flexural response of a tabular ice island to ocean swell. Ann. Glaciol., 1, 23–27, 1980
27. Holdsworth, G.: Tidal interaction with ice shelves. Ann. Geophys., 33, 133-146, 1977
28. Hughes, T. J.: West Antarctic ice streams. Reviews of Geophysics and Space Physics, 15(1), 1-46, 1977
29. Ilyas, M., Meylan, M.H., Lamichhane, B., Bennetts, L.G.: Time-domain and modal response of ice shelves to wave forcing using the finite element method. J. Fluids and Structures, 80, 113-131, doi:10.1016/j.jfluidstructs.2018.03.010, 2018
30. Kalyanaraman B., Bennetts L.G., Lamichhane B., Meylan M.H.: On the shallow-water limit for modelling ocean-wave induced ice-shelf vibrations. Wave Motion, 90, 1-16, doi: 10.1016/j.wavemoti.2019.04.004, 2019

31. Kalyanaraman B., Meylan M.H., Bennetts L.G., Lamichhane B.P.: A coupled fluid-elasticity model for the wave forcing of an ice-shelf. J. Fluids and Structures, 97, 103074, doi: 10.1016/j.jfluidstructs.2020.103074, 2020
32. Konovalov, Y.V. Abatement of Ocean-Wave Impact by Crevasses in an Ice Shelf. *J. Mar. Sci. Eng.*, *9(1)*, 46, 2021. https://doi.org/10.3390/jmse9010046
33. Lingle, C. S., Hughes, T. J., Kollmeyer, R. C.: Tidal flexure of Jakobshavns Glacier, West Greenland. J. Geophys. Res., 86(B5), 3960-3968, 1981
34. MacAyeal, D.R., Okal, E.A., Aster, R.C., Bassis, J.N., Brunt, K.M., Cathles, L.M., Drucker, R., Fricker, H.A., Kim, Y.-J., Martin, S., Okal, M.H., Sergienko, O.V., Sponsler, M.P., & Thom, J.E.: Transoceanic wave propagation links iceberg calving margins of Antarctica with storms in tropics and Northern Hemisphere. Geophys. Res. Lett., 33, L17502. doi:10.1029/2006GL027235, 2006
35. MacAyeal, D., Sergienko, O., Banwell, A.: A model of viscoelastic ice-shelf flexure. J. Glaciol., 61(228), 635-645, doi:10.3189/2015JoG14J169, 2015
36. McNeil, S., M.H. Meylan, Time-Dependent Modelling of the Wave-Induced Vibration of Ice Shelves. *J. Mar. Sci. Eng.*, *11*, 1191, 2023. https://doi.org/10.3390/jmse11061191,
37. Massom, R.A.; Scambos, T.A.; Bennetts, L.G.; Reid, P.; Squire, V.A.; Stammerjohn, S.E. Antarctic ice shelf disintegration triggered by sea ice loss and ocean swell. Nature, *558*, 383–389, 2018
38. Mei, C.C.: Resonant reflection of surface water waves by periodic sandbars. J. Fluid Mech., 152, 315-335, doi: S0022112085000714, 1985
39. Meylan, M., Squire, V.A., & Fox, C.: Towards realism in modelling ocean wave behavior in marginal ice zones. J. Geophys. Res., 102(C10), 22981–22991, 1997
40. Meylan, M., Bennetts, L., Hosking, R., Catt, E. On the calculation of normal modes of a coupled ice-shelf/sub-ice-shelf cavity system. J. Glaciol., 63(240), 751-754. doi:10.1017/jog.2017.27, 2017

41. Nekrasov, P. & D. MacAyeal. Ocean wave blocking by periodic surface rolls fortifies Arctic ice shelves. J. Glaciol., 1-11. doi:10.1017/jog.2023.58, 2023
42. Papathanasiou, T. K., Karperaki, A. E., Theotokoglou, E. E., and Belibassakis, K. A.: Hydroelastic analysis of ice shelves under long wave excitation, Nat. Hazards Earth Syst. Sci., 15, 1851–1857, doi:10.5194/nhess-15-1851-2015, 2015
43. Papathanasiou T.K., Karperaki, A.E., Belibassakis K.A.: On the resonant hydroelastic behaviour of ice shelves, Ocean Modelling, 133, 11-26, doi:10.1016/j.ocemod.2018.10.008, 2019
44. Reeh, N., Christensen, E.L., Mayer, C., Olesen, O.B.: Tidal bending of glaciers: a linear viscoelastic approach. Ann. Glaciol., 37, 83–89, 2003
45. Robin, G. de Q.: Seismic shooting and related investigations. In Norwegian-British-Swedish Antarctic Expedition, Sci. Results 5, Glaciology 3, Norsk Poarinstitutt (pp. 1949-1952). Oslo: University Press, 1958
46. Rosier, S.H.R., Gudmundsson, G.H., & Green, J.A.M.: Insights into ice stream dynamics through modeling their response to tidal forcing. The Cryosphere, 8, 1763–1775, 2014
47. Scambos, T.A., Hulbe, C., Fahnestock, M., Bohlander, J.: The link between climate warming and breack-up of ice shelves in the Atlantic Peninsula. J. Glaciol., 46(154), 516-530, doi:10.3189/172756500781833043, 2000
48. Shearman, E.D.R.: Radio science and oceanography, Radio Sci., 18(3), 299–320, doi:10.1029/RS018i003p00299, 1983
49. Sheng, P.: Introduction to wave scattering, localization and mesoscopic phenomena. Springer, Berlin, 2006
50. Schmeltz, M., Rignot, E., & MacAyeal, D.R.: Tidal flexure along ice-sheets margins: Comparison of InSAR with an elastic plate model. Ann. Glaciol., 34, 202-208, 2001
51. Schulson, E.M.: The Structure and Mechanical Behavior of Ice. JOM, 51 (2), 21-27, 1999

52. Sergienko, O.V.: Elastic response of floating glacier ice to impact of long-period ocean waves. J. Geophys. Res., 115, F04028. doi:10.1029/2010JF001721, 2010
53. Sergienko, O. Normal modes of a coupled ice-shelf/sub-ice-shelf cavity system. J. Glaciol., *59*, 76–80, 2013
54. Sergienko, O.V. Behavior of flexural gravity waves on ice shelves: Application to the Ross Ice Shelf. J. Geophys. Res. Oceans, 122, 6147–6164, 2017
55. Smith, A.M.: The use of tiltmeters to study the dynamics of Antarctic ice shelf grounding lines. J. Glaciol., 37, 51–58, 1991
56. Squire, V.A., Dugan, J.P., Wadhams, P., Rottier, P.J., & Liu, A.K.: Of ocean waves and sea ice. Annu. Rev. Fluid Mech., 27, 115–168, 1995
57. Stephenson, S.N.: Glacier flexure and the position of grounding lines: measurements by tiltmeter on Rutford Ice Stream, Antarctica. Ann. Glaciol., 5, 165-169, 1984
58. Turcotte, D.L., Schubert, G.: Geodynamics. (3rd ed.). Cambridge: Cambridge University Press, 2002
59. Van der Veen C.J.: Fracture mechanics approach to penetration of bottom crevasses on glaciers. Cold Reg. Sci. Technol., 27(3), 213-223, 1998
60. Vaughan, D.G.: Tidal flexure at ice shelf margins. J. Geophys. Res., 100(B4), 6213–6224, doi:10.1029/94JB02467, 1995
61. Wadhams, P.: The seasonal ice zone. In Untersteiner, N. (Ed.), Geophysics of sea ice (pp. 825–991), London: Plenum Press, 1986
62. Walker, R.T., Parizek, B.R., Alley, R.B., Anandakrishnan, S., Riverman, K.L., Christianson, K.: Ice-shelf tidal flexure and subglacial pressure variations. Earth and Planetary Science Letters, 361, 422–428, doi: 10.1016/j.epsl.2012.11.008, 2013